Università di Roma "La Sapienza"
Dipartimento di Meccanica ed Aeronautica
Dottorato di Ricerca in Meccanica Teorica ed Applicata

Francesca Magionesi

AN INVESTIGATION ON ENERGY DYNAMICS OF COMPLEX RESONATORS

Tutor: Prof. Aldo Sestieri

Supervisor: Prof. Antonio Carcaterra

ACKNOWLEDGEMENTS:

I owe my gratitude to many people for the achievement of this important result.
I would first like to express my gratitude to my thesis supervisor Prof. Antonio Carcaterra for his brilliant guidance and for his insights and suggestions that improved my research skills and prepared me for future challenges.
I wish to express my deepest gratitude to Dr. Elena Ciappi, who helped me to transform a confuse draft in a doctoral thesis. During these years her friendship and encouragement have been important in helping me complete this study.
I am thankful for those who kindly helped me in four years work at INSEAN. In particular, I am very grateful to Dr. Andrea DiMascio, who helped me making valuable comments on various parts of the many drafts of this thesis.
I gratefully acknowledge Prof. Aldo Sestieri who introduced me for the first time in the research community.
Part of this work has been accomplished in the Marcus Wallenberg Laboratory of the Kunglika Tekniska Hogskolan in Stockholm, in the framework of the European Doctorate in Sound and Vibration Studies (EDSVS) program. I would like to express my deep gratitude to Prof. Anders Nilsson, who gave me the possibility of spending seven months in that wonderful country and experiencing a stimulating and comfortable atmosphere. I would like to thank Prof. Svante Finnveden, without his technical skills, knowledge and advice, some of the results presented in this thesis would have not been possible.
Many thanks to Kent Lindgren and Danilo Prelevic for having helped me with my experimental measurements at MWL.
I cannot end without thanking my parents and my sister Laura for their encouragement, without their help and support none of this would be at all possible.
Last but not least, I would like to dedicate this work to Tomaso for having stood by me during all these years.

Francesca Magionesi
November 2006

CHAPTER 1: INTRODUCTION

In the last decades the design process of engineering structures was characterized by an increasing demanding of the prediction capabilities at the design stage, which would have allowed to asses not only the performance and the integrity of the structure but also the vibro-acoustic performances. The more realistic is the model, the greater the opportunity to produce optimal design; this implies the need of using a model with a very high number of degrees of freedom.

Predicting the response of a complex structural-acoustic system presents some difficulties. In fact, direct numerical solution of the governing equations of the system, while possible in principle, can be so computationally demanding as to be impractical. Furthermore, the application of deterministic methods of analysis to the prediction of its vibrational response would be not appropriate. In fact, in a complex system the presence of a high number of heterogeneous subsystems (beams, plates, acoustic cavities, etc.) and, above all, the high number of joints connecting the components are sources of a certain degree of variability of the system.

However, geometric and fabrication tolerances, variation in material properties, structural irregularities, non uniform damping distribution are some of the cause of variability that lead to different dynamical behaviours of samples of a set of nominally identical manufactures.

Moreover, many important engineering problems involve high frequency vibrations. In fact, especially in recent years, the use of light structures in aircraft and aerospace engineering, broad band excitations due to engines of increasing power and the increasing interest for the high speeds in ship, automotive and train engineering, created a general attention in the analysis of the high frequency vibration and of the acoustic problems. Approaching the high frequency problem both the difficulties above presented meet two serious limitations. In fact, high frequency problems involve vibrations characterized by short wavelengths compared with a typical length of the system. In conventional vibrational analysis based on a discretization of the continuum domains into small elements, being the size of these elements dependent on the minimum wavelength of interest, the computational time demanding could be so high that it would become prohibitive.

Besides the problem of high time demanding, which could be in principle overcome with the growth of the computer power, the use of a very fine mesh also implies an accurate

modelling of the system details. Obviously, such a modelling is difficult to obtain and it also introduces a certain degree of variability.

On the other hand, at high frequency the response of the system becomes increasingly sensitive to small perturbations of its parameters: even small variations in geometrical component dimensions, material properties and assembly tolerances imply large variations in the mid- and high- frequency responses. In fact, while low order eigenvalues of the system are lightly affected by small variation of the system parameters, the more the order of the eigenvalues increases the more their values are modified, such that the behaviour of the structure becomes unpredictable.

These considerations led to introduce a different way of tackling dynamic problems, based on a thermodynamic analogy. It is in fact in that frame that the problem related with system characterized by a high number of degrees of freedom (atoms) was studied for the first time. The necessity to reduce the computational cost has led to introduce global parameter as descriptor of the systems, rather than the local characterization, *i.e.* the punctual displacement. Further, to overcome the second problem, *i.e.* the inherent uncertainties of the system parameters, a statistical approach was favourite to a deterministic one, so that the attention is focused on an ensemble of similar system which characteristics are defined with a certain degree of variability.

The Statistical Energy Analysis (SEA) represents in this scenario the most fruitful method inspired up to now. For the first time, some concepts reminiscent of thermodynamic were applied on the analysis of the dynamical behaviour of a mechanical system. In fact, SEA states an analogy between the energy flow in mechanical systems and the heat flow in thermal problems, such that the energy diffuses from one substructure to another at a rate proportional to the difference in “temperature”, *i.e.* the modal energy, of the substructures and it is dissipated internally in each substructure at a rate proportional to the “temperature” of the substructure.

Even if the analogy with thermodynamic problems brought important results in the energy analysis of vibrating structures, this analogy still present limits not yet completely understood.

Moreover, the evaluation of the transient response to not steady excitation cannot be obtained by the classical SEA or other thermal-like approach, being their use limited at the steady state. Such an excitation is encountered in a large number of engineering structures: slamming load and breaking waves upon the bow of the ship hull, pyrotechnic

shock in space vehicle structures, earthquake in civil engineering are only few examples of this.

The impulsive excitation is particularly severe for the system, since can cause structural failure or unwanted noise.

This work is concerned with the development of a predictive method for describing in the time domain the energy sharing among complex vibrating systems, affected by inherent uncertainty of their parameters. Starting from a new approach to the problem, based on a suitable combination of statistical thermodynamics and classical structural dynamics, the goal relies in a better understanding of both the initial transient energy sharing among the subcomponents and the long term energy response of the subcomponents.

Before concluding this introduction, a brief description of the argument exposed in the following chapters is presented.

In the next chapter, a critical analysis of the available method that, up to now, can be used for the analysis of complex systems is given. The attention is mainly focused upon the discernment of the advantages of each method, as well as upon the difficulties and the limitations of their application. In particular, the attention is directed to those methods that are partially inspired by a thermal analogy.

In chapter 3 a new probabilistic energetic approach, (the Time Asymptotic Energy ensemble Average –TAEA), which has represented the foundation of the present work, is described. The originality of this methods lies in the development of an asymptotic expansion technique, that permits to evaluate the energy distribution between two subcomponents of a weakly coupled system, in both transient and steady state conditions with a low computational cost. As a particular result, this method also provides the long term energy responses of the two subsystems that, under some assumptions that will be later presented, expresses a condition reminiscent of the Energy Equipartition Principle (EEP) stated in Statistical Mechanics (SM).

In the light of this results, it seemed interesting to go deep into the principle of energy equipartition as stated in SM, trying to understand the conditions under which it holds, the definitions introduced in SM and how these last could be translated to structural dynamics. This analysis, described in chapter 4, underlines that the EEP is not an obvious result in the analysis of dynamical systems. This is clear through the consideration that to approach the EEP in SM a number of assumptions are necessary, that are often not satisfied for engineering systems.

This chapter is addressed investigating the conditions that can lead to the appearance of EEP and, as far as possible, a classification of the inhibiting or promoting factors for the reaching of energy equipartition conditions is presented. The analysis explores the field of linear and nonlinear vibrations, the effects of non-homogeneity and localization, the system dimension (*i.e.* its number of degrees of freedom), the weak or the strong coupling as well as the effect of the initial energy distribution among the subsystems.

Chapter 5 is focused upon the theoretical improvement of TAEA theory to include an arbitrary strong coupling between the substructures and the interaction among more than two subsystems. These analyses has led to reformulate the theory introducing a new energetic parameter, which is the sum of two terms: the "blocked energy term", which represents the sum of the kinetic and the potential energy terms of the subsystem when the other subsystems are considered blocked and the "mixed energy term", which provide the energy contribution to the subsystem energy due to the motion of the others. This new formulation allows the determination of the energy sharing among two or more subsystems even in presence of strong coupling among them.

In chapter 6 a validation of TAEA is presented through a comparison of the energy distribution among subcomponents of a system obtained applying the developed method and those obtained experimentally. Two different two-dimensional systems were analysed: the former is composed by two plates coupled by means of straps, while the second system is made up of three plates connected through straps among the subsystems.

Despite a small difference between the theoretical results and the measured energies at the first instants, the agreement between them is very satisfactory in both cases.

Chapters 7 and 8 close this thesis summarising the achieved results and showing some possible perspectives of the present study.

CHAPTER 2: HISTORICAL BACKGROUND

2.1 INTRODUCTION: THE ANALYSIS OF COMPLEX SYSTEM

Many efforts have been devoted to the development of methodologies for the analysis of complex and uncertainty systems. This chapter is addressed to present a classification of these methods and, as clearly as possible, to underline the advantages and the disadvantages of each of them.
In general, all the available methods belong to three different categories: the deterministic methods, the statistical methods and the hybrid ones, derived from a combination between these two approaches.

2.2 DETERMINISTIC APPROACHES

Nowadays current industrial procedures for structural product analysis usually employ deterministic Finite Element models (FEM) (Zienkiewicz and Taylor, 1989) or Boundary Element Method (BEM) (Brebbia, 1984) at low frequency range. At the basis of these methods there is a discretization of the continuum domains into small elements. The field variables within each element are described in terms of simple, approximate shape functions. Obviously to maintain the approximation error within acceptable values, the size of the finite element used to discretize the structure must be considerably smaller than the minimum structural wavelength excited. Since, as a general rule, the required number of points of the grid system increases with frequencies to a power of 1 to 3 (Carcaterra and Sestieri, 2003), depending on the specific structure (one-, two- or three-dimensional systems) for FEM (but a similar relation can be obtained also for the BEM, where the discretized system is reduced to a surface), and considered that the computational time needed to solve a vibro-acoustic problem at a given frequency ω is proportional to ω^m, where m is a positive parameter depending on the considered system and on the used numerical technique, it is evident the limitations encountered at high frequency. Thus, at high

frequency, the computational time for a complex system, already quite big at low frequency, would be so high to become prohibitive or inconvenient.

For a complex system, especially at high frequency, the limitations of applicability conventional deterministic FE or BE methods are not only related with the prohibitive computational efforts, but also with the impossibility to take into account the inherent uncertainty that affects the systems, as already underlined in the chapter 1. These considerations led the researcher to abandon the deterministic approach to study vibration for complex systems in favour of the statistical one.

2.3 STATISTICAL APPROACHES

2.3.1 METHODS BASED ON THE THEORY OF STOCHASTIC DIFFERENTIAL EQUATIONS

The analysis of uncertainty in structural dynamics belongs also to a class of problems approached by the theory of stochastic differential equations (Ghanem and Spanos 2003; Soong, 1973; Schuss, 1980). Although it was developed in the context of statistical mechanics, at present it goes beyond its limits.

Historically, the introduction of a statistical approach in the study of system dynamics was developed to study the problems related with deterministic systems excited by random forces. In fact, the analysis of stochastic differential equations began in the early ’20 of twentieth century from the Langevin’s studies upon Brownian motions (Nelson, 2001). The innovative element was given by the definition of the excitation forces in the equation of motion of a particle immersed in a fluid as a sum of a deterministic term and a stochastic one. The former is related with the fluid viscosity, the second one takes into account the random collision among the particles, instead. In that case the system dynamics is described through the equations of motion that are stochastic differential equations with deterministic coefficients and random excitation.

Starting from this pioneering work, this kind of systems has been deeply investigated and numerous results have been obtained (Newland, 1987). In fact, a wide class of engineering problems belongs to this type of problems: the vibro-acoustic analysis of structures which are moving in a fluid (for instance the hull of a ship and the fuselage

of an airplane excited by the turbulent boundary layer), offshore structures excited by the sea waves, etc.

The study of a dynamical system with stochastic parameters is an argument of more recent interest, instead. Its analysis is much more complicated than te one described above and the mathematical tools are still under development (Ghanem and Spanos, 2003; Ibrahim, 1987). From a mathematical point of view, one of the first work has been regarded the study of wave propagation in random media (Rice, 1954). This study involves partial differential equations whose coefficients are random functions of space and time. It is only in the early ’60, that this analysis were applied to the study of structural dynamics of simple structure (Kozin, 1961), and only in the last decades this approach began to spread to the study of engineering structures. A great incentive to the study of structural dynamics with parameter uncertainties has been provided by those applications where the uncertainty has a direct relationship to the reliability of such structures, for instance in civil engineering and in aerospace engineering. In particular, the necessity to obtain a deep knowledge of the risk of failure at the design stage has produced in the scientific community a great interest on the study of the system sensitivity to stochastic parameter variations (Szopa, 1986).

The theory of stochastic differential equations requires that the statistical characterization of the uncertainties that affect the system is available, for instance in terms of probability density function (PDF) of the parameters of interest: material properties, boundary conditions, initial conditions etc. Once this *a priori* probabilistic information is given, the statistics of the corresponding solution can be evaluated. In principle, the Fokker-Plank-Kolmogorov (FPK) parabolic differential equation, historically derived from the kinetic equation of Boltzmann, allows the correlation between the PDF of the equation’s parameters and the PDF of the solution (Soong, 1973).

On the other side, the great complexity of the FPK equation, especially for the nonstationary problem, allows to obtain a solution of this equation only for particular class of problems. To overcome these difficulties some new methods, based on averaging techniques, was developed providing good estimates of the first statistical moments (Soong, 1973; Ghanem and Spanos 1993; Bogadanov and Kozin, 1962). Among this class of methods, the weighted residual and the polynomial chaos

techniques are today two well established tools for the solution of stochastical differential problems.

A different approach is provided indeed by the Monte Carlo method (Pradlwarter and Schueller, 1997). It consists of solving a population of equations, where the stochastic parameter is randomly varied. Each equation is completely deterministic, thus it can be solved using standard algorithm. The obtained results are a random population of solutions and a statistics is performed on it. The great advantage of this method relies on the theoretical simplicity and in the few knowledge necessary of the stochastic process. However, the solution can be prohibitive in terms of computational time, since it requires the numerical solution of the equation of motion of the system for different set of the parameters obtained from their statistical distribution. However, a significant statistics can be performed only when a large enough number of solution samples are generated.

Another widely used technique for the analysis of stochastic system is the stochastic perturbation method, which consists of a natural generalization of the perturbation technique used in nonlinear problems to the case of stochastic systems (Soong and Bogdanoff, 1963; Carcaterra et al. 2005). The perturbation scheme consists of expanding all the random quantities around their respective mean values using a Taylor series. Even if this method is characterized by a high theoretical simplicity, its use is bound to a small class of problems involving small randomness.

2.3.2 ENERGETIC METHODS

To overcome the difficulties met in the analysis of complex systems a different way of tackling dynamical problems was developed. The necessity to reduce the computational cost has led to introduce global parameters as descriptor of the systems, rather than the local quantities. From this point of view, the use of the global energy of the whole mechanical system, or few energies characterizing some substructures, as global parameter was the most obvious choice, since for the energy variable is always possible to write the balance equations among the subsystems.

The use of global parameter to describe the system dynamic highly reduces the dimensions of the problem, but it also lead to loose all the local informations of the system behaviour.

Further, to overcome the problem of the inherent uncertainties of the system parameters, a statistical approach was favourite to a deterministic one.

It is interesting to notice that a similar approach was already used in the 19th century by Boltzmann and Gibbs to analyse the thermodynamical systems, leading to that part of physic called Statistical Mechanics (SM). In fact, dealing with the microscopic structure of matter, SM analyses systems that have such a large number of particle (atoms) as to be impossible to characterize the system in terms of motion of each particles. The descriptor of micro-scale phenomena of the analysed system, yet possible in principle, was skipped and replaced by an average macro-scale descriptor (the energy) and a statistical approach was used to consider the random nature of the system parameters. In section 2.5 a more detailed description of the analogies between structural dynamics of complex systems and SM will be exposed, trying to underline the concept that could be fruitful taken from this last.

Moreover, at the beginning of the last century the interest for room acoustics led the research community to analyse, for the first time in the vibration field, systems with a very high number of degrees of freedom. The study was focused on the laws that regulate the number of modes and their density in acoustic cavities as a function of the frequency and the distribution of the natural frequencies along the frequency axes. These researches were aimed to predict the property of the acoustic pressure in an acoustic room with respect to the mode distribution as a function of the frequency (Bolt and Roop, 1950; Morse and Ingard, 1968).

This is the background of Statistical Energy Analysis and of many satellite energy methods developed later.

Originating around 1960, early SEA resulted from a collaboration of two independent efforts by R.H. Lyon and P.W. Smith, that met to discuss how to predict the rocket noise and the vibrations of launch vehicles.

In the early 60, Lyon and Maidanik published their first work on Statistical Energy Analysis (Lyon and Maidanik, 1962), presenting a completely new point of view in tackling vibro-acoustic problem. In fact, for the first time some concepts reminiscent of thermodynamic were applied on the analysis of the dynamical behaviour of a mechanical system. SEA states an analogy between the energy flow in mechanical systems and the heat flow in thermal problems, such that the energy diffuses from one substructure to another at a rate proportional to the difference in “temperature”,

i.e. the modal energy, of the substructures and it is dissipated internally in each substructure at a rate proportional to the "temperature" of the substructure.

SEA deals with a population of similar systems, each of them shares the same macro characteristics with the others but differs in details, due to small variation of the physical parameters, as it was already described by the author himself in (Lyon and DeJong, 1995) during the explanation of the name chosen for this method:

"Statistical emphasizes that the systems studied are presumed to be drawn from populations of similar design construction having known distributions of their dynamical parameters".

Another possibility is to assume that the system itself is random, due to random irregularities in their construction, such that the mode shapes and the natural frequencies are not perfectly known.

The ensemble energy average is obtained by performing two different type of averaging: the first is a spatial average of the vibrational energy on the substructures, losing any information regarding the local behaviour; the second is a frequency band average of the energy.

SEA models a vibro-acoustic system as an assembly of subsystems, where a subsystem is defined as a group of modes with similar energetic properties, *i.e.* the modes belonged at each subsystem receives the same energy rate, they are similar coupled with the modes of the other subsystems and they are characterized by the same dissipation. That is when they have the same energy, since each mode receives the same energy and dissipates in the same way, establishing an energy equipartition among the modes of a subsystem.

Applying the energy conservation principle in terms of energy flow and the energy of each subsystem, similar with the Fourier law, a balance energy equation for each subsystem is obtained. In the hypothesis that the coupling among the subsystems is weak, the equations that results are linear and can be solved by the methods of matrix algebra.

Despite significant theoretical refinements and the development of complementary methods has occurred, the basic SEA theory has changed little from its first formulation.

Nowadays SEA can be considered the most widely used method for the high-frequency analysis in industrial applications, although it does not yet meet a general agreement for several reasons that are summarized in Fahy's review (Fahy, 1994).

Although the wide and successful use of SEA in a high number of different engineering applications, research on a more established theoretical base of SEA has still required.

Many critical points are still under analysis: the assumption of a thermal-like law for the exchange of the energy among the subsystems is one of this. In 1981 Woodhouse published an article (Woodhouse, 1981) that provides an important contribution in the attempt to understand the limit of validity of this assumption. Using a different mathematical foundation for the study of coupled subsystems with respect to Lyon and Maidanik's one, partially inspired by a technique described by Lord Rayleigh in (1945), he demonstrated that this assumption is not valid even in the case of three oscillators. In 1987 Keane and Price derived some hypothesis under which the thermal-like exchange of the energy distribution among the subsystems is valid: the excitation forces acting on the subsystems are statistically independent, the power flow and the energies of each subsystem are evaluated upon narrow band, anyhow containing a high number of modes, the damping of the system is proportional and the coupling is weak and conservative.

More recently, a significant contribution to the understanding of the physical aspects of SEA is given by Langley's work. Starting from the equation of motion in an elastic continuum and using a general and rigorous procedure, he manages to derive the SEA equations by assuming a random excitation in both time and space and a conservative coupling (Langley, 1989). The power flow is demonstrate to have a thermal-like expression when the mass density is uniform, the damping is mass proportional, the energy is averaged upon a population of random systems and the coupling among the subsystems is weak (in the sense that the Green function of each subsystem is approximately equal to that of the uncoupled system).

The implication of assuming proportionality between the average power flow between two subsystems and the difference of their average energies is still argument of discussions (Mace, 1994).

Even if we assume the validity of a thermal-like expression for the power flow, there are many other critical elements in SEA, starting even from the definition of a correct partition of the whole systems into appropriate subsystems (Totaro and Guyader, 2006). The establishment of the basic assumption of this method (*i.e.,* conservative, linear and weak coupling, equipartition of energy within the modal group, random excitation, etc.) is also difficult.

Despite SEA equations are formally quite simple, they need a preliminary evaluation of some coefficients, which represents other unknown parameter, *i.e.* the coupling loss factors, the internal loss factors and the input power. SEA does not provide any general criteria for their evaluation but, for each case, they can be theoretically or experimentally obtained using theoretical approaches, experimental measurements or computational techniques, such as FEM.

The evaluation of the coupling loss factors (CLF), which represent the proportionality coefficients between the energy power flow that a subsystem looses due to the coupling with another subgroup of modes and the energy stored in it, is a critical aspect. Even if in technical literature several methods are available for the determination of the CLFs (Fahy, 1994; Cacciolati and Guyader, 1997), a theoretical evaluation of these parameters is not always possible but can require experimental measurements (Bies and Hamid, 1980) or FE analysis (Maxit and Guyader, 2001).

Moreover, the determination of the damping loss factor and the power input in each subsystem are other sources of high uncertainty (Maidanik and Dickey, 1997).

Finally it is important to underline that SEA provides estimates of the ensemble average behaviour of population of systems having parameters drawn from random distributions, but no formal procedure are given for estimating the uncertainty of correspondence between the ensemble average behaviour and that of an individual sample. In the last years an increasing interest in extending this prediction to the variance of the energy has focus the attention of the research community (Fahy and Mohammed, 1992; Mace, 1992; Lyon and DeJong, 1995; Langley and Cotoni, 2004; Ichchou et al., 1997).

At the beginning of ’90, a new technique for the analysis of vibro-acoustic problem at high frequency was presented, namely Wave Intensity Analysis (WIA) (Langley, 1992). The basic idea is to represent the dynamical response of a component of a system as a superimposition of travelling waves in all the directions, each of them with a certain phase and amplitude. By neglecting the phase dependencies, which implies that the wave components are assumed uncorrelated (thus, the system response is considered homogeneous in space and the effects due to resonance and anti-resonance phenomena are neglected), at each wave-type component (the out-of plane bending waves, in-plane shear waves and in-plane longitudinal waves for a flat plate element) is associated an average energy. Assuming that the dissipated power is proportional to the energy stored, for each wave-type component an energy balance

equation can be obtained, providing a set of coupled equations (the coupling is given by the energy terms entering and exiting from the element boundaries).

To solve the system equations, the directional dependence of the wave energies of each component is represented by a finite Fourier series. Considering only the first term of the Fourier series (which implies the assumption of a diffusive wave field), the author demonstrates that WIA reduces to conventional SEA. In the analysis of plate assemblies, the author shown that the improvement in the response prediction which arises from WIA is obtained with a small additional effort, by introducing few terms in the expansion.

This leads to a significant improvement over conventional SEA, relaxing the SEA assumption of equipartition of energy between the modes of a particular subsystem and the diffuse wave field assumption. From a wave point of view this assumption implies to affirm that the vibrational wave-field in each element is diffuse. This hypothesis does not hold in general in fact, in some cases where the directional filtering effect of the junctions cannot be neglected, this assumption is not valid and consequently SEA does not provide good estimates of the vibrational energies.

On the contrary, SEA can be expected to provide better results for structure of more complex geometry, where the diffusive wave field approximation is more reasonable.

Following the hint from the Buvailo and Ionov's work of 1979, a number of papers (Nefke and Sung, 1987; Wolhever and Bernhard, 1992; Carcaterra and Sestieri, 1995, Xing and Price, 1997, Bouthier and Bernhard, 1995) were published attempting to extend the thermal laws used in SEA into differential terms. In 1987 Nefke and Sung proposed a new approach, namely Power Flow Method, where the same power relation used in SEA were proposed in differential terms to yield a smooth behaviour of the field variables along the structure under analysis.

The basic idea is that an elementar control volume of a generic continuous elastic vibrating system exchanges an amount of energies proportional to the energy stored in itself. Assuming that the energy flow is proportional to the gradient of the energy density and that the energy dissipated is proportional to the energy density, for a steady state problem the local energetic balance equation is a partial differential equation, formally equal to the heat conduction equation in thermal problems. Being the solution of this equation non-oscillating, the authors underlined the possibility to solve the problem using traditional FEM with a quite coarse mesh even at high frequency.

The great advantage of this approach is the possibility to obtain the local variation of the energy density along the structure, filling the SEA limitations.

Wohlever and Bernhard (1992) revisited the power flow method, defining a different energetic variable (the time average energy density) they obtained a similar thermal energy density equation. With this new variable definition, they manage to verify the validity of the thermal analogy for longitudinal vibrations of beams and plates for a point harmonic excitation. On the contrary, for flexural vibration of beam and plates this analogy does not hold, unless the near field and spatial oscillating terms of the new variable are neglected.

Despite the promising results obtained for rods and beams, up to now several points are still vague and not totally convincing.

Langley (Langley, 1995) demonstrated that the thermal analogy for two-dimensional systems is strictly not correct; he also showed that in the case of plates excited by a point load, the vibrational conductivity approach yields an energy distribution more uniform than the real one, underestimating the response in the vicinity of the loading point and over estimating it far from that.

In the meantime, a different approach for the prediction of the steady state response of one-dimensional structures, called General Energy Formulation (GEF) was presented in (Lase et al., 1998; Ichchou et al., 1997) where both the near field and the far field effects and both the active and the reactive part of the intensity vector are taking into account. This technique allows the determination of the spatial variation in the response within a subsystem and it can also incorporate different types of boundary conditions. A disadvantage is that the energy formulation becomes a more mathematically difficult problem than the equation of motion in terms of a displacement variable. For example, for a Bernoulli-Euler beam, instead of a single fourth-order partial differential equation of motion, the energy formulation requires two eighth-order partial differential equations. To overcome some of these difficulties, Le Bot et al. (1995) formulated the Simple or Smooth Energy Formulation (SEF) by introducing a smoothing function and performing spatial averaging on a single wavelength basis. Their results, for onedimensional systems, reduce to the heat (or diffusion) equation lending some credibility to the SEA thermal analogy. Le Bot et al. (1995) attempt to extend the SEF model to twodimensional system; however, their results in this case, do not reduce to the heat

equation. Despite the appealing results for simple structure, the GEF and SEF methods still require more studies before being applicable to engineering structures.

In (Carcaterra and Adamo, 1999) an investigation of the validity of the thermal wave approach is presented. They found that the energy transmission mechanism is controlled by a parameter, defined as the ratio between a characteristic dimension of the system and the excitation wavelength. For value less than one the thermal analogy fails, at higher values the thermal analogy is valid only for one-dimensional system.

A high number of engineering structures are subjected to transient excitation: the slamming load and breaking waves upon the bow of the ship hull, pyrotechnic shock in space vehicle structures, earthquake in civil engineering, etc. Such excitations can cause structural failure or unwanted noise. The evaluation of the transient response to this kind of excitation cannot be obtained by the classical SEA or PFM formulations, being their use limited to steady state condition. Moreover, considering the nature of the excitation (*i.e.* typically broadband), the use of classical deterministic approaches, such as the FEM, becomes impossible. Despite the above considerations, only a few papers deal with transient responses from an energetic point of view.

In particular the efforts were directed to partially reformulate the Statistical Energy Analysis, in order to allow the evaluation of the transient dynamics, leading to the Transient Statistical Analysis (TSEA). An earlier work has been published by Manning and Lee (Manning and Lee, 1968). Taking the same analytical procedure developed in SEA, the structure is divided into a set of coupled subsystems and the energy balance equations for each subsystem are similar to the SEA equation except for a term that provide the time dependent variation of energy.

The strong assumption that was made in this paper is that the damping and the coupling loss factors in transient conditions do not change from those defined in SEA for a steady state condition, thus the proportionality relation between the energy flow and the difference of the subsystem energies remains valid also for the transient dynamics. This element is particularly critic and, as demonstrated later by Lai and Soom (1990, 1990a), the time dependencies of the coupling loss factors must be taken into account. Besides they proposed an apparent time-varying coupling loss factor to describe transient power flow

As an alternative to TSEA, Nefske and Sung (1987) proposed an energy formulation, based on the assumption that the energy flow vector is proportional to the gradient of energy density, without obtaining better results than TSEA.

More recently, in (Pinnington, 1996; Pinnington 1996a) a comparison between the results obtained by applying the Transient Statistical Energy Average (TSEA) and the exact solution for a two degree of freedom system and for two coupled beams subjected to an impulse are analysed, respectively. Despite a general quite good agreement between the results obtained and those derived by the exact solution, some differences in the energy time histories are shown. In fact, by comparing the theoretical energy time histories of the non directly excited subsystems and their exact solution, they underlined that the maximum energy condition is reached faster than applying the exact solution (the rise time is approximately half the time of the exact solution for weak coupling) and also the maximum energy achieved by the receiver is higher than that obtained by the exact solution. After that the results obtained are totally similar: the ratio of the energy of the two subsystems becomes constant. This implies that an equilibrium condition between the two subsystem energies is reached and that their energies decay at the same rate.

In this paper the authors also provide interesting considerations upon the dependency of the energy sharing between the subsystems on the strength of the coupling, which confirms the presence of beating increasing the coupling strength as obtained experimentally by Fahy and James (1996). The dependency of the maximum value of energy reached by the receiver system on the coupling strength is also shown. Finally a different behaviour of the peak energy for different coupling is shown: for weak coupling the peak energy transmitted to the second system is controlled by the damping, while for strong coupling the rise time is controlled only by the coupling loss factor.

In (Pinnngton and Lednik, 1996a) a similar analysis was spread to the case of two beams coupled through a spring, which value was varied to analyse the effect of the variation of the coupling strength upon the energy distribution between the subsystems. An impulsive excitation is provided to one of this beam. The numerical results obtained by applying TSEA with a modified version of CLFs and a Wave Propagation Analysis (WPA) shown that: for modal overlap values greater than one, TSEA overestimate the transmitted energy but underestimates the rise time of the

receiver subsystem, while at lower values, even at strong coupling, it provides better estimates of the dynamical behaviour of the subsystems.
The authors affirm that the mismatch at modal overlap factor greater than one is due to TSEA inability to describe correctly the energy transfer between subsystems. In fact, in TSEA the energy transfer begins as soon as the excitation is applied, while no time delay due to the initial pulse travelling the length of the beams.
In (Ichchou et al., 2001), the authors demonstrated that the thermal analogy fails in representing the energy sharing even for very simple systems. Two different equations characterize the energy time histories: a wave type equation for an undamped structure and a telegraph type for a damped system.
From this brief description of the energetic approaches, it seems evident that while for steady state conditions, in spite of some problems still argument of debate, this kind of approach provides good estimates of the system dynamics for both simple and complex structures, for the unsteady state condition they do not offer satisfactory solution up to now.

2.4 HYBRID METHODS

In mid-frequency domain, a hybrid approach, in which deterministic and probabilistic techniques merged to create a hybrid method is usually used. At these frequencies the assumptions that underlie SEA break down and the method does not yield accurate prediction; on the other hand the use of a FE approach, especially for a complex structure, is not feasible due to the computational burden.
In the ’90 different ways of approaching to the analysis of the dynamical response of complex system at mid-frequency range start to be developed. The common idea is to include a locally averaged statistical behaviour into a global deterministic model of a system. One such hybrid approach is the Fuzzy Structure Theory, presented in Soize’s works (1993, 1999). In this theory, the whole structure is divided conceptually into a master structure and a fuzzy substructure. The dynamical properties of the master structure are known, while those of the fuzzy substructure are known only in some statistical sense. The influence of fuzzy attachments on the master structure is, upon a stochastic assumption, modeled as an increase of inertia and damping.

Langley and Bremner (1999) developed a hybrid FE-SEA approach based on a wave-number partitioning scheme. The system response is partitioned into two components, the first corresponds to long wavelength deformation, which is modeled deterministically and the second to short wavelength modeled by using SEA. In the global equation of motion the presence of the local response is taken into account through the introduction of an appropriate contribution to the dynamic stiffness matrix and in the forcing vector.

One of the basilary hypothesis used in this method is that the local modes have a high modal overlap factor; in this case the main effects of the local mode dynamics is to add damping and an effective mass to the global modes, in analogy with fuzzy structure theory.

Typically a FE-SEA method combined the use of FE method at low frequency and SEA at high frequency. Despite it seems an appealing way to solve the problem, this type of approach is not easy to apply. The difficulties met are basically two: the basic equation of these approaches are different (dynamic equilibrium against conservation of the energy flow) and a deterministic approach against a statistical one.

2.5 AN ATTEMPT TO APPLY STATISTICAL MECHANICS TO ENGINEERING VIBRATIONS

The term Statistical Mechanics (SM) was coined by Gibbs in 1884, for the kinetic theory's treatment of the thermodynamic issues. It concerns the connection between microscopic description of the matter and macroscopic models involving the evolution of global quantities.

Dealing with the microscopic structure of matter, SM analyses systems that have such a large number of particle (atoms) as to be impossible to characterize the system in terms of motion of each particles.

The basic idea was to abandon the attempt to follow the dynamical responses of each particle and to study instead the behaviour of an ensemble of similar systems. Once the average behaviour of the systems in a representative ensemble is chosen, it is possible to make predictions on what may be expected on the average for the particular system analysed. As the number of degrees of freedom increases, the

average behaviour is found to provide a completely characterization of the individual system.

More recently similar problems arise also for small scale engineering structures like micro/nano devices for which an analysis at molecular scale is often coupled to more conventional macro-structural models (Dowell and Tang, 2003).

The attention is here focused on the analysis of those elements that are already fruitfully kept from SM in the analysis of vibro-acoustic problem and in particular on underlining those that are still not considered.

In the previous section it was shown that SEA try to state an analogy between energy flow in mechanical system and heat flow in thermal problems. But only the first law of thermodynamics (the energy conservation principle) is used to provide the balance equations of the system components. Although the thermodynamic analogy for mechanical systems brought important results, as shown in the aforementioned works, an asymmetry between the SEA and SM is evident: despite the great number of hypothesis used in SEA for its validity, the obtained results are quite poor (*i.e.* only the estimates of the ensemble average of the subsystems). On the contrary, the analysis of the second order moment of the energy, that is an obvious output in SM (Landau, 1978), is still argument of debate in SEA and in the other energy methods for structural dynamics.

Moreover, none of the aforementioned SEA-related works address the second law of thermodynamics, involving entropy notions in the energy flow between subsystems.

Only recently, a first attempt to introduce this important result of thermodynamics in the analysis of energy flow between mechanical systems was presented by Carcaterra (Carcaterra, 2002). Revisiting the Khinchin's theory of Statistical Mechanics (Khinchin, 1949), the author introduces a general entropy concept for mechanical oscillators. Once obtained this definition, it would be possible to establish an equation similar to the Boltzmann inequality (Landau and Lifšitz, 1978). Unlike in classical thermodynamics, where the system moves towards an equilibrium condition with a continuous entropy increase, in mechanical energy processes the concept of irreversibility does not strictly hold. On the contrary, for mechanical oscillators a weak form of the Boltzmann inequality is presented, which implies the possibility of reversible processes.

In chapter 4 an investigation of the SM is presented, aimed to underline the difficulties met attempting to adapt the results obtained in SM to structural vibration in engineering.

It seems evident the necessity to develop a different way of approaching the energy problem in vibrations, based on a more deep theoretical foundation of SM. In the light of above considerations, in chapter 4 an investigation of the difficulties met attempting to adapt the results obtained in SM to structural vibration in engineering is presented.

CHAPTER 3: THE TIME ASYMPTOTIC ENSEMBLE ENERGY AVERAGE OF NONSTATIONARY VIBRATIONS (TAEA): WEAK-COUPLING OF TWO SUBSYSTEMS

As deeply investigated in chapter 2, in the last years a large number of new approaches [Carcaterra, 2005; Soize, 1993; Langley, 1992; Lyon, 1995; Mace, 1992] were developed to analyze the dynamical behavior of a system affected by inherent uncertainties. Among them, a probabilistic energetic approach by Carcaterra (2005) is the foundation of the present work. This method, named Time Asymptotic ensemble Energy Average (TAEA), allows the evaluation of the average energies of a population of similar systems. The statistical approach is achieved by introducing random natural frequencies, whose variability is due to stochastic perturbations of physical and geometrical parameters of the system. The originality of this methods lie in the development of an asymptotic expansion technique, that permits to evaluate the energy distribution among the subcomponents of a system in both transient and steady state conditions with a low computational cost.

With regard to the way the statistical method is introduced in treating the behavior of complex systems, this method has a different approach with respect to the classical Statistical Mechanics (SM). In fact, in SM a deductive approach is usually used, *i.e.* the evaluation of the average behavior is obtained by introducing some *a priori* hypotheses, drawn from preliminary studies on the nature of the system (as will be better described in the following chapter). In TAEA the energies of the subsystems are pseudo-analytically evaluated first and then an average on different samples of the system is obtained, no *a priori* hypothesis of the system behavior being required.

3.1 DESCRIPTION OF THE METHOD

TAEA provides the evaluation of the unsteady energy sharing between two coupled complex resonators, each of them consisting of a very large number of degrees of freedom (or modes), and affected by uncertainties in their parameters, together with the general relationship between power flow and the expected energies of the two subsystems. As a particular result, the analysis also provides the long term energy responses of the two subsystems.

The basic assumptions used to evaluate the energy distribution among the subsystems are briefly itemized below:

1. The system is conservative: this means that all the dissipative effects are neglected (this hypothesis is removed in the following paragraph, where the dissipation effect will be included in the analysis).
2. Only the interaction between two subsystems is considered.
3. The analyzed subsystems are of the same type, *i.e.* two beams, two plates, two acoustic cavities having homogeneous properties.
4. The coupling between the substructures is "weak", *i.e.* the energy associated to the interaction forces is negligible with respect to the energy stored in each subsystem.
5. In Carcaterra (2005) the author demonstrates that the time limit for the asymptotic expansion depends on the probabilistic properties of the natural frequencies, *i.e.* if we assume a Gaussian distribution of the natural frequencies of the whole system, the asymptotic probabilistic expansion used for the evaluation of the energy responses of the substructures hold when:

$$t >> \frac{1}{\sigma_{\omega_1}}$$

where σ_{ω_1} is the root mean square of the first natural frequency of the system.

A brief description of this method is given here for the sake of completeness; details can be found in Carcaterra (2005).

Consider a freely vibrating conservative system S ideally divided into two subsystems S_1 and S_2, such that $S \equiv S_1 \cup S_2$. Assume that the system S starts to vibrate due to given initial conditions. The motion of each subsystem is described by:

$$\boldsymbol{w}^{(1)}(\boldsymbol{x},t) = \sum_{i=1}^{N} \boldsymbol{\Phi}_i(\boldsymbol{x})\, q_i(t), \quad \boldsymbol{x} \in S_1; \quad \boldsymbol{w}^{(2)}(\boldsymbol{x},t) = \sum_{i=1}^{N} \boldsymbol{\Phi}_i(\boldsymbol{x})\, q_i(t), \quad \boldsymbol{x} \in S_2$$

where $\boldsymbol{\Phi}_i(\boldsymbol{x})$ and $q_i(t)$ are the orthonormal modes (vectors) and the Lagrangean co-ordinates of S, respectively, $\boldsymbol{x} \in S$ is the vector of space co-ordinates, t is the time and w is the displacement vector.

The energies of the two subsystems $E^{(1)}(t)$ and $E^{(2)}(t)$ are given by the sum of the kinetic and potential terms which, for a linear continuous system, are expressed as follows:

$$E^{(r)}(t) = \frac{1}{2}\int_{S_r} \rho |\dot{w}|^2 \, dV + \frac{1}{2}\int_{S_r} \sigma : \varepsilon \, dV \qquad \text{with } r = 1,2$$

where σ and ε are the stress and the deformation tensors respectively, ":" denotes the scalar product between the two tensors and $\dot{w}$ is the velocity vector.

Assuming that the system S satisfies the initial condition: $w(x,0)=0,\ \dot{w}(x,0)=\dot{w}_0(x),$ the Lagrangean coordinates are:

$$q_i(t)=A_i\sin\omega_i t \quad \text{and} \quad A_i=\frac{1}{\omega_i}\int_S \rho\dot{w}_0\cdot\Phi_j dV$$

In Carcaterra (2005) it is demonstrated that the total energy of the *r-th* (*r=1, 2*) sub-component, has the expression:

$$E^{(r)}(t)=\frac{1}{2}\sum_{i,j=1}^{N}\alpha_{ij}^{(r)}\dot{q}_i(t)\dot{q}_j(t)+\frac{1}{2}\sum_{i,j=1}^{N}\beta_{ij}^{(r)}q_i(t)q_j(t)$$

or equivalently:

$$E^{(r)}(t)=\sum_{i,j=1}^{N}\left[a_{ij}^{(r)}\cos(\omega_i+\omega_j)t+b_{ij}^{(r)}\cos(\omega_i-\omega_j)t\right] \tag{3.1}$$

where a_{ij} and b_{ij} are coefficients dependent on the initial conditions, on the mode-shapes of S and on its natural frequencies ω_i, defined as follows:

$$a_{ij}^{(r)}=\frac{1}{4}A_iA_j(\alpha_{ij}^{(r)}\omega_i\omega_j-\beta_{ij}^{(r)}) \qquad b_{ij}^{(r)}=\frac{1}{4}A_iA_j(\alpha_{ij}^{(r)}\omega_i\omega_j+\beta_{ij}^{(r)}) \tag{3.2}$$

where

$$\alpha_{ij}^{(r)}=\int_{S_r}\rho\,\boldsymbol{\Phi}_i\cdot\boldsymbol{\Phi}_j\,dV \qquad \beta_{ij}^{(r)}=\frac{1}{4}\int_{S_r}\left[\boldsymbol{D}\left(\nabla\boldsymbol{\Phi}_i+\nabla\boldsymbol{\Phi}_i^{T}\right)\right]:\left(\nabla\boldsymbol{\Phi}_j+\nabla\boldsymbol{\Phi}_j^{T}\right)dV$$

When inherent uncertainties affect the system S, the energies of each subsystem become stochastic variables. As a consequence expression (3.1) represents a stochastic process. As in Statistical Mechanics, the attention is now focused on the determination of the mean value of the ensemble energies of two coupled subsystems. The way the uncertainties of the system parameter are taken into account is through its natural frequencies ω_i, regarded as a set of random variables and characterized by a joint probability density function of the natural frequencies, $p(\omega_1,\omega_2,...,\omega_N)=p(\Omega)$

Thus, the ensemble energy average of the subsystems S_1 is:

$$\overline{E}^{(1)}(t)=\int_0^{\infty}\int_0^{\infty}\ldots\int_0^{\infty}E^{(1)}(t)\,p(\omega_1,\omega_2,...,\omega_N)d\omega_1\,d\omega_2\ldots d\omega_N=\int_{R^N}E^{(1)}(t)\,p(\Omega)d\Omega \tag{3.3}$$

where $d\Omega=d\omega_1 d\omega_2\ldots d\omega_n$; an analogous expression is valid for the second subsystem S_2.

Substituting eq.(3.1) into eq.(3.3) and integrating by parts the time dependent parts of the integral, leading to an asymptotic expansion of the integrals with respect to time, the following expression for the ensemble energy average is obtained:

$$\overline{E}^{(1)}(t)=\sum_{i=1}^{N}\int_{\omega_i^-}^{\omega_i^+}\Pi_i(\omega_i)b^{(1)}(\omega_i)d\omega_i+\frac{1}{2t}\sum_{i=1}^{N}\left[\Pi_i(\omega_i)a^{(1)}(\omega_i)\sin 2\omega_i t\right]\Big|_{\omega_i^-}^{\omega_i^+}+o\left(t^{-1}\right) \tag{3.4}$$

In eq.(3.4) only the first order terms (order $1/t$) are retained, while the others are neglected. The first integral, which is time independent, provides the energy distribution in the steady state; the second is instead a term that vanishes as t^{-1}, that is responsible of the initial energy sharing between the two subsystems.

3.2 THE ENERGY EQUIPARTITION AS A TIME ASYMPTOTIC RESULT OF TAEA

Let now consider only the steady state energy components (the time independent contribution) of the two subsystems, *i.e.* the equilibrium energies $\overline{E}_{eq}^{(1)}$ and $\overline{E}_{eq}^{(2)}$, of the system S_1 and S_2 respectively. They can be evaluated using the following expressions:

$$\begin{aligned}\overline{E}_{eq}^{(1)}&=\lim_{t\to\infty}\overline{E}^{(1)}(t)=\sum_{i=1}^{N}\int_R\Pi_i(\omega_i)\,b^{(1)}(\omega_i)\,d\omega_i\\ \overline{E}_{eq}^{(2)}&=\lim_{t\to\infty}\overline{E}^{(2)}(t)=\sum_{i=1}^{N}\int_R\Pi_i(\omega_i)\,b^{(2)}(\omega_i)\,d\omega_i\end{aligned} \tag{3.5}$$

where $\Pi_i(\omega_i)$ is the i-th marginal probability of the system, defined as:

$$\Pi_i(\omega_i)=\int_{R^{N-1}}p\,(\Omega)\;d\Omega_i\,,\qquad d\Omega_i=\frac{d\Omega}{d\omega_i}$$

Eqs (3.5) provide the expected energies approached asymptotically, *i.e.* when time becomes large in the sense described previously. In Carcaterra (2005) it is demonstrated that for two coupled homogeneous subsystems of the same type (such as two beams, two plates, two acoustical cavities), the following expressions can be obtained:

$$\overline{E}_{eq}^{(1)}=\frac{m^{(1)}}{m_0}\overline{E}_0,\qquad\qquad \overline{E}_{eq}^{(2)}=\frac{m^{(2)}}{m_0}\overline{E}_0 \tag{3.6}$$

where m_0, $m^{(1)}, m^{(2)}, \overline{E}_0$ are the total mass of S, the masses of S_1 and S_2, and the total energy of S, respectively.

Suppose now that the modal responses of the whole system includes the natural frequencies up to $\omega_{\max}$; since the mass of a system m and its number of degrees of freedom N are related through a function f, such that $m = N f(\omega_{\max})$, whose form depends on the kind of system considered and on its properties, it can be proved that if the two coupled subsystems have the same form of the function *f*, then eq.(3.6) can be written in the following way:

$$\frac{\overline{E}_{eq}^{(1)}}{N^{(1)}} = \frac{\overline{E}_{eq}^{(2)}}{N^{(2)}} = \frac{\overline{E}_0}{N} \tag{3.7}$$

where $N^{(1)}$ and $N^{(2)}$ are the number of modes of S_1 and S_2 contained into the frequency range $[0, \omega_{\max}]$, such that $N^{(1)} + N^{(2)} = N$. Eq.(3.7) states that, at steady state, the energy per mode of each subsystem is equal to the initial energy per mode of the whole system. This expresses a condition reminiscent of the energy equipartition principle (EEP) stated in Statistical Mechanics. It is important to underline that the last expression is valid only under the hypothesis of two coupled homogeneous subsystems of the same type. In fact eqs (3.6) and (3.7) provide two different energy distribution laws if the system under analysis is not homogeneous. In the following chapter a deeper investigation of the conditions that can lead to the appearance of EEP and, as far as possible, a classification of the inhibiting or promoting factors for the reaching of energy equipartition conditions will be presented.

3.3 THE NON-STATIONARY ENERGY TERM

Let us now consider the nonstationary energy term in equation 3.4. It was already shown that this term, which is a t^{-1} vanishing term, is responsible of the initial energy sharing between the two subsystems. In Carcaterra (2005) the author demonstrates that under the hypothesis of coupling between homogeneous systems of the same type, only few terms in the summation provide a significant contribution to the ensemble energy average, because it is given by:

$$\overline{E}^{(1)}(t) \approx \overline{E}_0 \frac{N^{(1)}}{N} + \frac{1}{t}\sum_{i=1}^{N} \left[\Pi_i(\omega_i^+) a(\omega_i^+) \sin 2\omega_i^+ t - \Pi_i(\omega_i^-) a(\omega_i^-) \sin 2\omega_i^- t\right] \tag{3.8}$$

where the coefficients $a(\omega_i)$ in the summation tend rapidly to zero as *i* increases. This means that the ensemble energy average can be obtained on the basis of the lowest natural frequencies and mode-shapes, once their statistics is known. The great potentialities of this method lie in this property of the coefficients $a(\omega_i)$; in fact, when this property holds, the

method can describe the energy sharing between two subsystems from the sole knowledge of a few macro parameters of the systems easy to evaluate. The procedure used to evaluate the energy distribution between the subsystems consists of three steps:

1) Identification of the first natural frequencies and mode-shapes. This analysis has low computational cost, since a numerical grid with few degrees of freedom is sufficient for their evaluation.

2) Determination of the parameters a_{ij} and b_{ij} using eq.(3.2)

3) Evaluation of the energy distribution between the subsystems through an implementation of eq.(3.8) in a numerical code.

For the time range over which the probabilistic asymptotic expansion holds, it is possible to define an envelop trend of the ensemble energy averages, denoted by $\left\langle \overline{E}^{(1)} \right\rangle$, accounting for both the stationary and nonstationary contributions, given by:

$$\left\langle \overline{E}^{(1)} \right\rangle = \overline{E}_0 \left(\frac{N^{(1)}}{N} + \frac{T}{t} \right)$$

where T is a suitable constant (positive or negative) having dimension of a time. A similar expression can be obtained for the second subsystem.

3.4 THE EFFECT OF DAMPING

In the previous paragraph the dynamical behavior of a couple of conservative complex resonators has been analysed. In what follows the dissipation effects are indeed included. In the presence of small damping the modes of the structure do not change significantly, while the natural frequencies are close to those of the undamped system. The system response can be expressed in the form:

$$q_i(t) = A_i e^{-\delta_i \omega_i t} \sin \omega_i t$$

where ω_i and δ_i are the damped natural frequencies $\left(\omega_i = \omega_i^{undamp} \sqrt{1 - \delta_i^2} \right)$ and the modal damping coefficients respectively. In Carcaterra (2005) it is shown that the expected value of the energy is:

$$\overline{E}^{(1)}(t)=\sum_{i=1}^{N}\int_{R}\Pi_i(\omega_i)\,b^{(1)}(\omega_i)\,e^{-2\delta_i\omega_i t}\,d\omega_i+\sum_{i=1}^{N}\int_{R}\Pi_i(\omega_i)\,a^{(1)}(\omega_i)\,e^{-2\delta_i\omega_i t}\cos 2\omega_i t\,d\omega_i+$$
$$\sum_{i=1}^{N}\int_{R^2}\Pi_{ij}(\omega_i,\omega_j)e^{-(\delta_i\omega_i+\delta_j\omega_j)t}\left[a^{(1)}(\omega_i,\omega_j)\cos(\omega_i+\omega_j)t+b^{(1)}(\omega_i,\omega_j)\cos(\omega_i-\omega_j)t\right]d\omega_i\,d\omega_j$$

An asymptotic expansion of the integrals with respect to t, obtained retaining only the terms up to t^{-2} and using a procedure analogous to the one shown in section 3.1, produces the following expressions:

$$<\overline{E}^{(1)}>=\mu^{(1)}\frac{e^{-\delta\omega t}}{t}\left(1+\frac{T^{(1)}}{t}\right),\qquad <\overline{E}^{(2)}>=\mu^{(2)}\frac{e^{-\delta\omega t}}{t}\left(1-\frac{T^{(2)}}{t}\right)$$

where $\mu^{(r)},\delta,\omega,$ and $T^{(r)}$ are suitable coefficients for the *r*-th subsystem.

It is interesting to investigate more deeply the order of the restrained of terms in the expression of the energy ensemble average. In a conservative system the ensemble energy average of each subsystem has a monotonical trend: the energy, initially stored in the system directly excited, is progressively transferred to the other one till equilibrium is reached, *i.e.* when the modal energies of the two subsystems are equal. In this case, it is sufficient to consider the term of the asymptotical expansion up to t^{-1}.

The dynamic of a non conservative system is indeed more complicated. While the trend of the system directly excited remains monotonic because of the dissipation effects and the energy flow to the receiver, this last undergoes two opposite effects: an energy increase due to the energy flow from the directly excited subsystem and a tendency to decrease due to its inherent dissipation. The combination of the two effects leads to an increasing of the energy of the receiver at the early stage, while its energy decays at later times because of the dissipation effects acting in both systems; hence, the resulting trend of the receiver energy exhibits a maximum. This leads to retain the terms up to t^{-2} in the asymptotic expansion.

The condition of maximum energy in the receiver deserves more attention for various reasons. James and Fahy (1997) proposed the rise time as an indicator of the coupling strength among the subsystems. In Fahy and James (1996) analysing numerical and experimental results obtained with different setup (two coupled rod, two beams in flexure coupled by a spring, two coupled plates and two acoustic cavities), the authors pointed out two different behaviours in the energy response of the non directly excited system. In fact, if the coupling between the subsystems is weak it is possible to distinguish two different temporal evolutions of the kinetic energies of the two subsystems and in particular it is possible to see a peak in the kinetic energy of the "receiver" system. Otherwise, i.e. strong coupling, the kinetic energies

of the direct excited and receiver systems show the same features and the slow rise of the local kinetic energy progressively disappears. Hence, from the analysis of a non-dimesional time for the average in space kinetic energy to reach its maximum value, it is possible to discern if the coupling among the subsystem is weak in a SEA sense.

Some critics raised on the possibility to use the rise time as an indicator of the coupling strength. In Finnveden (1998) the author underlined that the rise time is also sensitive to coincidence of the modal natural uncoupled frequencies and to the damping. This implies that in some cases, for instance in the case of a two unequal oscillators close to modal proximity and largely unequal damping, the rise time is large even if the coupling is strong.

A more practical reason of interest relies on the possibility to obtain information regarding the maximum energy reached in a component of a complex system at design stage, without using long and time consuming simulation of the system dynamics. TAEA can so be used as a useful tool for acoustic design for the prediction of the response of a system component and consequently (as the time derivative of the energy) the power flow between them.

In what follows some briefly remarks are itemized to capture the main results of this method:

1. in the analysis of the unsteady energy sharing between two coupled conservative resonators, two different phases can be distinguished: an initial transient controlled by a term vanishing with t^{-1}, which is responsible for the energy sharing between the two subsystems; a second phase where the energy flow tends to zero approaching to a steady-state condition, where a particular energy distribution that is something reminiscent of the EEP in statistical mechanics is obtained.
2. In steady conditions, the energies of each subsystem are independent of the natural frequencies; therefore they are not sensitive to their variations.
3. If the two coupled subsystems are of the same type, in steady conditions the energy per mode of each subsystem is equal to the initial energy per mode of the whole system.
4. The ensemble energy average of a system with N degrees of freedom can be described by considering only few modes of the system and the related marginal probabilities, determined with a low computational cost.
5. The system response in presence of damping exhibits a totally different energy trend of the receiver subsystem: an increase of the energy at early times and a decay at later times because of the dissipation effect acting in both the systems; hence the trend of the receiver energy exhibits a maximum.

3.5 ESTIMATORS FOR THE DEVIATION FROM THE EEP

In section 3.2 it was demonstrated that under some assumptions regarding the nature of the system, the interaction forces and the external forces it is possible to obtain a result similar to what EEP states in Statistical Thermodynamic. Since this result does not seem a general rule, it is necessary to analyze the conditions which inhibit or promote the reaching of energy equipartition conditions in engineering system. Before starting with this study, different estimators are defined to check the deviation from the energy equipartition principle. The basis for this estimation is the energy probability density function (Pdf) and its related statistical moments, especially that of first and second order.

The first step is the definition of a normalized energy e as the ratio between the energy of each individual degree of freedom $\hat{e}$ of the investigated system *S* and the energy obtained from EEP $\bar{\varepsilon}$, i.e.

$$e = \frac{\hat{e}}{\bar{\varepsilon}} \qquad \text{where} \quad \bar{\varepsilon} = \frac{E_{tot}}{N}$$

Now it is possible to define an energy pdf $p(e)$ such that:

$$n\left(e_1, e_2\right) = N \int_{e_1}^{e_2} p(e)\, de \tag{3.9}$$

where $n\left(e_1, e_2\right)$ represents the number of degrees of freedom of the system having expected energy within the interval $\left[e_1, e_2\right]$. This function, which provides the energy distribution within the system, allows estimating the deviations with respect the EEP. Other parameters can be used to provide indications on the correctness of the EEP; in particular, the first and the second order moments have special relevance:

$$\bar{e} = \int_0^{+\infty} e\, p(e)\, de, \quad \sigma_e^2 = \frac{1}{N} \int_0^{+\infty} (e - \bar{e})^2\, p(e)\, de \tag{3.10}$$

The first is naturally compared with the normalized value 1 (corresponding to the energy $\bar{\varepsilon}$), the second one expresses the deviation with respect to $\bar{e}$. In those cases for which $\bar{e} \equiv 1$, that however in not necessarily the rule as it will be clarified later, σ_e^2 provides a measure of the dispersion of the energy data around the average value predicted by the EEP.

In the following analysis the system is often partitioned in different subsystems, each one characterized by a certain number of degrees of freedom. Thus, besides σ_e^2 that relates the energy of each degree of freedom with the energy equi-distribution given by the EEP, a global

deviation estimator can be considered providing information about the deviation of the energy $E^{(k)}$ of each subsystem with respect to the value $N_k\bar{\varepsilon}$ predicted by the EEP. In this case:

$$\sigma_E^2 = \sum_{k=1}^{M} \frac{(E^{(k)} - N_k\bar{\varepsilon})^2}{E_0} \tag{3.11}$$

It is important to underline that in the numerical simulations, the energies *e* as well as $E^{(1)}, E^{(2)}$ are time dependent and consequently *p(e)* and the related statistical estimators $\bar{e}$, σ_e^2 and σ_{E}^2 are also time dependent.

CHAPTER 4: ENERGY STEADY CONDITIONS AND THE PRINCIPLE OF ENERGY EQUIPARTITION

4.1 THE ENERGY EQUIPARTITION PRINCIPLE IN STATISTICAL MECHANICS

The energy equipartition principle (EEP) can be considered one of the most important results obtained in Statistical Thermodynamics; its importance relies on the immediate prediction it provides of the energy distribution among the particles, or degrees of freedom, of the considered system. In several cases, this information would be sufficient for characterizing the response of the system for many practical purposes. In its simplest formulation the EEP states that, in thermodynamic equilibrium conditions (Tolman, 1980), a system of N particles with total energy E exhibits a mean energy for each particle $\overline{\varepsilon}$ equal to

$$\overline{\varepsilon} = \frac{E}{N}$$

The same difficulties met in thermodynamic arise in the analysis of complex engineering systems, whose mathematical models have such a large number of degrees of freedom as to reproduce, conceptually, the same difficulties met in molecular dynamics. Hence, the possibility to obtain an energy distribution law in structural dynamics of complex systems similar to the EEP stated in Statistical Mechanics has led to investigate the EEP in depth, trying to understand the conditions under which it holds, the definitions introduced in SM and how these last could be translated to the structural dynamics.

It is clear that when attempting to adapt Statistical Mechanics to structural vibration in engineering some problems arise. In particular the energy equipartition principle is not an obvious result in the analysis of dynamical systems. In fact, many assumptions made in SM to approach the EEP (Tolman, 1980; Kinchin, 1949) are often not satisfied for engineering systems.

These basic hypotheses and their likelihood with engineering systems are illustrated below.

▪ **Definition of ensemble**

In SM the system is usually described in the phase space whose axes, as natural when the Hamilton's equations, are q_i, p_i, with $i = 1,..,3N$. The q_i are the generalized coordinates (e.g. the space co-ordinates of a particle), the p_i are the generalized momenta, namely $p_i = \frac{\partial (T-U)}{\partial q_i}$ (T and U are the kinetic and potential energies, respectively), and N the number of particles. These phase coordinates define a $2N$ dimensional phase space Γ, in which a single point $P(q_1,...,q_N, p_1,..., p_N)$ is said to be a representative point, or a micro-condition, of the system and defines its state at a particular time. The representative point evolves through a transformation of the coordinates defined by the Hamilton's equations, describing a phase trajectory in the phase space. However, since statistical mechanics usually deal with constant energy systems (*i.e.* $H = T + U = const$), its dynamic is described in the phase space by a set of *6N* moving points that belong to the same hyper-surface (equal-energy-surface), characterized by an equal energy value.

The statistical element of the theory appears with the introduction of the concept of ensemble. The idea to treat the behaviour of a system, which knowledge is not completely specified, in terms of a representative ensemble of systems of similar structure was developed by Gibbs (Gibbs, 1902). The basic idea is expressed by Tolman in (Tolman, 1980) as follows:

"We shall wish to consider the average behaviour of a collection of systems of the same structure as the one of actual interest but distributed over a range of different possible states".

Different types of ensemble can be analyzed, as it will be presented in the third point. Once the average properties and behaviour of this ensemble are assumed, it provides the best estimates of the properties and behaviour of the system under analysis.

It is important to underline that the Tolman's definition of ensemble implicitly implies the choice of a set of systems having the same Hamiltonian function *H*, $T + U = H(p_1 p_2 ... p_{3N,} q_1 q_2 ... q_{3N})$. Each system of this ensemble consists of the same particles, the same interaction laws among the particles and has the same total energy as the others. The difference between them is only due to a different distribution of their

representative points in the phase space, *i.e.* the systems of the ensemble have different initial conditions that spread over the same equal-energy-surface.

In engineering problems, the choice of this kind of ensemble implies the study of a set of identical systems with different initial conditions. But this is only one of the possible aspects of uncertainty. The description of real-life engineering structural systems is inevitably associated with some amount of uncertainty in specifying material properties, geometric parameters, boundary conditions. Hence, in general, in the analysis of a structural engineering system the statistical ensemble of a system that should be taken is an ensemble of systems that do not exactly have the same structure, but rather present uncertainties in their constructive parameters. This is the case of a complex structure, like the aircraft fuselage or the ships hull, where the large number of components and even more the large number of joints affect the dynamical response of each sample of the collection. In this case, the Hamiltonians associated to each system are different, *i.e.* the form of $H(p_1 p_2 ... p_{3N,} q_1 q_2 ... q_{3N})$ is itself uncertain: this is not the kind of uncertainty claimed in SM.

● The dissipation effects

In classical SM only conservative systems are considered, whose Hamiltonian is constant. Obviously an important difficulty arises when we try to translate this hypothesis to the study of engineering systems which are often non conservative. How this hypothesis can be adapted to structural vibrations? The answer could rely in a new approach to the study of the damping in engineering models, which is partly inspired by SM (Çelik, and Akay, 2000). In fact, since this last deals with the microscopic structure of matter, no energy dissipation exists, but only an energy transfer among the particles of the system and eventually the energy spreading from lower order modes to higher order modes of an atomic lattice. In the light of the SM point of view, the dissipation in structural mechanics can be regarded as a transfer from the low order modes that, being characterized by a large amplitude, can be macroscopically observed, into a microscale vibration, that cannot be observed at macro-scale (Carcaterra, 2005a). This means that the energy is transferred to the modes of the atomic lattice with very short wavelengths and small amplitude. In this way mechanical energy is conserved in any system, but since in structural dynamic we are interested only to large amplitude motions (the macroscale phenomena), we interpret the damping as a progressive loss of energy.

● Equiprobability hypothesis in a stationary state: microcanonical ensemble.

The instantaneous state of any system of the ensemble is defined by the position of a representative point in the phase space, while the condition of the ensemble as a whole are specified by a cloud of its representative points, one for each system of the ensemble. Once a representative ensemble is chosen, the behaviour of a single system is totally lost, unless some hypothesis on the distribution of probability of finding representative points of the ensemble of the system over the equal energy surface is assumed. An ensemble is specified by fixing the list of allowed states, and the statistical weight for each state.

In the literature three different ways of assigning a probability function to each microstates are presented (Tolman, 1980): the micro-canonical, the canonical and the gran-canonical ensembles. These three ensembles are demonstrated to lead at the same results in the thermodynamic limits $(N \to \infty)$. Equilibrium statistics of finite Hamiltonian systems is fundamentally described by the microcanonical ensemble, that is an ensemble formed by isolated systems with the same energy, or more specifically the systems energies lie within a small range between E and $E + \delta E$.

Moreover, since there is no reason for the system to be in a particular microstate rather than in any other for a fixed macrostate, in SM it is assume that each microstate corresponding to the same energy is equally probable, *i.e.* the statistical weight is constant for each micro-state. In fact, in Tolman (1980) the author affirms that we have:" *no justification for proceeding in any manner other than that of assigning equal probabilities for a system to in different equal regions of the phase space that correspond ... with what knowledge we do have as to the actual state of the system*". Such an ensemble is called microcanonical (Tolman, 1980; Kinchin, 1949).

This element represents the statistical characterization of the ensemble, *i.e.* it is the *a priori* probabilistic information characterizing the investigated random process. On the basis of the aforementioned considerations, the chance of adapting the results of SM to engineering vibration holds only if the attention is restricted to an ensemble of systems of the same type and with initial conditions that are spread uniformly over the equal-energy-surface. This leads to investigate a very narrow class of uncertainties and too specific to cover the practical interests of engineering vibration. Thus, a suitable modification of this assumption must be introduced developing a statistical energy method for engineering structures as illustrated in Carcaterra (2005) and in Carcaterra (2005a).

A canonical ensemble in SM is an ensemble of dynamically similar systems, each of which can share its energy with a large heat reservoir, this means that in the canonical ensemble all energy values are permitted. This ensemble is used for systems where the interaction energy with the environment is negligible with respect to their internal energy. A typical example of applicability is the case of a molecule of an ideal gas. The distribution of the total energy among the possible dynamical states (*i.e.* the weight of each member of the ensemble) is given by:

$$W_j = C\,e^{-\beta E_j}$$

where β is the product of the temperature of a macroscopic system and the Boltzmann constant, E_j is the energy of the $j-th$ system and C is the normalization constant.

The gran-canonical ensemble can be considered as a generalization of the canonical ensemble, where all energy values are permitted and also N is allowed to vary. The applicability of this ensemble is restricted to few cases in structural dynamics, requiring a mass exchange among the subsystems.

● Energy partitioning

SM predicts the energy partitioning between two coupled sub-systems in steady state conditions through the Gibbs-Boltzmann distribution. Besides all the previous hypotheses, a fundamental assumption in Statistical Mechanics is that the coupling among the subsystems is "weak", *i.e.* in Khinchin's terminology the system must verify the "*decomposability principle*" (Khinchin, 1949). This means that the total energy of the whole system is just the sum of the partial energies of the subsystems, *i.e.* the energy associated to the interaction forces is negligible with respect to the energy stored in each subsystem.

● Energy equipartition

The EEP is derived on the basis of the Gibbs-Boltzmann distribution using all the previously mentioned hypotheses. In fact, once the Gibbs-Boltzmann probability density function is determined, the first moment of the energy is readily calculated. The result produces the EEP in the form given at the beginning of this section.

4.2 POTENTIAL ELEMENTS RESPONSIBLE FOR PROMOTING OR INHIBITING THE EEP IN DYNAMICAL SYSTEMS

In the last century great efforts were made by physicists to better understand the generic properties which allow the achievement of an equilibrium condition for mechanical systems similar to a thermodynamical equilibrium (Fermi et al., 1965). The remarks contained in the previous section show how the EEP is a property that is far from being strictly shared by dynamical systems. In fact, the hypotheses that allow its deduction in the frame of Statistical Thermodynamics are hardly realized in physical and engineering systems. Great progresses have been made in the last thirty years on the study of the evolution towards energy equipartition among systems (Ford, 1992), basically due to the increasing computer power, as to the author's knowledge, only results obtained from numerical simulation are presented in technical literature. Despite this great interest, a satisfactory understanding of this problem is still lacking. This justifies the attempt to define the conditions necessary for the validity of the EEP in engineering systems and support the research of new energy repartition principles with a more general validity. The aim of this chapter is to define the conditions that can lead to the appearance of EEP in engineering systems and, as far as it is possible, classify as inhibiting or promoting factors for the reaching of energy equipartition conditions.

The choice of these factors arises from a combined examination of the literature in physics as well as in engineering. In particular, in two recent works (Carcaterra, 2005; Carcaterra 2005a; Magionesi and Carcaterra, 2005) the authors have shown that under the hypotheses that two i) linear and ii) homogeneous resonators without localization effect are iii) weakly coupled and subjected to a iv) point power injection, then the EEP holds. Therefore it seems to be reasonable to consider the effect of each of these hypotheses on the appearance of the EEP. The above four factors in addition to the effects related with the system dimension are listed below:

1. Non-homogeneity of the subsystems and localization effects
2. Initial energy distribution
3. Non-linearity in the constitutive relationships
4. Degree of coupling between subsystems
5. Number of degrees of freedom

They seem, in different forms, potential responsibles for promoting or inhibiting the EEP in dynamical systems and their effect is examined separately in the next subsections for systems of engineering interest.

4.2.1 NON-HOMOGENEITY OF THE SUBSYSTEMS AND LOCALIZATION EFFECTS

The first test of validity of the energy equipartition principle has regarded the effect of the homogeneous properties within the considered system. In fact, despite the large number of articles devoted to this topic, the results are quite often in disagreement even for very simple cases, like harmonic and anharmonic chains. For instance in Kato and Jou (2001), a harmonic chain composed by alternating masses, which models a bi-atomic gas, is analysed. From the analysis of the energy means assumed by those two kinds of particles, the authors conclude that the biggest amount of energy is stored in the heaviest particles. In Garrido et al. (2001), when considering the same system, the results was instead the opposite, since the lightest ones seem to be responsible for the higher absorption of energy. In Baowen et al. (2001), a random distribution of the masses in anharmonic chain is analysed. Using numerical simulation the authors affirm that it is not possible to define a unique condition of equilibrium of the energy, since the solution is highly dependent on initial conditions. The authors also show that as soon as a small fraction of nonlinearity is added to the system, the dynamical behaviour changes totally, being characterized by a unique equilibrium condition (in the following paragraph a deep investigation on the nonlinear effect on the reaching an equilibrium condition will be presented). When the inhomogeneity of the system becomes important, the lack of an energy equipartition principle was shown. Nowadays there is not a clear understanding of the effects that “impurities” on a chain of masses have on the transition to an equilibrium state in nonlinear systems. In this scenario the problem related to Anderson localization (Anderson, 1958) seems to be relevant. In his work, the author showed that if a quantum-mechanical system is sufficiently disordered, the system states have a finite probability to return to a given site in a long time limit. This localization of the states in a finite region of space implies the absence of diffusion.

In Snyder and Kirkptrick (1999) the effect of disorder achieved by randomly changing the value of a certainly number of masses in a nonlinear chain described by the classical Fermi-Pasta-Ulam (FPU) Hamiltonian is studied. In this context the energy equipartition

principle is not valid. Further, the responses of the systems depends on whether the impurities are heavier or lighter than those of the original system. For both cases the energy is basically stored around the impurities, but different behaviors are shown in the two cases. If the impurities are heavier than the original one, they release their energies very slowly, while lighter masses expel energy through large oscillations, speeding up the diffusion process at low concentration; on the contrary, they slow down this process at higher concentrations.

In particular, it has been recently shown in Weaver and Lobkis (2000) how the effect of mode localization can inhibit acoustic energy diffusion in coupled reverberation rooms, something that has a direct correlation with the inhibition of the mechanism leading to energy equipartition.

In the previous chapter it was demonstrated that for an homogenous system under steady conditions, the energy partitioning between two coupled sub-systems can be predicted from an expression coincident with the energy equipartition principle stated in Statistical Mechanics. In fact, the energy per mode of each subsystem is equal to the initial energy per mode of the whole system (eq 3.7). Different sets of numerical simulations were performed for three test cases (one-two-three dimensional systems) to explore the effects of non-homogeneity on the reaching of the energy equipartition condition.

The first test case is a homogeneous rod, with Young modulus E=1 Nm^2, mass per unit length ρ=1 Kg/m and total length L= 1m. The rod is ideally divided into two homogeneous subsystems, as shown in figure 1.

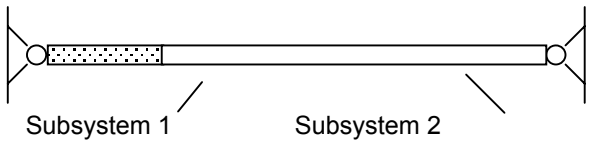

Fig.1

The one-dimensional set up

The initial conditions are given by:

$$\mathbf{u}(x,0) = 0,$$
$$\dot{\mathbf{u}}(x,0) = \delta(x - x_0)$$

where u and $\dot{u}$ are the displacement and the velocity vectors and x_0 is the point of application of a velocity spike, given as initial condition. The first simulation is

performed using a finite difference scheme with 2000 points. The discretized system corresponds to two coupled linear chains of masses, each with a mass of $5 \cdot 10^{-3}$ Kg, connected with linear springs, all with the same stiffness equal to 1 N/m (see figure 2). The two subsystems have the same number of masses, equal to 1000.

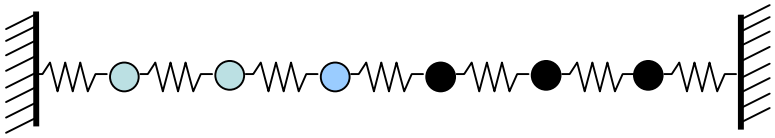

Fig.2
The one dimensional setup:
discretized system

In figure 3, the time histories of the subsystem energies are shown and compared with the theoretical results, obtained by applying eqs 3.6 and 3.7 that provides the same asymptotic energy distributions for the case under analysis. It is evident a perfect agreement between the theoretical and the numerical results. In figure 4 the results obtained for a similar geometrical system, where now the homogeneity condition is not valid anymore, are shown. The first system consists of 1000 masses each one equal to $1 \cdot 10^{-3}$ kg and the second one consists of 1000 masses with mass equal to $5 \cdot 10^{-4}$ kg.

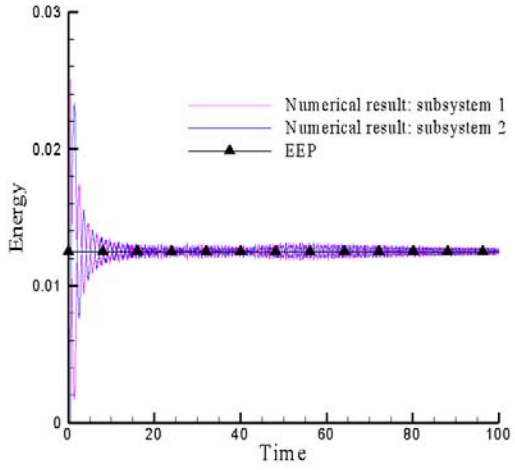

Fig.3
1D Homogeneous rod: test case 1

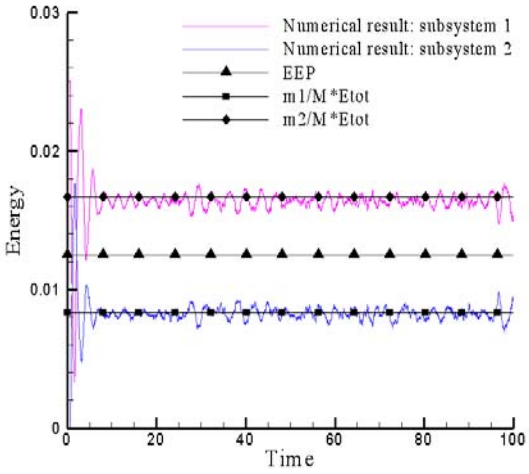

Fig.4
1D Inhomogeneous rod: test case 1

Since the number of degrees of freedom in the two subsystems is equal, the expected energies of the two chain obtained by applying the EEP should be the same. As shown in

figure 4, the energetic responses of the subsystems are not identical, thus in this case the EEP does not hold. On the other hand, by applying eq.(3.6), which basically expresses the energy equi-distribution among the systems masses, the obtained results are in good agreement with the numerical simulation.

To generalize the obtained results, other numerical simulations were performed on the same structure, varying the subdivision between the subsystems and their densities.

In figure 5 the results obtained for an homogeneous system divided into two subsystems of 500 and 1500 masses, each of them with a value of the mass equal to $5 \cdot 10^{-4}$ kg, are shown. The agreement between the numerical results and the EEP is still very good. If an inhomogeneity is set in the system such that each mass of the first systems is equal to $2 \cdot 10^{-3}$ kg and to $1 \cdot 10^{-4}$ kg for the second one, the results totally change, as displayed in figure 6. In this case, if the EEP was verified, the ratio between the subsystems energies should be 1:3 (like in the homogenous case), this ratio is instead equal to 1,5:1, that is exactly the value obtained by applying eq. (3.6).

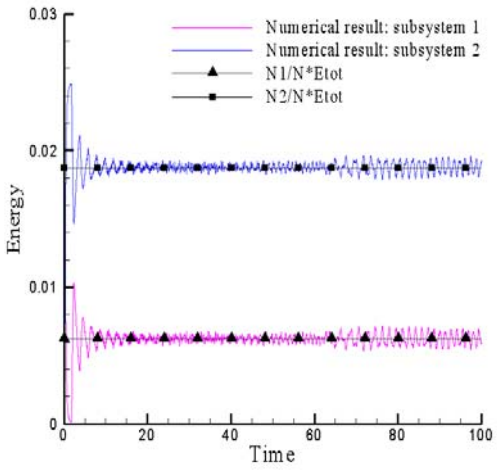

Fig.5

1D Homogeneous rod: test case 2

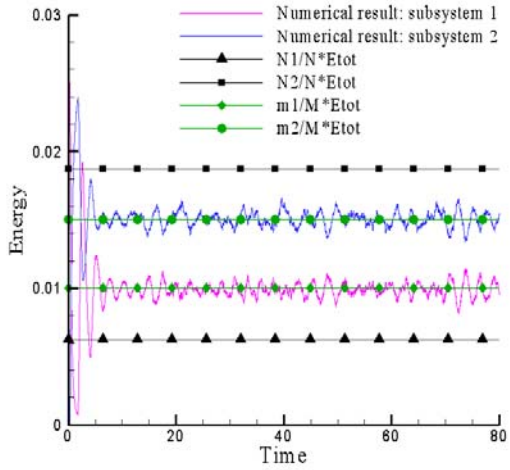

Fig.6

Inhomogeneous rod: test case 2

In figure 7 and 8 a comparison of the global deviation parameters, defined in chapter 3, for the previous homogenous and inhomogeneous cases are presented. In the homogeneous case the global deviation has a general trend characterized by an initial decrease during the period of energy sharing among the substructures, followed by an asymptotic very low value reached in the equilibrium condition, which states the good agreement with the EEP. On the contrary, in the inhomogeneous case the transient is followed by a quite high asymptotic value, which demonstrates the high disagreement

between the numerical result and the EEP.

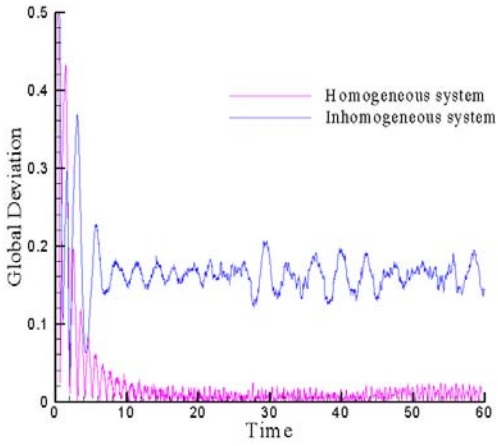

Fig.7

1D: test case 1

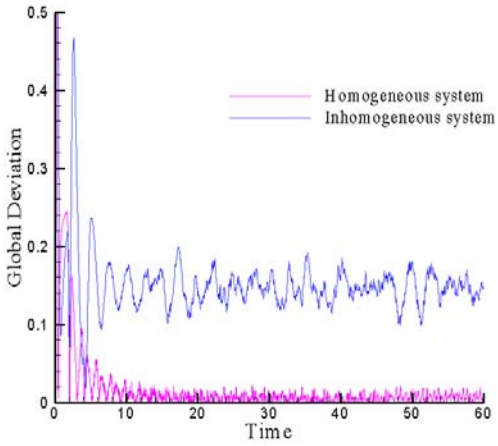

Fig.8

1D: test case 2

The second sets of numerical simulation is performed on a square membrane with a side of length L=1m, a density ρ = 1Kg/m^2 and ideally divided into two systems with different area, see figure 9. Initial conditions are given as follows:

$$\mathbf{u}(\mathbf{x},0) = 0,$$
$$\dot{\mathbf{u}}(\mathbf{x},0) = \delta(\mathbf{x}-\mathbf{x}_0)$$

The dynamical response of the systems is governed by the Poisson's equation:

$$\frac{1}{c^2}\frac{\partial^2 \mathbf{u}(\mathbf{x},t)}{\partial t^2} = \nabla^2 \mathbf{u}(\mathbf{x},t)$$

This equation was numerically solved using a finite different scheme with 1600 degrees of freedom. The investigated model corresponds to a two dimensional lattice composed by masses, each of them with a value equal to $6.06\cdot10^{-4}$ kg, connected through springs with the same stiffness, as shown in figure 10.

In the first case analyzed, the system is divided into two homogeneous subsystems, with 440 and 1160 masses respectively, each of them equal to $6.25\cdot10^{-4}$ kg. In figure 11 the time histories of the subsystem energies are shown and compared with the asymptotic energy values predicted applying the EEP.

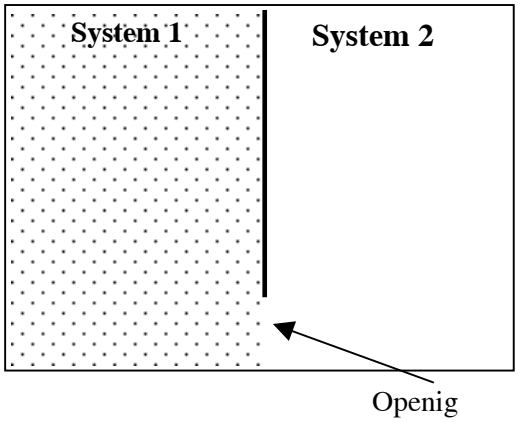

Fig 9

The two-dimensional set up

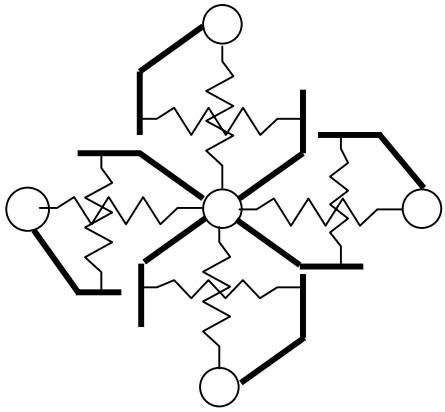

Fig.10

The two-dimensional set up: discretized system

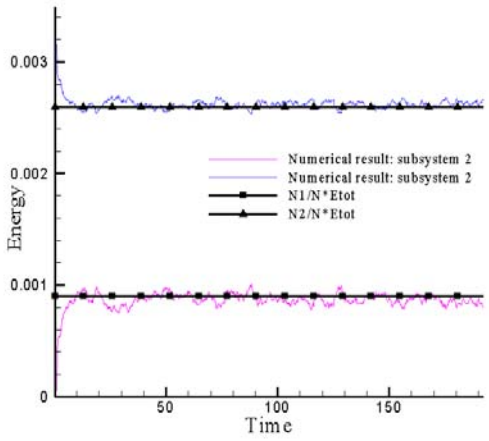

Fig.11

2D: Homogeneous system

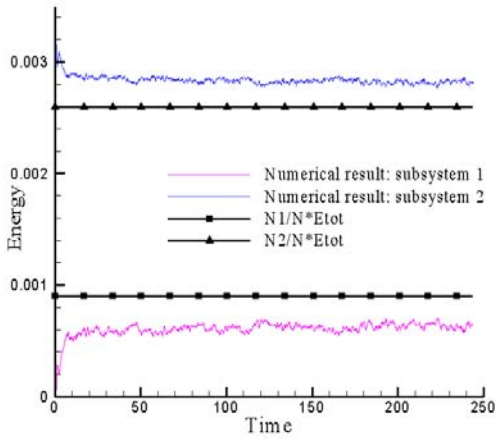

Fig.12

2D:Inhomogeneous system

As already done for the one-dimensional test case, another numerical experiment was performed on the same geometrical 2D system, but now the system is divided into two inhomogeneous systems with different densities. The first system, characterized by a density equal to 2 Kg/m^2 , has 440 masses each equal to $1.25 \cdot 10^{-3}$ Kg, while the second system, characterized by a density equal to 1 Kg/m^2 , has 1160 masses of $6.25 \cdot 10^{-4}$ Kg. In figure 12 the time histories of the subsystems energies are shown and compared with the asymptotic energy values predicted by eq. (3.7). Similar results were obtained for different system configurations and different densities. The time histories of the global deviation parameter are in this case not shown, being its trend for the homogeneous and inhomogeneous case totally similar with the results shown in figures 7 and 8.

The last test case is a three-dimensional cubic acoustic cavity divided into two cavities by a rectangular rigid panel, as shown in figure 13. The side of the panel is shorter than the sides of the box, leaving a rectangular opening between the subsystems. A set of numerical simulations was performed by varying the sound speed of the first subsystem. The volumes of the two cavities are approximately in the ratio 1:2,5. The initial condition is a velocity spike inside the first subsystems(chamber 1 in Fig. 13).

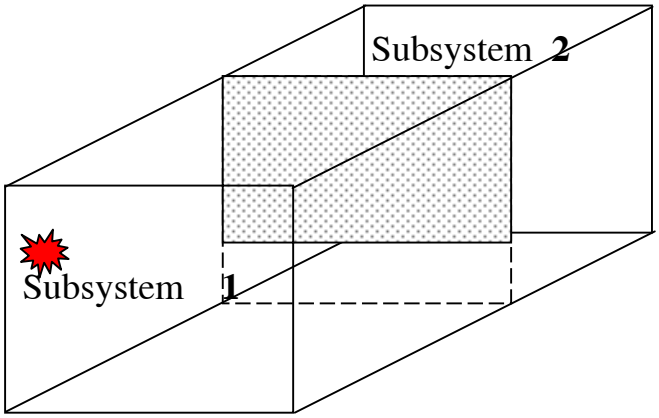

Fig.13

The three-dimensional set up

A finite difference scheme with grid 24 x 24 x 24, corresponding to 13824 degrees of freedom, is used for the numerical solution of the acoustic wave equation. The discretized system corresponds to the coupling of two three-dimensional lattices, divided into two subsystems with 3950 and 9874 masses of mass equal to $7.23 \cdot 10^{-5}$ kg. In figure 14 the energy time histories of the two connected subsystems are displayed, showing a very good agreement with the asymptotic energy distribution given by the EEP. If the speed of sound in the first chamber is set different from the second one, such that each mass is equal to $1.44 \cdot 10^{-4}$ kg and $7.23 \cdot 10^{-4}$ kg respectively, the responses of the two subsystems changes. In figure 15 the time histories of the two subsystem energies are shown. In the same figure the asymptotic equilibrium energies evaluated by equation (3.7) are plotted.

In conclusion the obtained results for these three different setup allow to conclude that the presence of inhomogeneity in the system inhibits the reaching of energy equipartition conditions.

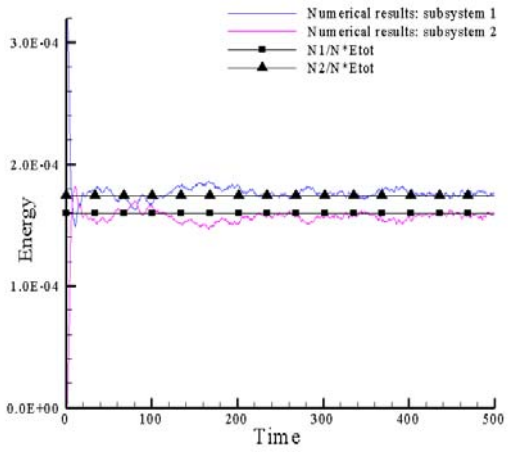

Fig.14

3D: homogeneous acoustic cavity

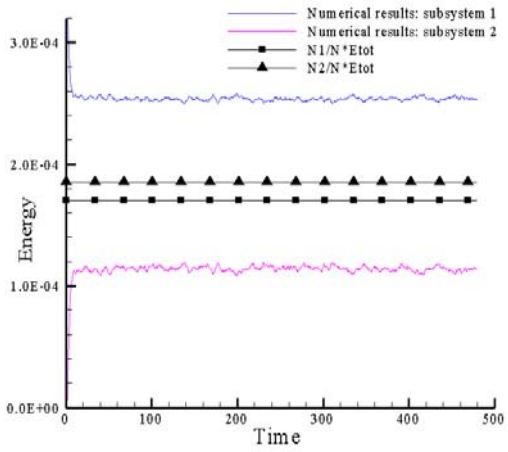

Fig.15

3D: Inhomogeneous acoustic cavity

4.2.2 INITIAL ENERGY DISTRIBUTION

The same three test cases analysed in the previous section are here used to show the influence of the number of modes involved in the process of energy sharing between the subsystems upon the achievement of a condition of energy equipartition. For the first test case, a homogeneous rod (see figure 1), a different initial condition is now considered: the initial displacement of the first system is coincident with its second uncoupled mode is given. The initial conditions are expressed as below:

$$u(x,0)=\begin{cases}\sin\left(\dfrac{2\pi x}{L_1}\right) & x<x_1\\ 0 & x>x_1\end{cases}$$

$$\dot{u}(x,0)=0$$

where x_1 is the coordinate corresponding to the separation between the two subsystems and L_1 is the length of the first subsystem.

The simulations are performed using the same model and with the same finite different scheme described in the previous paragraph, allowing a direct comparison of the energy time histories of the three different test cases for the two set of initial conditions. In figures 16 and 17 the time histories of the system energies are shown and compared with the theoretical results obtained by applying eq.(3.7) for the two different initial conditions.

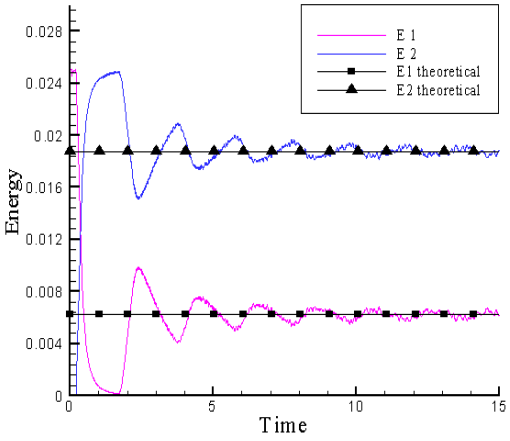

Fig.16

1D: velocity spike

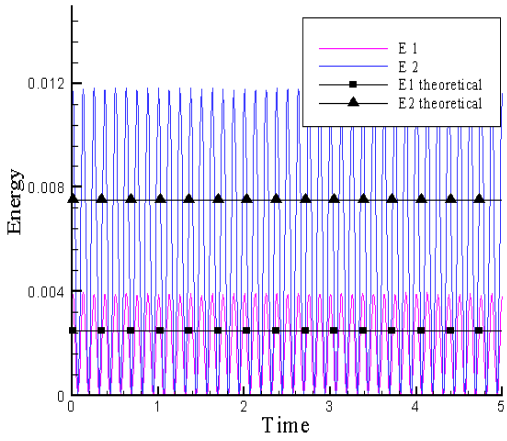

Fig.17

1D: local mode

The same type of initial conditions (*i.e.* an initial displacement of the fisrt subsystem coinciding with its second uncoupled mode) is also analysed in the two- and three-dimensional test cases (see figures 18 and 19). The results confirm the strong dependency on the initial conditions of the energy distribution between the subsystems. In fact, in both cases the time histories of the energy subsystems are far from being well represented by the asymptotic energy values obtained applying the energy distribution law expressed in eq.(3.7).

It is evident that if the initial condition is a velocity spike (figures 5, 11 and 14), except for a short transient, the agreement between the numerical and the theoretical results is fairly good. On the contrary, if the initial condition approaches a local mode (figures 17, 18 and 19), the dynamics of the systems are not caught by eq.(3.7), being also difficult to define an equilibrium condition for the subsystem energies. In fact, even if the level of the oscillations around the mean values become smaller when increasing the connectivity degree of the system, it still remains large enough not to allow a complete definition of the system with only an asymptotic value.

Thus, the need to introduce another parameter that provides the amplitude of the oscillations is evident.

In figures 20, 21 and 22 a comparison of the global deviation parameters obtained for the two different couple of initial conditions for a one-, two- and three-dimensional systems are shown. In all of those figures it is evident that the deviation from the EEP is much smaller when the initial condition is a velocity spike rather than the local mode.

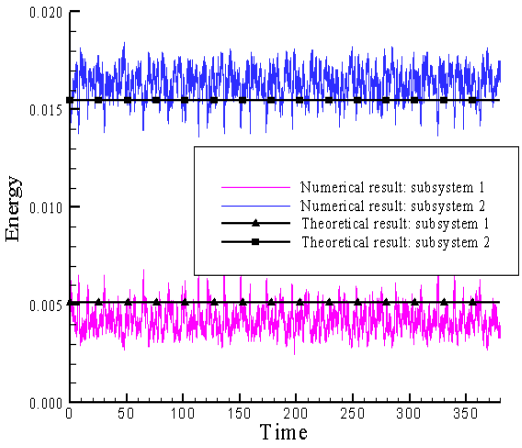

Fig.18

Two-dimensional test case

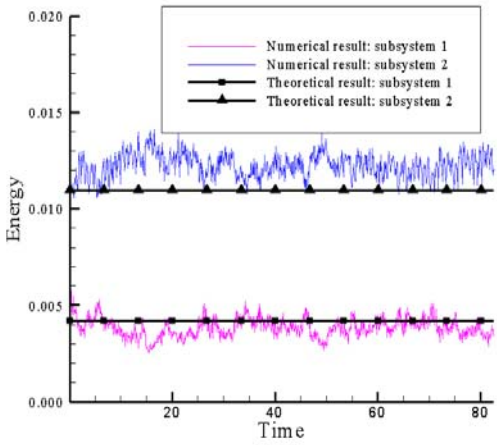

Fig.19

Three-dimensional test case

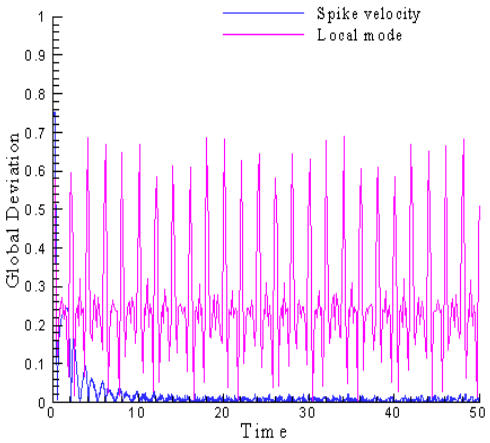

Fig.20

One-dimensional system

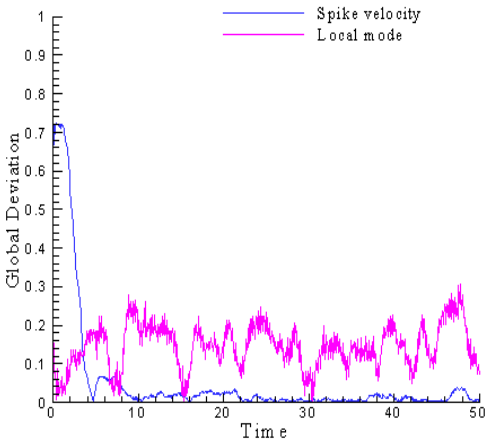

Fig.21

Two-dimensional system

In figure 23 a comparison of the global deviation parameter for the three test cases under analysis is shown. Passing from the one-dimensional test case to the three-dimensional one, a high decrease of this parameter is evident, implying a decrease of the deviation of the energy distribution from the EEP. In fact, while for the rod the deviation from the EEP varies from 10% up to 60% with a mean value of 25 %, in the case of an acoustic cavity the deviation is approximately equal to 6 %. Moreover, increasing the dimensionality of the of the system under analysis a decrease of the fluctuations around the mean value is also evident; this means that an equilibrium condition, different from that stated by EEP, is achieved.

It is also interesting to analyse the energy distribution among each degree of freedom (i) of the system and its time evolution. In figures 24 and 25 the time histories of the normalized energy distributions (defined in section 3.5) among the degrees of freedom for the two different initial conditions (the spike velocity and the local mode, respectively) are shown for the mono-dimensional system. If the EEP holds in this case, the value of the normalized energy should be equal to 1. When the initial condition is a velocity spike it is evident (see figure 24) that after the first instants ($t > 6$ sec), when the energy, initially stored in only one Dof, is basically convected along the rod, a tendency to obtain an uniform distribution can be observed. This condition of equal energy distribution among the modes demonstrates the presence of a diffusive condition, where the EEP is valid. On the contrary, as shown in figure 25, if the initial condition coincides with a local mode of the structure, the EEP does not hold, being the energy distribution periodical changing with the time. This can be seen also in figures 26, where a comparison of the time histories of the normalized energies at different points of the rod for the spike velocity excitation are presented, while in figure 27 the same quantities for the local mode are shown. While in the first case it is evident a tendency to a energy equipartition among the degrees of freedom, in the second case the energetic response of each degree of freedom is oscillating around a mean value different from that foreseen by EEP.

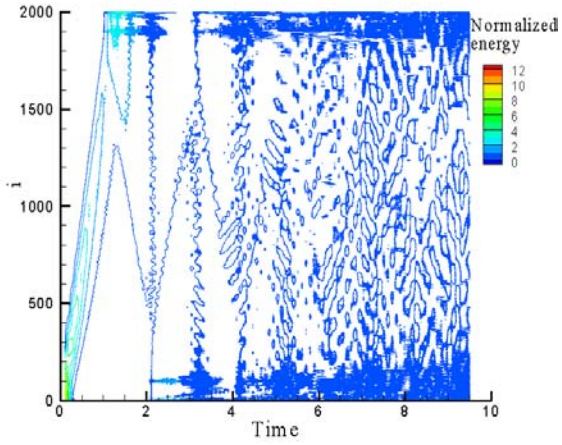

Fig.24

1D: spike velocity

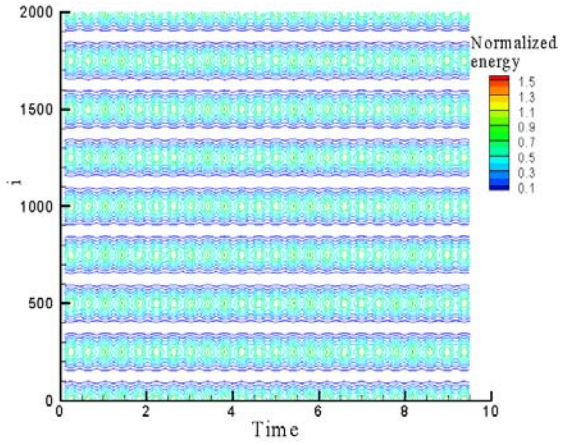

Fig.25

1D: local mode

In conclusion, an investigation to verify the dependencies on the initial condition in reaching the EEP was performed. The results show that the energy distribution between the subsystems is strongly dependent on the initial energy distribution among the degrees

of freedom. This fact is related with the orthogonal properties of the natural modes of the system. In fact, for a linear system, since the modes are decoupled and energy independent, only those which are initially excited with the initial conditions take part to the process of energy sharing. Hence, unless the initial conditions excite all the modes or degrees of freedom, like a velocity spike, it is not possible to obtain an equipartition of the energy among the degrees of freedom.

4.2.3 NON-LINEARITY IN THE CONSTITUTIVE RELATIONSHIPS

It seems reasonable to expect that the introduction of a nonlinearity in the elastic constitutive relationship of the system under analysis, which effect is to couple its modes, can affect the asymptotic values in the process of energy sharing.

Although the effects introduced by nonlinearities in the system dynamical behavior have been deeply investigated by physicists in the last century, a satisfactory understanding of the generic properties of a non linear systems and its effect on the reaching the EEP is still lacking. It is not the aim of this work to provide a detailed historical survey of the efforts made to understand the EEP in non linear systems, which can be found *e.g.* in Ford (1961): nevertheless in what follows a brief description of those results that are relevant for the analyzed problem, *i.e.* the lack of validity of the EEP, are presented.

The numerical experiment made by Fermi Pasta Ulam in 1940 (FPU) (Fermi et al., 1965) represents the first attempt to check the validity of the prediction of classical Statistical Mechanics concerning the dynamics of a Hamiltonian system of coupled oscillators with a large number of degrees of freedom. In this work the authors analysed the energy distribution in a long anharmonic chain composed by masses connected through non linear springs, where the energy is initially stored in a low frequency mode. If q_i and p_i are the coordinates and the momenta of the oscillators respectively, the model is defined by the following Hamiltonian:

$$H = \sum_{i=1}^{N} \frac{p_i^2}{2} + \sum_{i=1}^{N} \left[\frac{1}{2}(q_{i+1} - q_i)^2 + \frac{\beta}{3}(q_{i+1} - q_i)^3 \right] \tag{4.1}$$

Before the definition of the Kolmogorov-Arnold-Moser (KAM) (Arnlod et Avez, 1968) theorem, it was generally assumed that energy redistribution through nonlinear couplings would bring a nonintegrable system to a condition of approximate equipartition. The FPU experiment was intended to show such scenario. On the contrary, the expected

relaxation to equipartition of energy among the normal modes of the system was not achieved during the time of observation. After an initial increase of the energy in the neighbouring modes as expected, they observed that the energy sharing was restricted only to the first modes with a quite regular dynamics, rather than demonstrating a gradual and continuous energy flow from the first excited mode to the higher ones and a stochastic dynamics. Even more surprisingly, at farther times almost all the energy has gone back into the initially excited mode, so that the system showed quasi-periodicity properties which were later explained in terms of beating among the system modes (Ford, 1961).

This paper proved for the first time that ergodicity, which is a basic hypothesis in SM, is not an obvious consequence of the non existence of analytical first integrals of the motion. This implies that a weak nonlinearity could be not sufficient to lead a Hamiltonian system to equipartition of the energy among the degrees of freedom.

The explanation of this different dynamical behaviour was already furnished in the KAM theorem, enunciated few years before in 1954 but ignored by Fermi. The Kolmogorov-Arnold-Moser theorem shows that energy redistribution does not always occur in nonintegrable systems, like a nonlinear Hamiltonian system. Redistribution is only possible when the nonintegrable part of the Hamiltonian (the non linear one) is sufficiently large. Once the perturbation ε is fixed, the energy density assumes a relevant importance, being the parameter that controls the energy distribution. In fact, for energy level lower than a critical value E_c, that depends on the number of degrees of freedom, the system behaviour is similar to the linear case (which implies the lack of equi-distribution of the energy), due to the presence of survived invariant torus in the equal energy iper-surface in the phase space. Beyond this critical value the energy is instead uniformly distributed among the modes according to Statistical Mechanics, since great part of KAM tori are destroyed. Starting from these results, Izrailev and Chirikov (Chirikov et al. 1973) proved later with numerical experiments that at sufficiently high energy, when the KAM theorem cannot be applied, the FPU model relaxes to the equipartition state on times which become smaller and smaller as the energy is increased. Although more than 50 years passed since the first formulation of the FPU experiment, the problem is still the subject of numerous publications(Livi et al., 1995; Kato and Jou, 2001; Benettin 2005).

Several problems are still opened: the presence of the Chaotic breather (Cretegny et al., 1998), the dependency of the minimum energy value from the number of degrees of freedom, the initial conditions effects, etc.

The great difficulties of the topic and the non complete understanding of this phenomena suggested the use of numerical simulations to investigate the effects on energy distribution of the presence of non-linear term in the constitutive relationship of the system. The setups are the same described in a previous paragraph.

The first set of numerical simulation were performed on the one dimensional system, a nonlinear relationship is introduced in the elastic constitutive relationship, namely by a hardening effect $\sigma = E\varepsilon + \gamma\varepsilon^3$, where σ and ε are stress and deformation tensor, respectively and γ a suitable material coefficient equal to $3 \cdot 10^{-3}$ Nm^2. A second order semi-implicit Runge Kutta algorithm was used for the numerical integration. The systems are indeed identical for any other respects. A local mode deformation is given to the system as initial condition. Except for the transient, the dynamical behaviour of the linear and the non linear systems are totally different: in the former the energies of the two subsystems do not reach any asymptotic value (see figure 28), but they continues to oscillate around their mean values. In the second case the energies achieve instead their asymptotic values, which coincide with the results obtained by applying the EEP, reducing rapidly their oscillations around their mean value as shown in figure 29. The same kind of analyses were performed on the other two setup, the 2 and 3 dimensional systems, leading to the same conclusions (see figures 30,31,32 and 33).

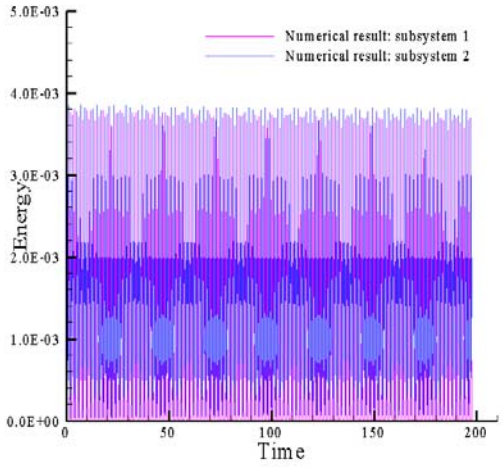

Fig.28

1D: linear system

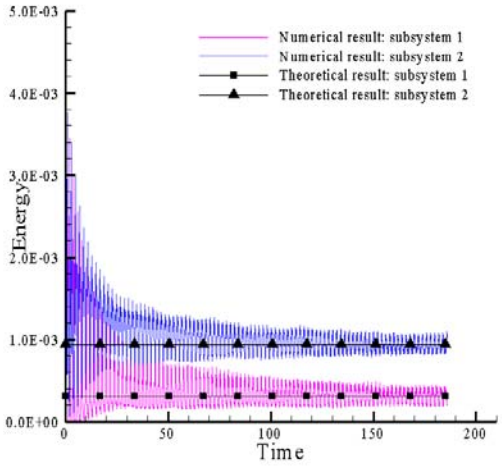

Fig.29

1D: non linear system

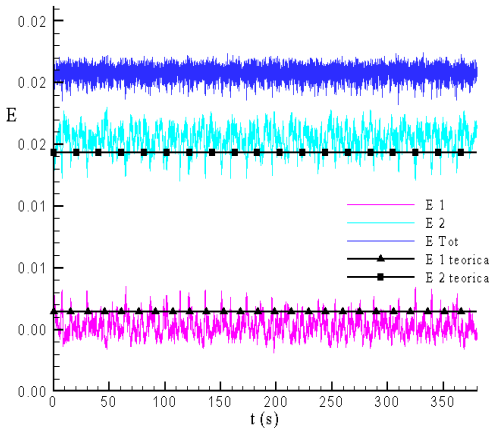

Fig.30

2D: linear system

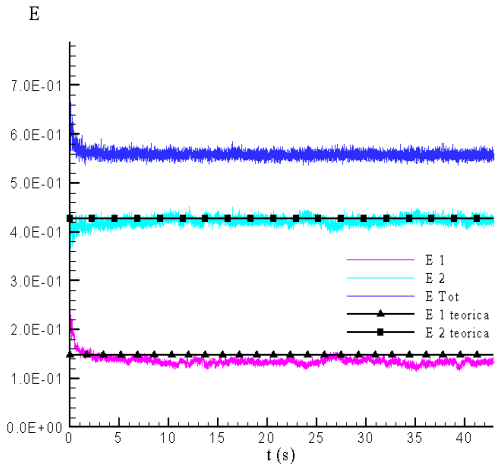

Fig.31

2D: non linear system

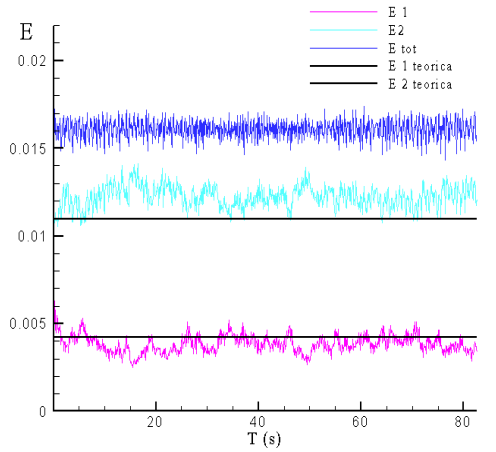

Fig.32

3D: linear system

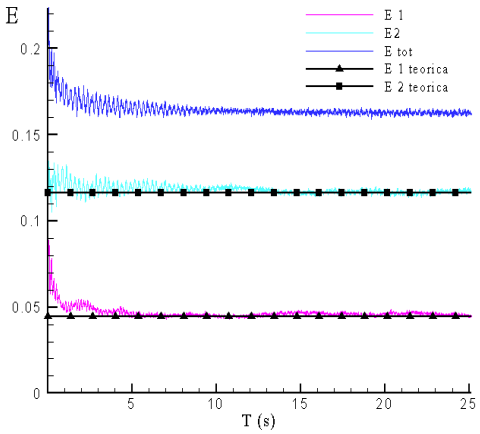

Fig.33

3D: non linear system

In figure 34 a comparison of the global deviation parameter of the energy fluctuations with respect to the EEP for the linear and nonlinear rods is shown.

Except for the transient, the two systems show totally different behaviours. In fact, while for the linear system the global deviation continues to oscillate around high value, for the nonlinear system both its amplitude and fluctuations decrease rapidly with the time. Similar results were obtained analysing the plate and the acoustic cavity.

It is now interesting to make an analysis of the dependencies of the energy distribution among the modes or degrees of freedom from the dimension of the nonlinear parameter.

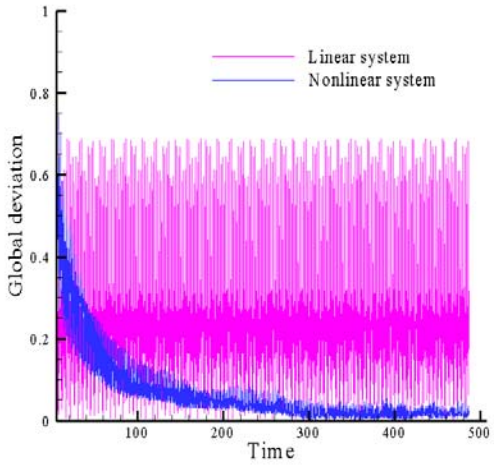

Fig.34

1D: Global deviation

Except for the transient, the two systems show totally different behaviours. In fact, while for the linear system the global deviation continues to oscillate around high value, for the nonlinear system both its amplitude and fluctuations decrease rapidly with the time. Similar results were obtained analysing the plate and the acoustic cavity.

It is now interesting to make an analysis of the dependencies of the energy distribution among the modes or degrees of freedom from the dimension of the nonlinear parameter.

Chirikov et al. (1973), by applying the nonlinear resonance theory, predicted the existence of a KAM tori, and the chaotic dynamics, which implies the reaching of an equilibrium condition similar to the one stated in statistical thermodynamic. For this reason a set of numerical simulations were performed on the one dimensional test case, varying the value of γ. The global and local deviation parameters were evaluated for different values of the nonlinearity, the obtained results are displayed in figure 35 .

It is possible to distinguish three different behaviours in the dynamical responses of the system: for low values of the nonlinear parameter the deviation from the EEP is quite high and independent on the value assumed by γ. This means that the trajectories in the phase space are quite regular, no energy equipartition is achieved, and the system behaves as a linear Hamiltonian system.

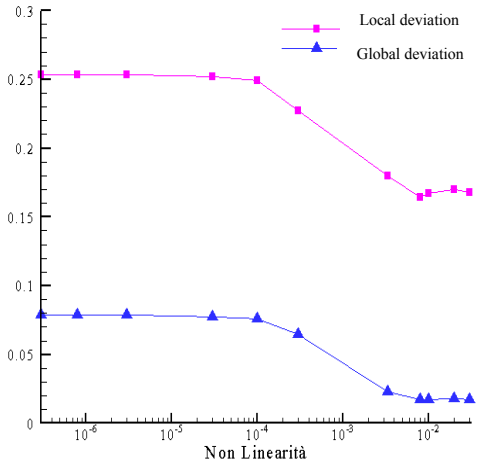

Fig. 35

1D: local and global deviation as a function of the nonlinear parameter

This is true until a critical value is reached where the deviation between the numerical results and the EEP is depends almost linearly on this parameter. This is due to an increasing destruction of the KAM tori with a tendency on a chaotic region in the phase space. It is also possible to define another critical value of γ; beyond this value the system dynamic does not change increasing the nonlinearity. This means that all the Kam tori have been already destroyed, and the motion of the system can be described using the equilibrium theory stated in Statistical Mechanics.

Conversely, as it is more natural, for a fixed γ, the increasing departure from the harmonic behaviour is controlled by increasing the energy initially stored in the system.

4.2.4 DEGREE OF COUPLING BETWEEN SUBSYSTEMS

A fundamental assumption in Statistical Mechanics is that the coupling among the subsystems is "weak", *i.e.* in Khinchin's terminology the system must verify the "*decomposability principle*" (Khinchin, 1949). This assumption derives from the hypothesis that the components S_i of a system S are stochastically independent and that the phase function f of S may be written as the sum of individual functions f_i, as in the following expression

$$f = \sum_{i=1}^{N} f_i$$

where N is the number of components. In this way the possibility of any energetic interaction between the subsystems is excluded. Since the Hamiltonian function, which basically expresses the energy of the system, is a sum of functions each depending only on the dynamical coordinates of a single component, then the whole system equations are split into component systems each describing the motion of some separable component and it is not connected in any way with other components. In other words, the energy of a system is just the sum of the energy of the substructures that compos the system; consequently, the energy associated to the interaction forces is negligible with respect to the energy stored in each subsystem.

This paradox can be easily understood by analyzing a thermodynamic system where the whole idea is to provide a treatment of heat as a form of energy, and the transfer of heat is achieved only by some form of intermolecular interaction.

In classical mechanics is also possible to verify that this assumption is often not satisfied. A typical example used to show that is the system composed by two masses connected through a linear spring (figure 36)

If the system is divided in two subsystem S_1 and S_2, characterized by the energies E_1 and E_2 respectively, the energy of the whole system is given by the following expression:

$$E_{Tot} = E_1(\mathbf{x}_1) + E_2(\mathbf{x}_2) + E_{12}(\mathbf{x}_1, \mathbf{x}_2) \tag{4.2}$$

where E_{12} is the energy associated with the interaction force.

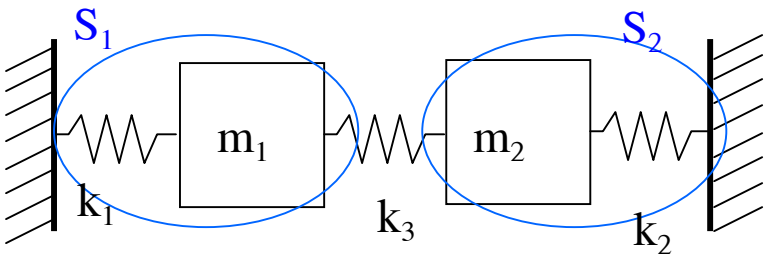

Fig.36

2DOF system

In order to avoid this difficulty it is necessary to consider that the substructures are not totally separated but they interact, exchanging energy in very small quantity with respect to the total energy of the system. If the structures verify this property, namely they are "weak coupled" in a SM sense, the dynamic correlation that arises from their interaction are rapidly lost. Moreover as the number of degrees of freedom increase, as was

demonstrated in Khinchin (1949), the dynamical correlation between the subcomponents tends to zero.

As shown in the previous chapter, in the TAEA method a basic assumption is that the total energy of the whole system is just the sum of the partial energies of the subsystems, *i.e.* the energy associated to the interaction forces is negligible with respect to the energy stored in each subsystem.

This is something different with respect to the "weak coupling" condition states in Statistical Energy Analysis. It is interesting to notice that also the SEA equations are based upon the hypothesis that the energy of the whole system can be written as the sum of the energy of each subsystems (DeRosa et al., 1999). Moreover, taking into account the different nature of the system analysed in SM and SEA, this last needs to introduce other hypothesis upon the coupling. In SEA different ways are used to verify if the coupling among the substructures can be considered weak. Among the others the "Smith criterion" (Smith, 1979) provides the simplest expression, which related the coupling loss factor η_{12} with the damping η_1. It states that the coupling among two substructures can be considered weak if $\frac{\eta_{12}}{\eta_1} << 1$.

A set of numerical simulation were performed to better understand the dependency of the EEP from the strength of the coupling between the subsystems. The investigated model corresponds to a two-dimensional lattice composed by masses, divided in two different subsystems with different densities (see figure 37). The dynamical response of the systems is governed by the Poisson's equation:

$$\frac{1}{c^2}\frac{\partial^2 \mathbf{u}(\mathbf{x},t)}{\partial t^2} = \nabla^2 \mathbf{u}(\mathbf{x},t)$$

The dimension of the second subsystem was changed in order to vary the ratio between the energy stored in the subsystems and the energy stored in the coupling between the systems.

The first step is the definition of a degree of coupling η as the ratio between the energy stored in the coupling and the lowest energies of the two subsystems.

$$\eta = \frac{E_{junction}}{\min\{E_1, E_2\}}.$$

The definition of this parameter allows to obtain a new criteria for the identification of the coupling strength:

for $\eta << 1$ the coupling is weak

for $\eta \cong 1 \quad or \, \eta > 1$ the coupling is strong

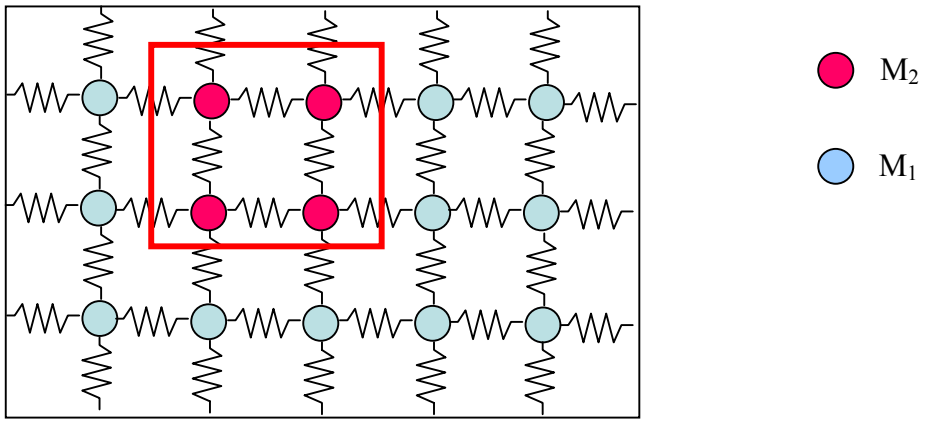

Fig.37

Two-dimensional lattice

If the EEP hold the degree of coupling is only dependent on the geometrical parameter of the partition. Two different set of simulations were performed for a homogeneous and an inhomogeneous systems. The results obtained are shown in figure 38 and 39 and compared with the one deduced from the EEP. In the abscissa there is the number of junction between the two subsystems, while in the ordinate the value of the degree of coupling is presented. It is evident that for a low level of η (basically obtained when the two subsystems have the same area for the homogeneous test case) the EEP and the numerical results are in good agreement, but as soon as the coupling become stronger the numerical curve deviates from the theoretical one.

The symmetry that characterizes the homogeneous case is lost when an nonhomogeneity is introduced in the system.

This analysis confirms the key role assumed by the strength of the weak coupling upon the achievement of the EEP. Without this assumption, as already shown by Khinchin, all the most important results obtained in SM cannot be reached.

The above consideration together with the actual interest to overcome the same problem in SEA, has led attempting to improve the TEAE method in order to include the case of strong coupling.

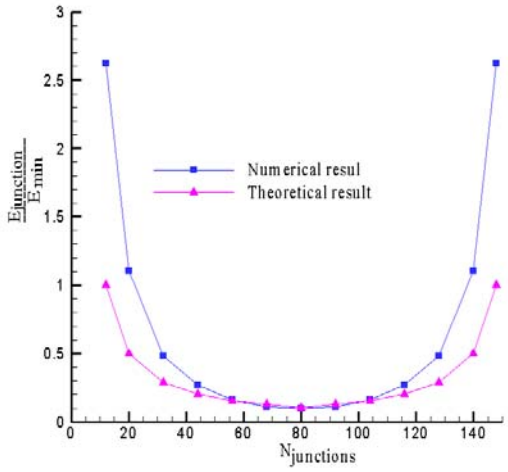

Fig.38

Homogeneous system

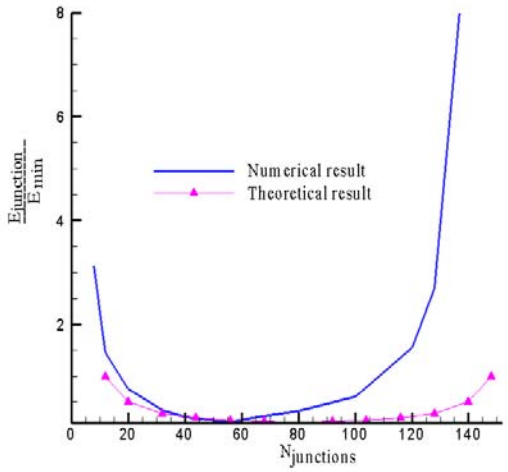

Fig.39

Nonhomogenous system

4.2.5 NUMBER OF DEGREES OF FREEDOM

In a previous paragraph it was shown that for a nonlinear Hamiltonian system, at a fixed value of the nonlinear coupling coefficient γ, there is a critical energy E_c such that below E_c a lack of energy equipartition is observed due to the presence of ordered orbits in the phase space. On the contrary, for energy values larger than E_c, the trajectories are dominated by a chaotic motion, implying the achievement of an energy distribution defined by the EEP.

Great efforts were done to understand better the behaviour of a nonlinear Hamiltonian systems with a small number of degrees of freedom, trying to demonstrate the obtained results through the KAM theorem. There are not so many papers indeed regarding the reaching of a chaotic motion or ordered motion in the thermodynamic limit $N \to \infty$. In Livi et al. (1985) an interesting study of the energy distribution in nonlinear large Hamiltonian system is presented. In particular the authors focalized their attention on the critical energy E_c and its dependencies on the number of degrees of freedom. The analyzed system is a nonlinear one-dimensional system, where not only the number of the masses which composed the system is varied, but also the initial conditions are changed in order to maintain the ratio between the number of degrees of freedom and the

number of the initially excited modes. The results show that the E_c does not change significantly with increasing *N*.

Different results were obtained in De Luca et al. (1999) where above the critical energy the system is found to reach a near-equipartition state in a time proportional to N^2; below this critical energy, the time needed to reach the equilibrium increases even faster with *N* (the author suggests an exponential increase). This holds when the initial energy is given to a subset of low modes whose number do not increase with N. If the excited modes are indeed a subset proportionally to N, the typical time scale to reach quasi equipartition increases like N.

Another interesting aspect to analyze is provided by Khinchin, who affirmed that considering a phase function f, defined as a sum of the corresponding phase functions f_i for each of the components N of the system, i.e.

$$f = \sum_{i=1}^{N} f_i$$

The dispersion of this parameter is of the order of N. This means that the single trajectory size of the energy, which is a sum-function, is linked to the number of degrees of freedom.

In (Carcaterra, 2005), a general argument to derive the dispersion of the energy samples around the mean value is provided for stationary conditions. The obtained expression

$$\frac{\sqrt{\overline{\left(E^{(1)} - \overline{E}^{(1)}\right)^2}}}{\overline{E}^{(1)}} \propto \frac{1}{\sqrt{N^{(1)}}}, \qquad \frac{\sqrt{\overline{\left(E^{(2)} - \overline{E}^{(2)}\right)^2}}}{\overline{E}^{(2)}} \propto \frac{1}{\sqrt{N^{(2)}}} \tag{4.3}$$

shows that the dispersion around the mean value is sensitive to the number of modes *N*, *i.e.* to the complexity of the system. In fact, for *N* large, a small deviation with respect to the ensemble average is expected. This result is referred to stationary conditions, but it is reasonable that this property, at least qualitatively, holds over the whole time axis, including the transient.

As additional result eq (4.3) also allows to affirm that if the system has a large number of modes or degrees of freedom, *i.e.* it is complex, the ensemble average is a rather good representation of the energy behaviour of each sample of the population.

CHAPTER 5: THE TIME ASYMPTOTIC ENSEMBLE ENERGY AVERAGE OF NON-STATIONARY VIBRATIONS (TAEA): STRONG COUPLING OF TWO OR MORE SUBSYSTEMS

In this chapter the results obtained in the attempt to overcome some limitations of the TAEA method, that were pointed out in chapter 3, are presented.

Among the list of assumptions necessary to evaluate the energy distribution between two complex coupled resonators itemized in section 3.1, it has already shown in section 3.4 the possibility to extend the method also for a non conservative system, so that the first assumption can be overcome.

In the following sections the TAEA theory is expanded to include i) an arbitrary strong coupling between the substructures ii) the interaction among more than two subsystems.

The considerations that have led to expand the TAEA theory in these directions are related with the need to obtain a theory that could be easily applied to a real structure, that is usually composed by more than two components and their interaction forces cannot be usually neglected. In the first part of this chapter a theoretical analysis of the energy related to the coupling is presented, followed by a modification of the TAEA method to include arbitrary strong coupling. The validation of this new TAEA formulation is obtained using both numerical simulations (in this chapter) and experimental measurements (in the following chapter).

In the second part of this chapter, the theory is extended to include also the case of coupling among more than two subsystems. Also in this case some numerical simulations and experimental measurements allow to verify the effectiveness of the changes performed.

5.1 THE NATURE OF THE COUPLING

In chapter 3 the ensemble energy average distribution between two substructures is evaluated in the hypothesis that their coupling is “weak”. It has also underlined that the

meaning of this hypothesis is something different with respect to the "weak coupling" condition stated in Statistical Energy Analysis. In fact, in TAEA the "weak coupling" hypothesis means that the energy associated to the interaction forces among the subsystems is considered negligible with respect to the energy stored in each subsystem. This concept reminds of Khinchin's "*principle of decomposability"*, expressed in the frame of Statistical Mechanics.

The key role assumed by the interaction forces in the energy repartition among subsystems in steady state was already studied in section 4.2.4. Numerical experiments performed upon a two dimensional system demonstrate the strong dependence of the energy distribution on the strength of the coupling, such that for weak coupling the system behaviour in steady state can be characterized by means of the EEP, for stronger value of the coupling the solution diverges from the EEP, instead.

This lack of knowledge of the system behaviour at strong coupling, as well as the interest to render the method applicable to a real structure, lead to modify the TAEA method in order to include arbitrary strong coupling firstly.

In the development of TAEA the hypothesis of weak coupling is introduced in the evaluation of the subsystem energies when the term due to the motion of the other subsystem is neglected, *i.e.* the energy of each subsystem is evaluated in the hypothesis that the other subsystem is blocked.

A theoretical analysis of the energy related with the coupling in a discretized system is here presented, followed by a modification of the TAEA method to include arbitrary strong coupling.

The dynamical behaviour of a discretized multiple degree of freedom (N) mechanical system can be described by the following governing equation in matrix form:

$$[M]\{\ddot{\mathbf{x}}\}+[K]\{\mathbf{x}\}=0 \tag{5.1}$$

where M and K are the $N\times N$ dimensional mass and stiffness matrices respectively, and x is the N-dimensional vector of space coordinates. Introducing the orthonormal modes Φ and the Lagrangean coordinates q, such that: $x=q\Phi$ and substituting in (5.1), the equation of motion of the system becomes:

$$M\Phi\ddot{q}+K\Phi q=0\,. \tag{5.2}$$

It is easy to demonstrate that the energy of the whole system, obtained as a sum of the kinetic and potential terms, can be expressed as follows:

$$E^{Tot}(t)=\frac{1}{2}\sum_{i=1}^{N}\sum_{j=1}^{N}\alpha_{ij}\dot{q}_i\dot{q}_j+\frac{1}{2}\sum_{i=1}^{N}\sum_{j=1}^{N}\beta_{ij}q_iq_j \tag{5.3}$$

where

$$\alpha_{ij} = \mathbf{\Phi}^T M \mathbf{\Phi}$$

$$\beta_{ij} = \mathbf{\Phi}^T K \mathbf{\Phi}$$

It is customary to orthonormalize the mode shape, namely:

$$\Phi_i^T M \Phi_i = I \quad \text{and} \quad \Phi_i^T K \Phi_i = \omega_i^2 I$$

where I is the identity matrix and ω_i is the *i*-th natural frequency.

If the whole system is divided into two sets of oscillators S_1 and S_2, the vector of displacement $\mathbf{w}$ of the whole system can be also partitioned into two sub-vectors $\mathbf{w}_1$ and $\mathbf{w}_2$, such that $\mathbf{w} = [\mathbf{w_1}, \mathbf{w_2}]$. Similarly the mass and stiffness matrices and the *i*-th eigenvector matrices can be partitioned as follows:

$$M = \begin{bmatrix} M_{11} & M_{12} \\ M_{21} & M_{22} \end{bmatrix} \quad K = \begin{bmatrix} K_{11} & K_{12} \\ K_{21} & K_{22} \end{bmatrix} \quad \Phi_i = \begin{Bmatrix} \mathbf{\Phi}_i^{(1)} \\ \mathbf{\Phi}_i^{(2)} \end{Bmatrix} \tag{5.4}$$

Introducing the partitioning stated in (5.4) in expression (5.3), the expression of the energy of the whole system assumes the following form:

$$\begin{aligned} E^{Tot}(t) = & \sum_{i=1}^{N}\sum_{j=1}^{N} \begin{bmatrix} \Phi^{(1)T} & \Phi^{(2)T} \end{bmatrix} \begin{bmatrix} M_{11} & M_{12} \\ M_{21} & M_{22} \end{bmatrix} \begin{bmatrix} \Phi^{(1)} \\ \Phi^{(2)} \end{bmatrix} \dot{q}_i \, \dot{q}_j + \\ & \sum_{i=1}^{N}\sum_{j=1}^{N} \begin{bmatrix} \Phi^{(1)T} & \Phi^{(2)T} \end{bmatrix} \begin{bmatrix} K_{11} & K_{12} \\ K_{21} & K_{22} \end{bmatrix} \begin{bmatrix} \Phi^{(1)} \\ \Phi^{(2)} \end{bmatrix} q_i \, q_j = 0 \end{aligned} \tag{5.5}$$

The α and β matrices can also be partitioned as:

$$\begin{aligned} \alpha_{ij} &= \Phi^T M \Phi = \alpha_{ij}^{(1)} + \alpha_{ij}^{(2)} + \alpha_{ij}^{(12)} + \alpha_{ij}^{(21)} \\ \beta_{ij} &= \Phi^T K \Phi = \beta_{ij}^{(1)} + \beta_{ij}^{(2)} + \beta_{ij}^{(12)} + \beta_{ij}^{(21)} \end{aligned} \tag{5.6}$$

where $\alpha^{(r)} = \Phi^{(r)T} M_{rr} \Phi^{(r)}$ and $\beta^{(r)} = \Phi^{(r)T} K_{rr} \Phi^{(r)}$ while $\alpha^{(rs)} = \Phi^{(r)T} M_{rs} \Phi^{(s)}$ and $\beta^{(rs)} = \Phi^{(r)T} K_{rs} \Phi^{(s)}$ with $r, s = 1, 2$

Introducing the last expression, eq.(5.5) can finally be written as:

$$\begin{aligned} E^{Tot}(t) = & \sum_{i=1}^{N}\sum_{j=1}^{N} \left(\Phi^{(1)} M_{11} \Phi^{(1)} + \Phi^{(2)} M_{21} \Phi^{(1)} + \Phi^{(1)} M_{12} \Phi^{(2)} + \Phi^{(2)} M_{22} \Phi^{(2)} \right) \dot{q}_i \dot{q}_j + \\ & \sum_{i=1}^{N}\sum_{j=1}^{N} \left(\Phi^{(1)} K_{11} \Phi^{(1)} + \Phi^{(2)} K_{21} \Phi^{(1)} + \Phi^{(1)} K_{12} \Phi^{(2)} + \Phi^{(2)} K_{22} \Phi^{(2)} \right) q_i q_j \end{aligned}$$

Assembling the kinetic and potential term of the same substructure, the energy of the whole system is given by:

$$E^{Tot}(t) = E^{(1)}(t) + E^{(2)}(t) + E^{(12)}(t) + E^{(21)}(t) \tag{5.7}$$

where

$$E^{(r)}(t) = \frac{1}{2}\sum_{i=1}^{N}\sum_{j=1}^{N}\alpha_{ij}^{(r)}\dot{q}_i\dot{q}_j + \frac{1}{2}\sum_{i=1}^{N}\sum_{j=1}^{N}\beta_{ij}^{(r)}q_i q_j \tag{5.8}$$

$$E^{(rs)}(t) = \frac{1}{2}\sum_{i=1}^{N}\sum_{j=1}^{N}\alpha_{ij}^{(rs)}\dot{q}_i\dot{q}_j + \frac{1}{2}\sum_{i=1}^{N}\sum_{j=1}^{N}\beta_{ij}^{(rs)}q_i q_j \quad \text{with } r,s = 1,2 \tag{5.9}$$

The terms in eq.(5.7) have different physical meanings:

- $E^{(r)}(t)$ represents the sum of the kinetic and the potential energy terms of the *r*-th subsystem when the *s*-th subsystem is considered blocked.
- $E^{(rs)}(t)$ is the sum of the kinetic and the potential energy terms of the *r*-th subsystem due to the motion of the *s*-th subsystem.

In the hypothesis of weak coupling the energies $E^{(rs)}(t)$ and $E^{(sr)}(t)$ are negligible with respect to the energies $E^{(r)}(t)$ and $E^{(s)}(t)$. Considering the expression of the mixed energy terms (eq. 5.9), this condition is reached when:

$$\begin{aligned} \alpha_{rs} &= \frac{1}{2}\Phi_i^{(r)T} M_{rs} \Phi_j^{(s)} \quad << \quad \alpha_{rr} = \frac{1}{2}\Phi_i^{(r)T} M_{rs} \Phi_j^{(r)} \\ \beta_{rs} &= \frac{1}{2}\Phi_i^{(r)T} K_{rs} \Phi_j^{(s)} \quad << \quad \beta_{rr} = \frac{1}{2}\Phi_i^{(r)T} K_{rr} \Phi_j^{(r)} \end{aligned} \tag{5.10}$$

Before starting with the determination of the energy terms due to the coupling, a trivial example is shown in order to underline better the importance of this mixed energy terms and to show some properties of the mass and stiffness matrices.

Let us consider a one-dimensional chain (see figure 1), partitioned into two subsystems with different masses m_1 and m_2, respectively.

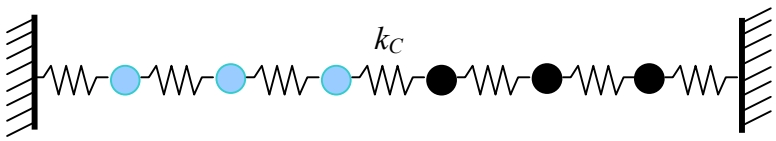

Fig.1

The one-dimensional linear chain

Each mass is connected with the adjacents through kinear springs, with a stiffness k equal to 1 kg/s^2, except that one coupling the two subsystems, which is equal to

$k_C = \varepsilon k$, where ε is a parameter that was changed to provide different strength of the coupling. To analyze the effect induced by the strengthening of the coupling on the energy distribution among the subsystems, a set of numerical simulations was performed varying the strength of the coupling through the variation of the value of the coupling spring, *i.e.* ε. The system, composed by 400 degrees of freedom, is divided into two subsystems of 160 and 240 Dof, respectively. The equation of motion of the *i-th* mass is obtained applying D'Alambert equation. Repeating the operation for each mass and rearranging the terms, a system of differential equations of the 2nd order, that describes the motion of the whole systems, is obtained:

$$\begin{cases} m_1\ddot{x}_1 + 2kx_1 - kx_2 = 0 \\ m_2\ddot{x}_2 - kx_1 + 2kx_2 - kx_3 = 0 \\ \ldots\ldots\ldots\ldots\ldots\ldots\ldots\ldots \\ m_i\ddot{x}_i - kx_{i-1} + (k + k_C)x_i - kx_{i+1} = 0 \\ m_{i+1}\ddot{x}_{i+1} - k_C x_i + 2kx_{i+1} - kx_{i+2} = 0 \\ \ldots\ldots\ldots\ldots\ldots\ldots\ldots\ldots \\ m_N\ddot{x}_N - kx_N + 2kx_N = 0 \end{cases}$$

For the system shown in figure 1 the mass and stiffness matrices assume the following shapes:

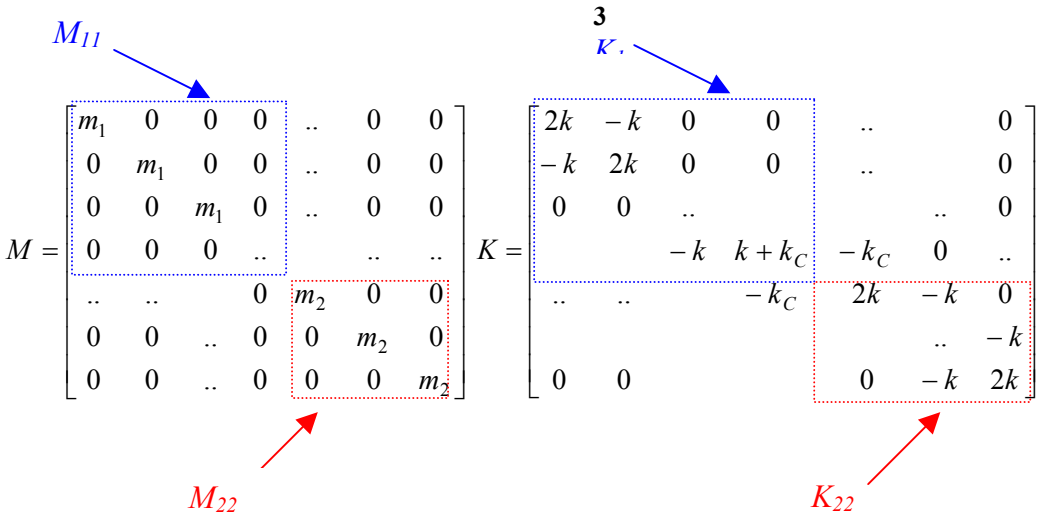

Since in the expression of the kinetic energy of the system, no mixed term ($\dot{x}_i\dot{x}_j$) are present, the off-diagonal elements of the mass matrix are equal to zero and in particular M_{12} and M_{21} thus, the kinetic energy terms due to the coupling are equal to zero. The stiffness matrix is symmetric and the off-diagonal terms are not identically zero instead, but they depend on the strength of the coupling among the subsystems. Hence in the determination of the potential energy of the whole system is necessary to take into

account also the contribution due to these off-diagonal elements. Preliminary, a set of numerical simulations was performed to analyse what happens to the matrices β_{12} and β_{21}, defined in the eq.(5.6), varying the strength of the coupling. Their behaviour can be used as an indicator of how far we are from the condition of weak coupling. In fact, if the coupling among the subsystems is weak, *i.e.* the conditions expresed in eq.(5.10) are valid, the orthonormality condition can be expressed as follows:

$$\alpha_{ij}^{(1)} + \alpha_{ij}^{(2)} = \delta_{ij} \quad \text{and} \quad \beta_{ij}^{(1)} + \beta_{ij}^{(2)} = \omega_i^2 \delta_{ij} \tag{5.11}$$

If the coupling become stronger, the second equality is not valid anymore, since it is necessary to take into account the effect of coupling by introducing the matrices β_{12} e β_{21}.

A good indicator of the validity of this hypothesis can be obtained using the Frobenius norm of the matrix given by the difference between the sum of β_1 and β_2 and the eigenvalue matrix, which is given by the following expression:

$$\|A\|_2 = \sqrt{\left(\sum_i \sum_j \left(\beta_{ij}^{(1)} + \beta_{ij}^{(2)} - \omega_i^2 \delta_{ij} \right)^2 \right)}$$

To have a measure independent of the system dimension, this value is normalized with respect to the norm of the eigenvalues matrix, obtaining:

$$\vartheta = \frac{\sqrt{\left(\sum_i \sum_j \left(\beta_{ij}^{(1)} + \beta_{ij}^{(2)} - \omega_i^2 \delta_{ij} \right)^2 \right)}}{\sqrt{\left(\sum_i \sum_j \left(\omega_i^2 \delta_{ij} \right)^2 \right)}} \tag{5.12}$$

Figure 2 shows the normalized norma ϑ for the one-dimensional system under analysis. It is evident that increasing the strength of the coupling the error committed applying eq.(5.11) becomes greater because the difference between the sum of β_1 and β_2 and the eigenvalue matrix increases. This means that in the evaluation of the energy of each subsystem the component due to the coupling must be taken into account for stronger coupling. It is also possible to distinguish two different behaviours: at low-middle value of ε the increase of θ is monotonic with ε and seems to follow a logarithmic law until a critical value is reached, that corresponds to a "saturation" condition where, even if ε increases, the discrepancy remains the same and equal to 70%.

Another important aspect to analyze is the dependency of this error on the number of degrees of freedom considered in the system under analysis. A set of numerical

simulations were performed to fill up this lack of knowledge. The same setup is used, but both the number of masses, which composed the subsystems, and the strength of the coupling are varied.

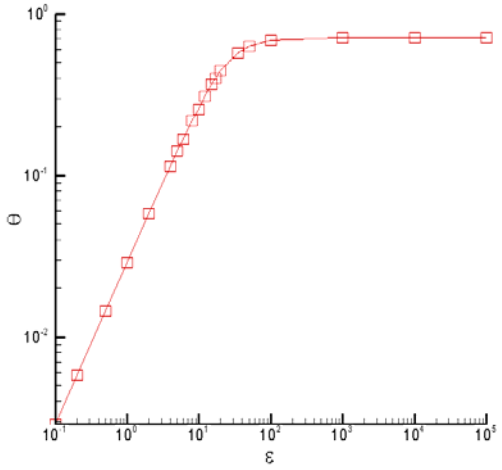

Fig.2

Normalized norm of θ

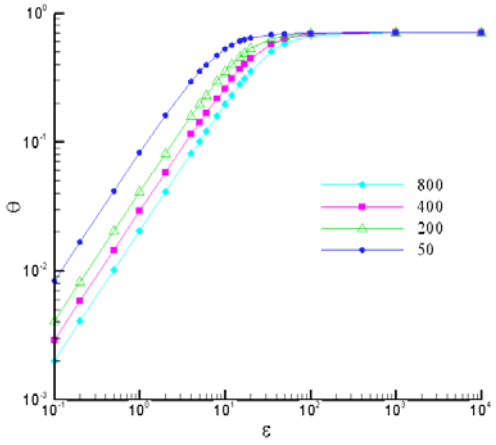

Fig.3

Normalized norm of θ for different values of the DOF

The results, shown in figure 3, demonstrate that the parameter θ is sensitive to the number of degrees of freedom N; in particular with the growth of N a decrease of θ for the same ε is obtained. This means that with the increase of the Dof, the system becomes less sensitive to the strengthening of the coupling.

Using the same setup, in figure 4, 5, 6 and 7 the time histories of the subsystem energies for different values of the coupling parameter ε are shown.

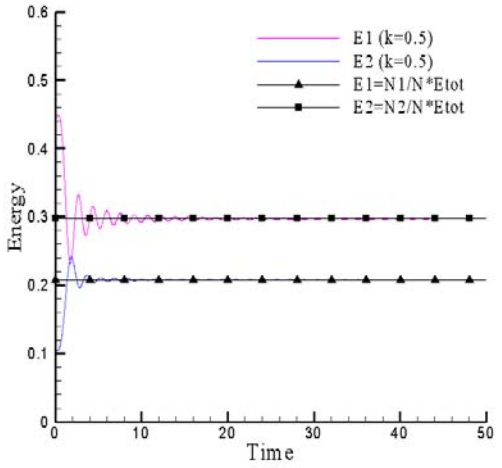

Fig.4

Subsystem time histories for $\varepsilon = 0.5$

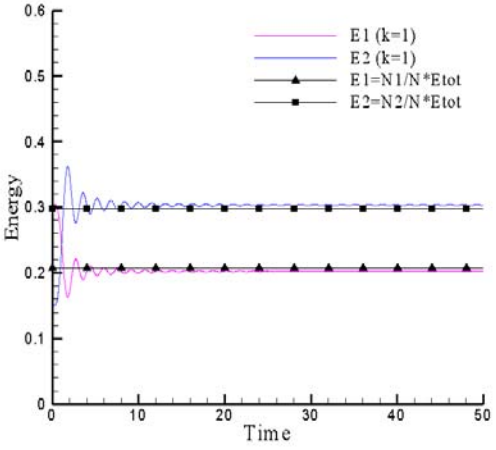

Fig.5

Subsystem time histories for $\varepsilon = 1$

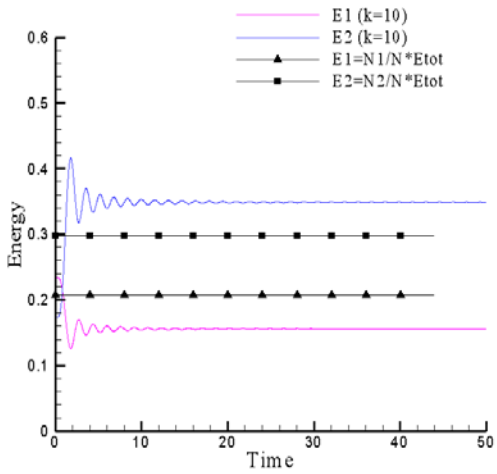

Fig.6

Subsystem time histories for $\varepsilon = 10$

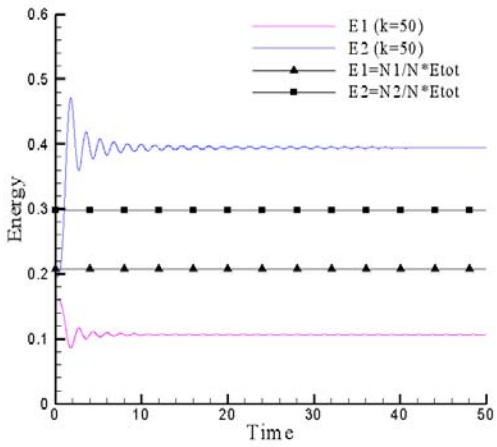

Fig.7

Subsystem time histories for $\varepsilon = 50$

It is evident that increasing the strength of the coupling, *i.e.* for growing ε, the energy distribution between the subsystems diverges from the EEP.

In fact, for ε less than 1, the theoretical and numerical results are in good agreement (the error is less than 3%), at higher value the dynamics of the two subsystems are totally different from the theoretical ones, instead.

To overcome the inability to predict the energy distribution between two strongly coupled subsystems, some modifications in the development of TAEA method are necessary.

Firstly the subsystem energies are now defined as a sum of two terms: the first is the energy component obtained when the other subsystem is considered blocked, the second is related with the coupling instead. The following expressions provide the two new energies:

$$\begin{aligned} E_1^{new}(t) &= E^{(1)}(t) + E^{(12)}(t) \\ E_2^{new}(t) &= E^{(2)}(t) + E^{(21)}(t) \end{aligned} \tag{5.13}$$

Assuming that the system S satisfies the initial condition $w(x,0) = 0$, $\dot{w}(x,0) = \dot{w}_0(x)$, the Lagrangean coordinates are :

$$\begin{cases} q_i(t) = A_i \sin \omega_i t \\ A_i = \dfrac{1}{\omega_i} \displaystyle\int_S \rho \dot{\mathbf{w}}_0 \cdot \Phi_j \, dV \end{cases}$$

Substituting the last expression in (5.13) and considering the eqs.(5.8) and (5.9), the explicit time dependencies of the subsystem energies are given by:

$$E_1^{new}(t)=\frac{1}{2}\sum_{i,j=1}^{N}\left[\alpha_{ij}^{(1)}\omega_i\omega_j A_i A_j\cos(\omega_i t)\cos(\omega_j t)\right]+\frac{1}{2}\sum_{i,j=1}^{N}\left[\beta_{ij}^{(1)}A_i A_j\sin(\omega_i t)\sin(\omega_j t)\right]+$$
$$\frac{1}{2}\sum_{i,j=1}^{N}\left[\alpha_{ij}^{(12)}\omega_i\omega_j A_i A_j\cos(\omega_i t)\cos(\omega_j t)\right]+\frac{1}{2}\sum_{i,j=1}^{N}\left[\beta_{ij}^{(12)}A_i A_j\sin(\omega_i t)\sin(\omega_j t)\right]$$

$$E_2^{new}(t)=\frac{1}{2}\sum_{i,j=1}^{N}\left[\alpha_{ij}^{(2)}\omega_i\omega_j A_i A_j\cos(\omega_i t)\cos(\omega_j t)\right]+\frac{1}{2}\sum_{i,j=1}^{N}\left[\beta_{ij}^{(2)}A_i A_j\sin(\omega_i t)\sin(\omega_j t)\right]+$$
$$\frac{1}{2}\sum_{i,j=1}^{N}\left[\alpha_{ij}^{(21)}\omega_i\omega_j A_i A_j\cos(\omega_i t)\cos(\omega_j t)\right]+\frac{1}{2}\sum_{i,j=1}^{N}\left[\beta_{ij}^{(21)}A_i A_j\sin(\omega_i t)\sin(\omega_j t)\right]$$

where the first two terms of each equality provide the kinetic and potential energy of a subsystem when the other is considered blocked, while the remainders are the energy terms due the motion of the other subsystem.

In chapter 3, the determination of the ensemble energy average of two subsystems weakly coupled has already discussed, hence nothing regarding the energy of each subsystem in the hypothesis that the other one is blocked will be added. The attention is here focused on the coupling terms and on the evaluation of their energy ensemble averages. The guide line of the following analysis can be summarized in the following two points:

- Introduction of a variability in the system parameters, through the introduction of a joint probability density function for the natural frequencies;
- Use of an asymptotic expansion technique to deduce the energy ensemble average of a population of similar systems.

The explicit time dependencies of the energy component of the first subsystems due to the coupling with the second one is obtained as:

$$E^{(12)}=\frac{1}{2}\sum_{i,j=1}^{N}\left[\alpha_{ij}^{(12)}\omega_i\omega_j A_i A_j\cos(\omega_i t)\cos(\omega_j t)\right]+\frac{1}{2}\sum_{i,j=1}^{N}\left[\beta_{ij}^{(12)}A_i A_j\sin(\omega_i t)\sin(\omega_j t)\right]$$

This expression can be also written as follows:

$$E^{(12)}=\frac{1}{4}\sum_{i,j=1}^{N}\left[\left(\alpha_{ij}^{(12)}\omega_i\omega_j-\beta_{ij}^{(12)}\right)A_i\,A_j\cos\left(\omega_i+\omega_j\right)t\right]+$$
$$\frac{1}{4}\sum_{i,j=1}^{N}\left[\left(\alpha_{ij}^{(12)}\omega_i\omega_j+\beta_{ij}^{(12)}\right)A_i\,A_j\cos\left(\omega_i-\omega_j\right)t\right]$$

The terms of the summations can be divided into two parts: the terms for which $i=j$, *i.e.* those related with the coefficients belonging to the diagonals of the matrices $\alpha^{(12)}$ and $\beta^{(12)}$, and those for which $i\neq j$.

$$E^{(12)} = \frac{1}{4}\sum_{i=1}^{N}\left[\left(\alpha_{ii}^{(12)}\omega_i^2 - \beta_{ii}^{(12)}\right)A_i^2\ \cos 2\omega_i t\right] + \frac{1}{4}\sum_{i=1}^{N}\left[\left(\alpha_{ii}^{(12)}\omega_i^2 + \beta_{ii}^{(12)}\right)A_i^2\ \right] +$$
$$+\frac{1}{4}\sum_{\substack{i,j=1\\ j\neq i}}^{N}\left[\left(\alpha_{ij}^{(12)}\omega_i\omega_j - \beta_{ij}^{(12)}\right)A_i\ A_j\cos\left(\omega_i+\omega_j\right)t\right] + \frac{1}{4}\sum_{\substack{i,j=1\\ j\neq i}}^{N}\left[\left(\alpha_{ij}^{(12)}\omega_i\omega_j + \beta_{ij}^{(12)}\right)\cdot\right. \quad (5.14)$$
$$\left.A_i\ A_j\cos\left(\omega_i+\omega_j\right)t\ \right]$$

Assuming that inherent uncertainties affect the subsystem, the last expression is not deterministic anymore, since it represents a stochastic process. The way the uncertainty of the system parameters is considered is through its natural frequencies ω_i, that are now characterized by a probability density function $p(\omega_i,\omega_2,..,\omega_N) = p(\Omega)$. The energy ensemble average of a population of similar subsystems are given by:

$$\overline{E}_1^{new}(t) = \overline{E}^{(1)}(t) + \overline{E}^{(12)}(t) = \int_{R^N}\left(E^{(1)}(t) + E^{(12)}(t)\right)p(\Omega)d\Omega \quad (5.15)$$

where $R \equiv [0,\infty)$.

Let us consider only the energy term due to the coupling $\overline{E}^{(12)}(t)$ in eq.(5.15). Introducing its expression, given by eq.(5.14), in eq.(5.15), we obtain:

$$\overline{E}^{(12)}(t) = \int_{R^{N-2}}\left(\frac{1}{4}\sum_{i=1}^{N}\left[\left(\alpha_{ii}^{(12)}\omega_i^2 - \beta_{ii}^{(12)}\right)A_i^2\ \cos 2\omega_i t\right] + \frac{1}{4}\sum_{i=1}^{N}\left[\left(\alpha_{ii}^{(12)}\omega_i^2 + \beta_{ii}^{(12)}\right)A_i^2\ \right] +\right.$$
$$+\frac{1}{4}\sum_{\substack{i,j=1\\ j\neq i}}^{N}\left[\left(\alpha_{ij}^{(12)}\omega_i\omega_j - \beta_{ij}^{(12)}\right)A_i\ A_j\cos\left(\omega_i+\omega_j\right)t\right] + \frac{1}{4}\sum_{\substack{i,j=1\\ j\neq i}}^{N}\left[\left(\alpha_{ij}^{(12)}\omega_i\omega_j + \beta_{ij}^{(12)}\right)\cdot\right.$$
$$\left.\left.A_i\ A_j\cos\left(\omega_i+\omega_j\right)t\ \right]\right)p(\Omega)d\Omega$$

Let:

$$d\Omega_{ij} = \frac{d\Omega}{d\omega_i\, d\omega_j}, \qquad d\Omega_i = \frac{d\Omega}{d\omega_i}$$

$$\Pi_{ij}(\omega_i,\omega_j) = \int_{R^{N-2}} p\ (\Omega)\ d\Omega_{ij} \quad \text{and} \quad \Pi_i(\omega_i) = \int_{R^{N-1}} p\ (\Omega)\ d\Omega_i$$

where $\Pi_{ij}(\omega_i,\omega_j)$, $\Pi_i(\omega_i)$ are the marginal probabilities; the following expression for $\overline{E}^{(12)}(t)$ is obtained:

$$\overline{E}^{(12)}(t)=\frac{1}{4}\sum_{i=1}^{N}\int_{R^N}\Pi(\omega_i)c_{ii}^{(12)}\,d\omega_i+\frac{1}{4}\sum_{i=1}^{N}\int_{R^N}\Pi(\omega_i)d_{ii}^{(12)}\,\cos(2\omega_i t)d\omega_i+$$

$$+\frac{1}{4}\sum_{i=1}^{N}\sum_{\substack{j=1\\ j\neq i}}^{N}\int_{R^N}\Pi(\omega_i,\omega_j)d_{ij}^{(12)}\,\cos(\omega_i+\omega_j)t\;d\omega_i\,d\omega_j+ \tag{5.16}$$

$$+\frac{1}{4}\sum_{i=1}^{N}\sum_{\substack{j=1\\ j\neq i}}^{N}\int_{R^N}\Pi(\omega_i,\omega_j)\,c_{ij}^{(12)}\,\cos(\omega_i-\omega_j)t\;d\omega_i\,d\omega_j$$

where $c_{ii}=\frac{1}{4}A_i^2\left(\alpha_{ii}^{(12)}\omega_i^2+\beta_{ii}^{(12)}\right)$ and $d_{ii}=\frac{1}{4}A_i^2\left(\alpha_{ii}^{(12)}\omega_i^2-\beta_{ii}^{(12)}\right)$

Using an asymptotic expansion of the integrals with respect to time and considering only the first order terms (see appendix A), the expression of the energy due to the coupling is:

$$\overline{E}^{(12)}(t)=\sum_{i=1}^{N}\int_{R^N}\Pi(\omega_i)c_{ii}(\omega_i)d\omega_i+\frac{1}{2t}\left[\Pi(\omega_i)d_{ii}(\omega_i)\sin(2\omega_i t)\right]\Big|_{\omega_i^-}^{\omega_i^+}+o\left(t^{-1}\right) \tag{5.17}$$

In a similar way, it is possible to evaluate the energy $\overline{E}^{(21)}(t)$ of the second subsystem due to the coupling with the first one. Hence, the effect of the coupling is relevant for both the transient and steady state condition. In Appendix B the same procedure is used to evaluate the asymptotic energy distribution among two damped substructures.

In the system under analysis (figure 1), a simplification arises due to the fact that the kinetic energy term due to the coupling is equal to zero. In this case the explicit time dependencies of the energy related to the coupling is obtained as:

$$E^{(12)}(t)=\frac{1}{2}\sum_{ij=1}^{N}\beta_{ij}^{(12)}A_iA_j\sin\omega_i t\sin\omega_j t=-\frac{1}{4}\sum_{ij=1}^{N}\beta_{ij}^{(12)}A_iA_j\left[\cos(\omega_i+\omega_j)t-\cos(\omega_i-\omega_j)t\right]$$

$$=-\sum_{ij=1}^{N}\tilde{c}_{ij}^{(12)}\left[\cos(\omega_i+\omega_j)t-\cos(\omega_i-\omega_j)t\right]$$

where:

$$\tilde{c}_{ij}^{(12)}=\frac{1}{4}A_iA_j\beta_{ij}^{(12)}$$

Following the same procedure used for the general case, it is possible to obtain the ensemble energy average of a population of similar systems, affected by inherent uncertainty of their paramter as:

$$\overline{E}^{(12)}(t)=\sum_{ij=1}^{N}\int_{R^N}\tilde{c}_{ij}^{(12)}\left[\cos(\omega_i+\omega_j)\,t-\cos(\omega_i-\omega_j)\,t\right]p(\Omega)d\Omega$$

If we divide the terms in the summation into a part for which $i = j$ and the others, the last expression becomes:

$$\overline{E}^{(12)}(t) = \sum_{i=1}^{N} \int_{R} \Pi(\omega_i)\, \widetilde{c}_{ii}(\omega_i) d\omega_i - \sum_{i=1}^{N} \int_{R} \Pi(\omega_i)\, \widetilde{c}_{ii}(\omega_i) \cos 2\omega_i t \; d\omega_i + \sum_{\substack{i,j=1 \\ j \neq i}}^{N} \int_{R^2} \Pi(\omega_i, \omega_j)\, \widetilde{c}_{ij}(\omega_i, \omega_j) \left[\cos(\omega_i + \omega_j)t - \cos(\omega_i - \omega_j)t\right] \cos 2\omega_i t \; d\omega_i d\omega_j$$

Using an asymptotic expansion of the integrals with respect to time and considering only the first order terms, the expression of the energy due to the coupling is:

$$\overline{E}_C(t) = \sum_{i=1}^{N} \int_{R} \Pi_i(\omega_i) \widetilde{c}_i(\omega_i) d\omega_i - \frac{1}{2t} \sum_{i=1}^{N} \left[\Pi_i(\omega_i) \widetilde{c}_i(\omega_i) \sin 2\omega_i t\right] \Bigg|_{\omega_i^-}^{\omega_i^+} + o\left(t^{-1}\right) \qquad (5.18)$$

Using the same setup shown in figure 1, a set of numerical experiments were performed in order to verify if the changes introduced in the method well represent the dynamical behaviuors of two strongly coupled subsystems. The analysed system is composed by 400 degrees of freedom, divided into two identical subsystems, each of them with 200 degrees of freedom, connected through springs, each equal to $1\,{kg}/{s^2}$. The stiffness of the coupling spring is varied in order to verify the effect of the increase of the strength of the coupling in the energy distribution among the subsystems. The initial condition is a velocity spike in the first subsystem, that provide an intial energy equal to 0.5 $Kg\frac{m^2}{s^2}$. The theoretical value of the two energies in the steady state condition should be equal to $0.25\, Kg\frac{m^2}{s^2}$. In figure 8, 9 and 10 the time histories of the subsystem energies, obtained using the new expression $E_1^{new}(t)$ and $E_2^{new}(t)$ (see eq.(5.13)), are plotted and compared with the energetic term computed with the other subsystem blocked, for different strength of the coupling $E^{(1)}(t)$ and $E^{(2)}(t)$.

For value of spring's stiffness lower than 1 it is not possible to see any difference between the energy evaluated with or without the coupling terms. On the countrary, with the increase of the coupling strength it is evident that, if the terms due to the coupling are not included the error in the evaluation of the total energy becomes not negligible. In fact, even if the ratio among the subsystems remains the same, the total energy is incorrect because the contribution of the coupling energy is not considered.

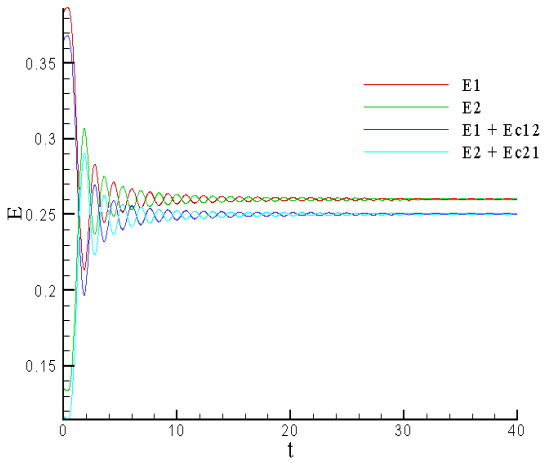

Fig.8

Energy time histories for $\varepsilon = 1$

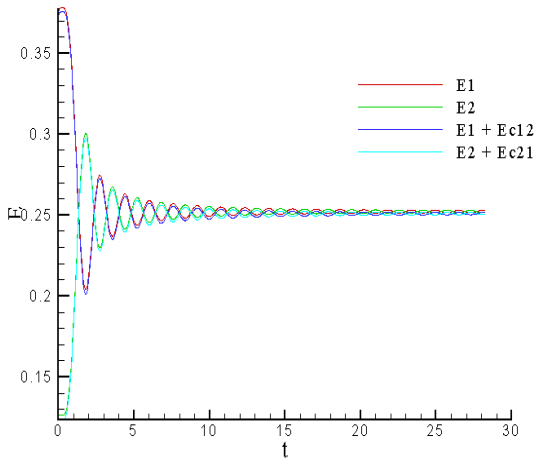

Fig.9

Energy time histories for $\varepsilon = 5$

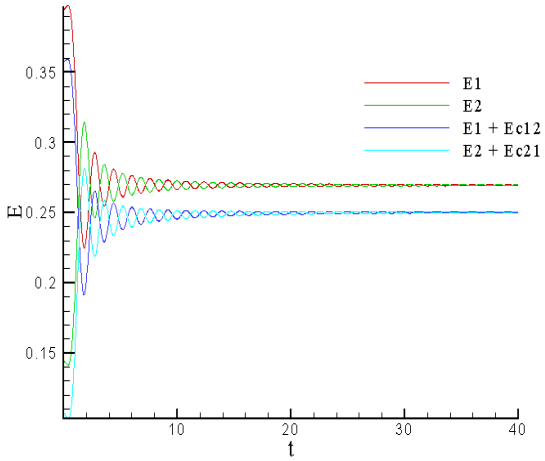

Fig.10

Energy time histories for $\varepsilon = 10$

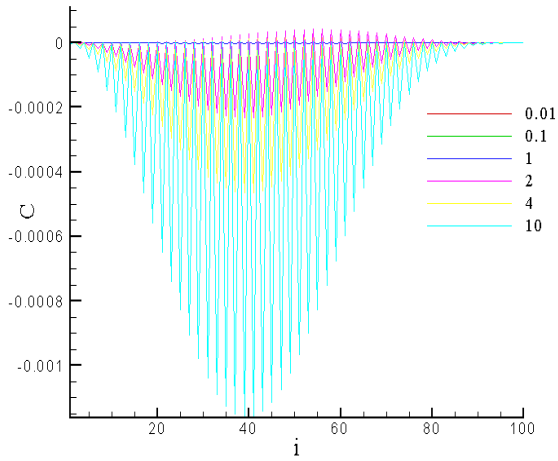

Fig.11

The effect of the coupling strength on the coefficient $\widetilde{c}_{ii}$

It is also interesting to compare the coefficients $\widetilde{c}_{ii}$ with the increase of the coupling strength. In figure 11 the behaviour of these coefficients for each degree of freedom is plotted for different values of ε. The rapid increase of the absolute value of this parameter when increasing the strength of the coupling demonstrates the necessity to use the new developed formulation for the evaluation of the energy distribution between strongly coupled subsystems. It is also interesting to compare the order of magnitude of the coefficients a_{ii}, related to the "blocked energy term" in each subsystem, and the $\widetilde{c}_{ii}$, that provide a measure of the coupling strength. In figures 12 and 13, a comparison of of

these two parameter distributions along the chain is shown for two different cases: a weak coupling (figure12) and a quite strong coupling (figure 13). While in the first case the a_{ii} are undoubtedly higher than the $\tilde{c}_{ii}$, so that the effect of coupling can be neglected, in the second case the two coefficients are of a comparable order of magnitude instead, implying the necessity to take into account in the energy evaluation of each subsystem the term due to the coupling forces.

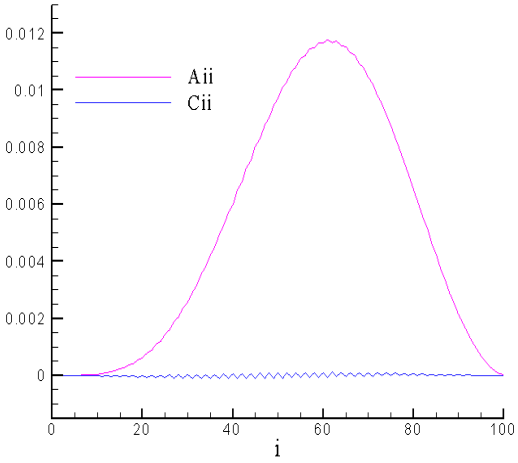

Fig.12

Comparison between coefficients a_{ii} and c_{ii} for ε=1

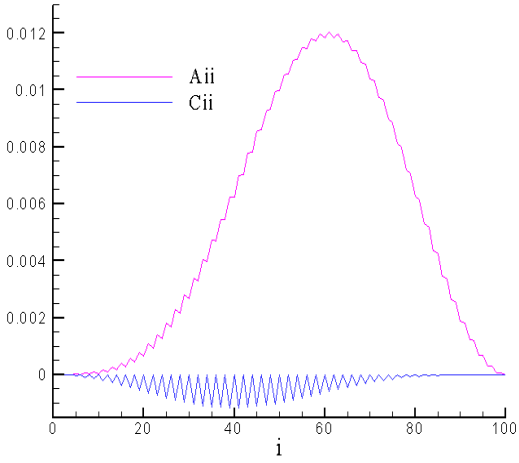

Fig.13

Comparison between coefficients a_{ii} and c_{ii} for ε=10

5.2 INTERACTION AMONG MORE THAN TWO SUBSYSTEMS

In this section the TAEA theory is extended to include the case of coupling among more than two subsystems. Consider a freely vibrating system S, isolated and conservative, divided into three parts S_1, S_2 and S_3, such that $S = S_1 \cup S_2 \cup S_3$. Assume that the system S starts to vibrate due to given initial conditions. Applying the same notation used in chapter 3, the dynamical behaviour of each system can be expressed in terms of orthonormal modes and Lagrangean coordinates of the whole system S, as shown below:

$$\mathbf{w}^{(1)}(\mathbf{x},t)=\sum_{i=1}^{N}\Phi_i(\mathbf{x})q_i(t) \quad \mathbf{x}\in S_1$$

$$\mathbf{w}^{(2)}(\mathbf{x},t)=\sum_{i=1}^{N}\Phi_i(\mathbf{x})q_i(t) \quad \mathbf{x}\in S_2$$

$$\mathbf{w}^{(3)}(\mathbf{x},t)=\sum_{i=1}^{N}\Phi_i(\mathbf{x})q_i(t) \quad \mathbf{x}\in S_3$$

The energies of the three subsystems S_1, S_2 and S_3 are $E^{(1)}(t)$, $E^{(2)}(t)$ and $E^{(3)}(t)$, respectively. For a continuous, linear, elastic system they can be expressed as follows:

$$E^{(r)}(t)=\frac{1}{2}\int_{S_r}\rho|\dot{w}|^2\,dV+\frac{1}{2}\int_{S_r}\sigma:\varepsilon\,dV$$

with $r=1,2,3$

In (Carcaterra, 2005) it is demonstrated that the total energy of each subsystem can be written concisely as:

$$E^{(r)}(t)=\frac{1}{2}\sum_{i,j=1}^{N}\alpha_{ij}^{(r)}\dot{q}_i(t)\dot{q}_j(t)+\frac{1}{2}\sum_{i,j=1}^{N}\beta_{ij}^{(r)}q_i(t)q_j(t) \tag{5.19}$$

With the positions:

$$\alpha_{ij}^{(r)}=\int_{S_r}\rho\,\Phi_i\,\Phi_j\,dV \quad \text{and} \quad \beta_{ij}^{(r)}=\frac{1}{4}\int_{S_r}\left[D\left(\nabla\Phi_i+\nabla\Phi_i^T\right)\right]:\left(\nabla\Phi_i+\nabla\Phi_i^T\right)dV$$

For weak coupling, the orthonormality conditions imply in the case of three coupled systems the equalities:

$$\begin{cases}\alpha_{ij}^{(1)}+\alpha_{ij}^{(2)}+\alpha_{ij}^{(3)}=\delta_{ij}\\ \beta_{ij}^{(1)}+\beta_{ij}^{(2)}+\beta_{ij}^{(3)}=\omega_i^2\delta_{ij}\end{cases} \tag{5.20}$$

On the countrary, for strong coupling the "mixed" term $\alpha^{(rs)}$ and $\beta^{(rs)}$ for $r=1,2,3$ must be taken into account in eq.(5.20).

Consider now the discrete system, in this case the continuous system is discretized by a set of masses which are partitioned into three sets S_1, S_2 and S_3. The vector of displacement w of the whole system can be partitioned into three sub vectors referred to the displacement of the three sets of masses $w=\left[w^{(1)},w^{(2)},w^{(3)}\right]^T$. The mass and the stiffness matrices and the *i*-th eigenvector of the whole system are partitioned as follows:

$$M=\begin{bmatrix}M_{11}&M_{12}&M_{13}\\M_{21}&M_{22}&M_{23}\\M_{31}&M_{32}&M_{33}\end{bmatrix},\ K=\begin{bmatrix}K_{11}&K_{12}&K_{13}\\K_{21}&K_{22}&K_{23}\\K_{31}&K_{32}&K_{33}\end{bmatrix} \text{ and } \boldsymbol{\Phi}_i=\begin{Bmatrix}\boldsymbol{\Phi}_i^{(1)}\\\boldsymbol{\Phi}_i^{(2)}\\\boldsymbol{\Phi}_i^{(3)}\end{Bmatrix}.$$

Where the α_{ij} and β_{ij} coefficients are now expressed by the following expressions:

$$\alpha^{(rs)} = \frac{1}{2}\Phi_i^{(r)^T} M_{rs} \Phi_j^{(s)} \qquad \text{and} \qquad \beta^{(rs)} = \frac{1}{2}\Phi_i^{(r)^T} K_{rs} \Phi_j^{(s)} \quad \text{with} \quad r,s = 1,2,3 \qquad (5.21)$$

As already shown in the previous section, the weak coupling hypothesis implies that the matrices defined above (eq.(5.21)) for $r \neq s$ are negligigle respect to those for which $r = s$.

In the same way shown for the coupling between two subsystems, in the expression of the energy of each subsystem it is possible to discern the term related to the coupling (the mixed energy term) and the term of energy stored in the subsystem when the others are considered blocked (the blocked energy term). As to the energy term obtained considering the others blocked, there are not significant changes with respect to the case with only two coupled subsystems. This term can be expressed for each sub-component as shown previously:

$$E^{(r)}(t) = \sum_{i,j=1}^{N} a_{ij}^{(r)} \cos\left(\omega_i + \omega_j\right) t + b_{ij}^{(r)} \cos\left(\omega_i - \omega_j\right) t \qquad (5.22)$$

where $a_{ij}^{(r)} = \frac{1}{4} A_i A_j \left(\alpha_{ij}^{(r)} \omega_i \omega_j - \beta_{ij}^{(r)}\right)$, $b_{ij}^{(r)} = \frac{1}{4} A_i A_j \left(\alpha_{ij}^{(r)} \omega_i \omega_j + \beta_{ij}^{(r)}\right)$ and the $\alpha_{ij}^{(r)}$ and $\beta_{ij}^{(r)}$ are obtained from eq.(5.21).

Assuming that inherent uncertainties affect the systems, and that this uncertainty in the system parameters is charcterized through its natural frequencies ω_i, which are now regarded as a set of random variables, characterized by a joint probability function $p(\Omega) = p(\omega_1, \omega_2, ..., \omega_N)$, the ensemble energy average of the *r*-th subsystem is :

$$\overline{E}^{(r)}(t) = \int_0^\infty \int_0^\infty ... \int_0^\infty E^{(r)}(t)\, p(\omega_1, \omega_2, ..., \omega_N)\, d\omega_1\, d\omega_2 ... d\omega_N = \int_{R^N} E^{(r)}(t)\, p(\Omega)\, d\Omega$$

Using an asymptotic expansion of the integrals with respect to time and considering only the first order terms, the following expression for the ensemble energy average is obtained:

$$\overline{E}^{(r)}(t) = \sum_{i=1}^{N} \int_{\omega_i^-}^{\omega_i^+} \Pi_i(\omega_i) b^{(r)}(\omega_i) d\omega_i + \frac{1}{2t} \sum_{i=1}^{N} \left[\Pi_i(\omega_i) a^{(r)}(\omega_i) \sin 2\omega_i t\right]\Big|_{\omega_i^-}^{\omega_i^+} + o\left(t^{-1}\right) \qquad (5.23)$$

Applying an analysis similar to that exposed in section 3.2, it is possible to obtain an energy distribution in the steady state which, under some assumptions as the coupling among homogeneous subsystems, can be described through the following expression:

$$\frac{\overline{E}^{(1)}}{N_1} = \frac{\overline{E}^{(2)}}{N_2} = \frac{\overline{E}^{(3)}}{N_3} = \frac{\overline{E}_0}{N} \tag{5.24}$$

where N_r and $\overline{E}^{(r)}$ are the number of modes contained in the frequency range $[0, \omega_{\max}]$and the ensemble energies of the *r*-th subsystem, respectively. Equation (5.24) states that the energy per mode of each subsystems is equal to the initial energy per mode of the whole system.

Some differences arise in the evaluation of the energy stored in the coupling, in fact in the determination of the energy of the *r*-th system it is necessary also to consider the effect due to the other two subsystems. This implies a change in the expression of the energy term related with the coupling forces $E_c^{(r)}(t)$, that can now be expressed as follows:

$$E_c^{(r)}(t) = \frac{1}{2}\sum_{ij=1}^{N} \Phi^{(r)^T} M_{rs} \Phi^{(s)} \dot{q}_i \dot{q}_j + \frac{1}{2}\sum_{ij=1}^{N} \Phi^{(r)^T} K_{rs} \Phi^{(s)} q_i q_j + \\ + \frac{1}{2}\sum_{ij=1}^{N} \Phi^{(r)^T} M_{rp} \Phi^{(p)} \dot{q}_i \dot{q}_j + \frac{1}{2}\sum_{ij=1}^{N} \Phi^{(r)^T} K_{rp} \Phi^{(p)} q_i q_j$$

where the first two summations are related with the coupling between the subsystems *r* and *s* and the last two with the coupling between *r* and *p*.

The same analysis developed in the previous section can be applied for the determination of each coupling energy term through eqs.(5.13-5.18).

Different conditions of coupling can be analysed in the case of three systems. In the first case, that is shown in figure 1, the systems are in “cascade”, which implies that the first and the third systems are connected only with the middle one.

An example of this kind of configuration is the solar panel mounted exterior to the spacecraft. In fact, they are composed by three plates belonging to parallel planes, connected thought bolts.

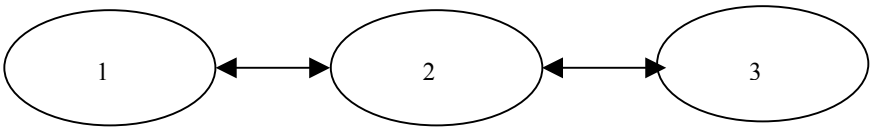

Fig.15

Three system assembly: configuration 1

In this case the terms K_{13} and K_{31} are obviously equal to zero, since there is not a direct connection between the systems. This configuration is particularly interesting from a

theoretical point of view, since it is sometimes critical in a SEA modelling. In fact, a "tunnelling" mechanism can occur, as shown in Heron (1994), *i.e.* non zero coupling loss factors (CLF) may be found between two SEA subsystems that are physically separated. This doesn't mean that there is an energy flow between two systems not physically connected, but means that in the evaluation of the energy flow between two coupled systems it is necessary to consider an energy contribution of a third system. This condition is particularly critical, since the basic SEA assumption of coupling power proportionality does not hold. The mechanism of indirect coupling was later analysed in Mace (2005), where the author provides the conditions under which the indirect CLFs are zero, such that the system can be described by a "proper SEA" model.

It seemed to be interesting to verify if, in this critical configuration for SEA, TAEA model could provide significant results. In TAEA the mass and the stiffness matrices can be evaluated using a FE-model, hence if the systems are not connected the terms of these matrices related to their interaction are zero. Consequently, if two subsystems are not physically connected, no energy term related with the coupling are present. As a support of this, a set of numerical simulations upon two simplified structures were perfomed, allowing to check the validity of the developed model.

A first set of numerical simulation were performed on a two-dimensional system (1m x 1m) divided into three homogeneous plates through two separator lines shorter than the length of the plate side in order to allow the energy exchange (figure 16). The area of the plates are in the ratios 1:1,3 and 1:1,5. Since only the intermediate plate exchange energy with both the other systems, this configuration is equivalent to the one shown in figure 15. The initial conditions imposed are a displacement equal to zero for all points and a velocity spike in the centre of the first plate.

In figure 17 the energetic behaviour of the systems are shown and compared with the theoretical results obtained by applying eq.(5.24), showing a good agreement.

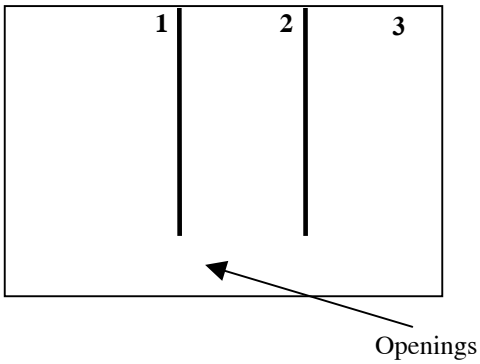

Fig.16

Three plates assembly: configuration 1

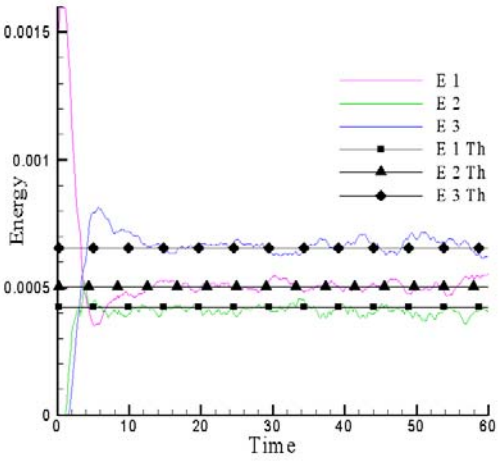

Fig.17

Energy time histories

The second set of numerical simulations was performed upon a three dimensional acoustic cavity (1 m x 1m x 1m) divided into three homogeneous cavities by two rectangular panels, as shown in figure 18. The volumes of the three cavities are approximately in the ratio 4:1 and 5:1 with respect to the smallest one. The sides of both panels are shorter than the sides of the box, leaving rectangular openings between the subsystems. A pressure spike is generated at the initial time inside the first subsystem (chamber 1 in Fig. 18).

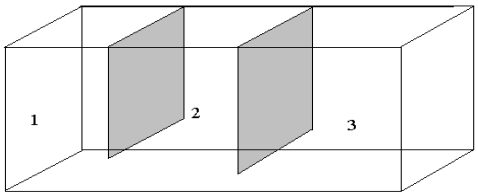

Fig.18

Three acoustic cavitues assembly: configuration 1

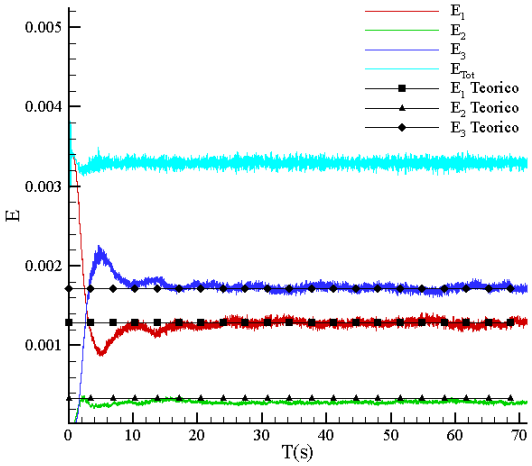

Fig.19

Energy time histories

A finite difference scheme with grid 24 x 24 x 24, corresponding to 13824 degrees of freedom, was used for the numerical solution of the acoustic wave equation.

In figure 19 the time histories of the subsystems energies are shown and compared with the asymptotic energy values predicted by eq.(5.24), showing a very good agreement. Similar results are obtained for different system configurations and different pressure spike locations.

A second way to couple three plate is the one shown in figure 20:

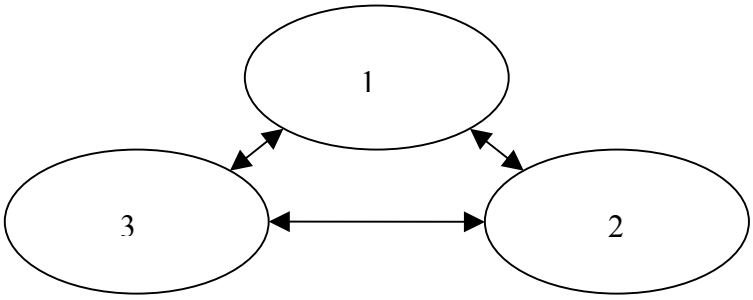

Fig.20

Three system assembly: configuration 2

In this case each system is connected with the other two. An example of this kind of coupling is provided by the setup shown in figure 21, where the panel positions allow the energy exchange from one to all the other subsystems.

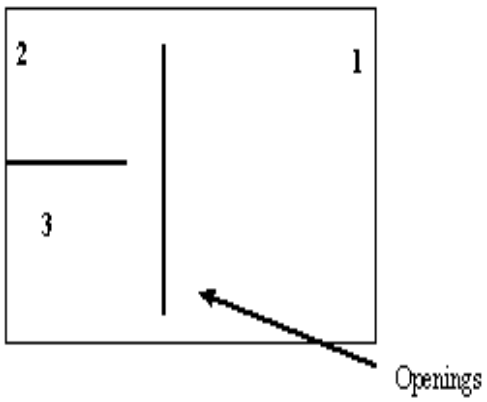

Fig.21

Three plates assembly: configuration 2

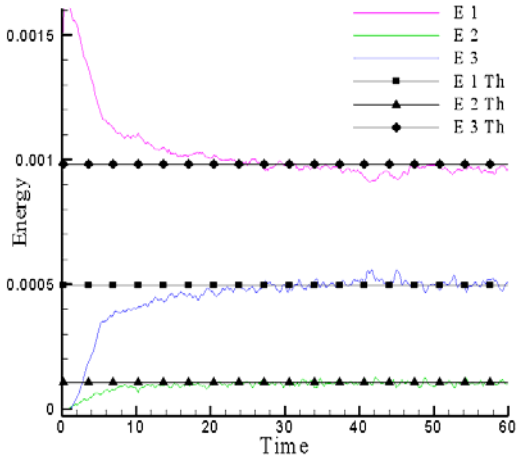

Fig.22

Energy time histories

Also in this case the agreement between the theoretical results and the numerical one is really good, as shown in figure 22.

The last setup is an acoustic cavity, where the panels are now inserted as shown in figure 23, recreating a type of connection among the substructure similar to that shown in figure 20. Chamber 1 and 2 have the same volume while the third subsystem is twice the volume of chamber.

In figure 24 the numerical results are compared with the theoretical results obtained by applying eq.(5.24), showing a very good agreement.

Since similar results were obtained for different system configurations and different pressure spike locations, the validity of TAEA can be considered verified.

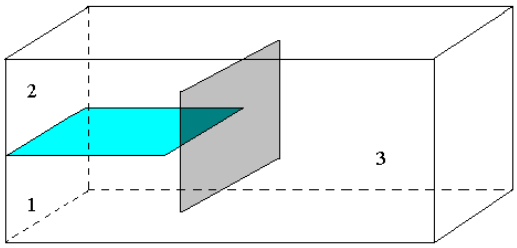

Fig.23

Three acoustic cavitues assembly:

configuration 2

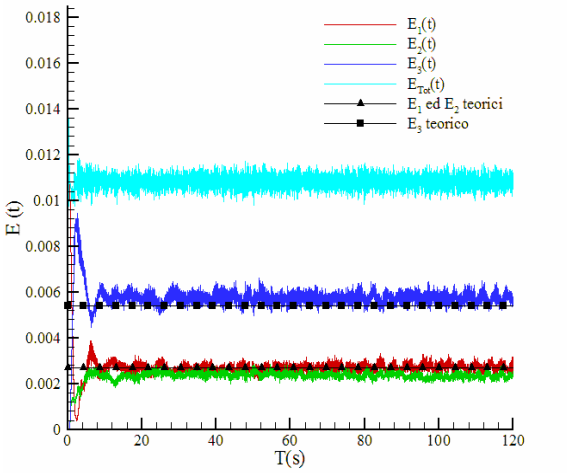

Fig.24

Energy time histories

CHAPTER 6: EXPERIMENTAL VALIDATION

In this chapter a validation of the theoretical-numerical procedure, previously described, is presented through a comparison of the energy distribution among subcomponents of a system obtained applying the developed method and those obtained experimentally. Two different two-dimensional systems were analysed: the former is composed by two plates coupled by means of straps, while the second system is made up of three plates connected through straps among the subsystems. In section 6.1 the measured transient responses of these systems are shown, while in section 6.2 these results are compared with those obtained applying the modified TAEA method.

6.1 EXPERIMENTAL MEASUREMENTS

In this section the results of an experimental campaign performed at the Marcus Wallenberg Laboratory for Sound and Vibration at Kungliga Tekniska högskolan in Stockholm in the frame of the European Doctorate in Sound and Vibration (EDSVS) are shown.

The typical experiment has consisted of a transient excitation on a subcomponent of the structure and a measure of the dynamical responses of the plates at different locations upon all the subsystems, in order to derive a space-average value of the vibrational energies. Several repetitions of the tests under nominally equal conditions were done to verify the repeatability of the measurements.

In subsection 6.1.1 some preliminary studies concerning the design of the experiment are shown, while in the following one (6.1.2), a description of the instrumentation used is presented. Subsections 6.1.3 and 6.1.4 represents the core of this experimental section, since the results of the energy time histories for the two and three plate assembly respectively are presented.

6.1.1 PRELIMINARY CONSIDERATIONS FOR THE DESIGN OF THE EXPERIMENTAL SETUP

A preliminary analysis was performed to choose the plates characteristics, *i.e.* material, shape, area and thickness, taking into account different necessities. The first step was

the choice of the material among aluminium, steel and perspex. In table 1 the main mechanical characteristics of these materials are compared.

MECHANICAL PROPERTIES				
	Density [kg/m^3]	**Poisson ratio**	**Young modulus [Pa]**	**Loss factor**
Aluminium	2700	0.34	$6.\cdot10^{9}$	10^{-4}
Steel	7860	0.33	$2\cdot10^{11}$	$0.2\text{-}3\ 10^{-4}$
Perspex	1190	0.37	$3.3\cdot10^{9}$	$2\text{-}4\ 10^{-2}$

Tab.1

The choice of the material was basically obtained analysing their loss factors. In fact, for this kind of experiment, it is important to have a high damping for two different motivations: the first is the possibility to neglect other losses, in particular the acoustic energy radiated by the plates during their vibration, and the second is related to the reduction of the length of the time window necessary to produce accurate estimates of the impulsive responses. Regarding the first motivation, it is interesting to notice that the internal loss factor of a built-up structure includes several different energy-loss mechanisms: the structural loss factor, the radiation loss factor, the one associated with energy dissipation at the boundaries of structural element and the energy dissipation at the junctions. The only two terms that are considered here are those related with the structural loss factor and with the energy radiated from the vibrating plate.

Among these three materials, perspex is characterized by the highest loss factor, in fact its magnitude is two order greater than the others. Moreover, taking into account the easiness to work this material and its lightness, the choice fell to perspex.

A preliminary analysis of the energy component radiated from the plate was numerically performed, in order to verify if this kind of loss was of the same order of magnitude of the internal dissipation or if it could be neglected. Using the hypothesis of thin plate, the radiation loss factor was evaluated as in Cremer et al. (1987):

$$\eta_{rad} = \frac{\rho_0 c \sigma}{\omega \rho_s} \tag{6.1}$$

where σ is the radiation efficiency, ρ_0 and ρ_s are the fluid and plate densities respectively, c is the velocity of the waves in the fluid and ω is the centre frequency of the band.

In Maidanik (1962) the radiation efficiency was evaluated as a function of the coincidence frequency f_c defined as:

$$f_c = \frac{c_f^2}{2\pi}\sqrt{\frac{\rho h}{D}} = \frac{c_f^2}{2\pi h}\sqrt{\frac{\rho\left(1-\upsilon^2\right)}{E}} \tag{6.2}$$

In table 2 the coincidence frequencies for different thickness and materials are shown.

COINCIDENCE FREQUENCY (Hz)			
Thickness	**Perspex**	**Steel**	**Aluminium**
3 mm	12000	4000	10500
5 mm	7300	2400	6200
10 mm	3600	1200	3100

Tab.2

Under some assumptions regarding the boundary conditions (all edges simply supported), but also on the behaviour of the modes (the amplitude of the resonant modes are equal to their average and their phases are randomly distributed) the radiation efficiency can be evaluated (Maidanik, 1962) using the following expression:

$$\sigma = \begin{cases} \dfrac{4 L_x L_y f^2}{c_f^2} & for\ f < f_1 \\ \lambda_c^2 g_1(\alpha) + 2\left(L_x + L_y\right)\lambda_c g_2(\alpha) & for\ f_1 < f\ < f_c \\ \sqrt{\dfrac{L_x}{\lambda_c}} + \sqrt{\dfrac{L_y}{\lambda_c}} & for\ f \approx f_c \\ \sqrt{\dfrac{1}{1-\dfrac{f_c}{f}}}_{c} & for\ f > f_c \end{cases} \tag{6.3}$$

where $\alpha = \sqrt{\frac{f}{f_c}}$, L_x and L_y are the length of the plate sides and λ_c is the wavelength at the critical frequency. Moreover, $g_1(\alpha)$, which represents the modal average radiation efficiencies for the so-called corner modes, assumes the following values:

$$g_1(\alpha) = \begin{cases} \dfrac{8}{\pi^4}\dfrac{1-2\alpha^2}{\alpha\sqrt{1-\alpha^2}} & for\ f\ < \dfrac{f_c}{2} \\ 0 & for\ f\ > \dfrac{f_c}{2} \end{cases}$$

and the edge mode contribution, provided by $g_2(\alpha)$, is given by:

$$g_2(\alpha) = \frac{1}{4\pi^2} \frac{\left(1-\alpha^2\right)\ln\left\{\left(1+\alpha\right)/\left(1-\alpha\right)\right\}+2\alpha}{\sqrt{\left(1-\alpha^2\right)^3}}$$

Analysing eq.(6.3), it is evident that below the critical frequency, some parameters regarding the geometry of the system, like the perimeter and the area, are requested. Thus, it is not easy to obtain significant results since, at this time, the real geometry is not already known. Moreover at low frequency the radiation is sensitive to boundary conditions. Taking into account different needs (among the others the geometrical limitation for the experimental apparatus, the possibility to use commercial Perspex sheets but also the availability of the measurement systems) the behaviour of two different plates were analysed: the former with an area equal to 0.5 $m^2$and a thickness of 5 mm and the second with an area of 0.3 m^2 and a thickness of 3 mm. In figure 1 a comparison of the internal loss factor and the radiation loss factors, evaluated for the two different plates, is shown. Being the critical frequency for the chosen material quite high and the radiation efficiency very low up to the critical frequency, in the evaluation of the energy loss the radiation efficiency can be neglected in both cases with respect to the internal damping in the frequency range between 0 and 5 KHz.

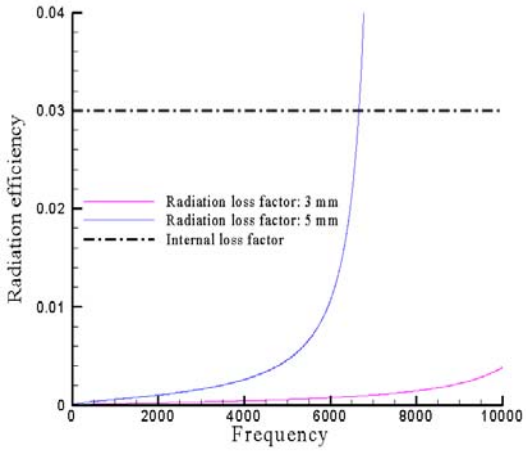

Fig.1

Comparison between the radiation efficiency for the two plates and the internal loss factor

The shapes of the three plates were chosen irregular, in order to avoid problems of modal localization. Mace and Rosemberg (1998), analysing different combinations of regular and irregular plates, underlined that, for a regular shape plate, at low modal

overlap, there is a stronger tendency of the global modes to be localized within only one plate. In other words, in the coupling between plates with a regular shape the energy tends to be stored in one of the two plates. For a coupling between plates with irregular shapes, the energy for each of the global modes tends to be more spread between them, instead. However, at higher value of modal overlap this difference of the dynamical behaviours in regular and irregular coupled plates becomes small.

Even if the choice of the material with a high damping (that corresponds to a weak coupling between the systems) allows reducing the frequency range inside which the problem of modal localization can appear, the shapes of the plates were chosen irregular, so that the problem can be reduced.

The upper frequency limit was chosen in order to verify the equation:

$$kh < 1$$

In fact, below this value the shear deformation in the plate vibration can be neglected, otherwise it must be necessary to model the system using the Mindlin theory (Graff, 1975). For a perspex plate 5 mm thick the last expression provides a value of the frequency equal to 16 KHz.

On the basis of the above considerations, three different perspex plates were chosen to perform the experiment. The main geometrical characteristics of those plates are presented in the table 3.

GEOMETRICAL CHARACTERISTICS			
	Area [m^2]	**Thickness [m]**	**Weight [kg]**
Plate 1	0.464	$3 \cdot 10^{-3}$	1.656
Plate 2	0.637	$5 \cdot 10^{-3}$	3.790
Plate 3	0.382	$3 \cdot 10^{-3}$	1.363

Tab.3

6.1.2 EXPERIMENTAL SETUP

Two different configurations were analysed: the former (see figure 2) consisted in two plates assembly connected by straps which number can be varied, the second is composed by three plates assembly with the same connecting elements (see figure 3).

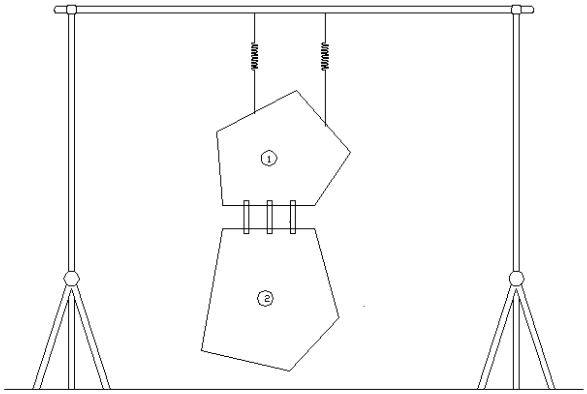

Fig.2

Two plates assembly

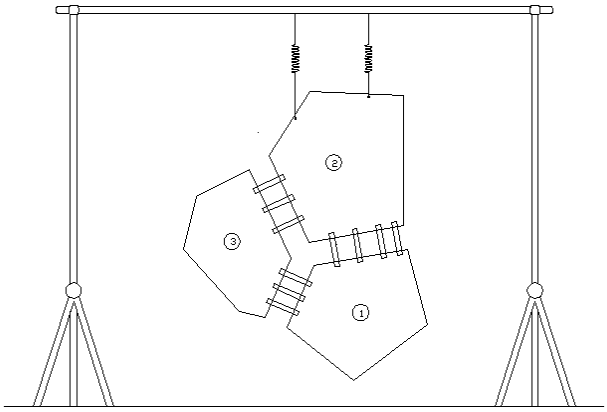

Fig.3

Three plates assembly

The typical experiment consists of a measurement of the plate responses to an impulsive excitation provided to one subsystem. The use of a shaker to excite the structure was preferred to the hammer, being in the first case the results perfectly reproducible and implying a reduction of the time window necessary for the achievement of the equilibrium condition. The impulsive response was derived by the inverse Fourier transform of the frequency response function (FRF). The structural excitation experiments were conducted with a LDS's electrodynamics V203 shaker, providing the excitation input to the plate. The shaker was connected to the plate using a steel stinger. The signal provided to the shaker is a white noise in the frequency range between 0-5 KHz. A Bruel & Kjaer 8200 force transducer characterized by a reference sensitivity equal to 4.07 pC/N was connected to the end of the shaker to measure the

input force signal. This was force transducer. The weight of this type of force transducer is 21 g. A Bruel & Kjaer charge amplifier provided the amplification from the force sensor to the analyser (see figure 4).

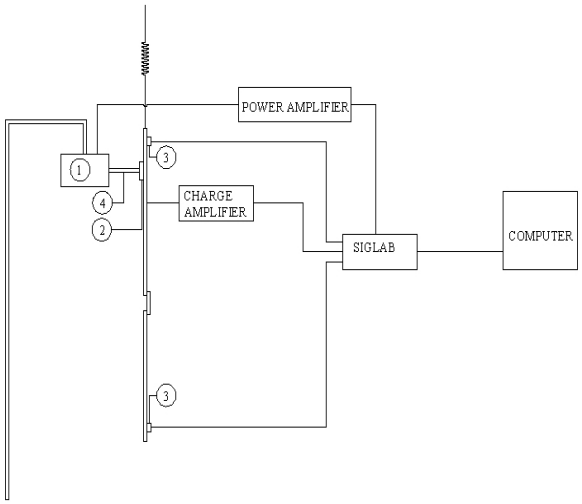

1 shaker

2 force transducer

3 accelerometers

4 stinger

Fig.4

Experimental setup

For the plate response measurements three piezoelectric accelerometers Bruel & Kiar 4507 were used. The reference sensitivities of these accelerometers are 100 mV/ms^{-2}. The working frequency range is [0.3-6000] Hz, with a resonance frequency at 18 KHz. The masses of those instruments are 4.8 gr, that is quite low compared with the masses of each plate.

However, the presence of instrumentation upon the measuring plate is responsible for a modification of the system response. This effect is obviously as much pronounced as lighter is the system under analysis with respect to the mass of the instrumentation. A preliminary analysis of the mass loading effect, induced by the accelerometers mounted upon the plate, has shown that at frequency below 2.5 KHz the frequency response function (FRF) of the system is not sensitive to the accelerometer mass. On the contrary, at higher frequency, the measured system response becomes sensitive to the presence of the accelerometer mass. In appendix C the results of some preliminary measurements, specifically carried out to show the mass loading effect in the system under analysis, and a correction formula (Sestieri et al., 1991), which provide the real FRF from the knowledge of the accelerometer mass and of the measured FRF, is provided.

The force transducer and the accelerometers were fixed to the plate using bee wax.

The structure is tested in a "free" condition, being connected to a rigid supporting structure through soft springs, so that the rigid body modes have natural frequencies lower than those of the bending modes. Thus, the rigid body (inertia) properties don't have any significant influence on the flexural modes.
The accelerometer responses were time integrated and squared to evaluate the kinetic energy. The total energy of each system was obtained as twice the kinetic energies.

6.1.3 TWO-PLATES ASSEMBLY

The first experiments were performed on two coupled plates connected by three straps of the same material with a width of 3·mm a length of 0.15·m and a thickness equal to 5·mm. To fix the straps upon the plates, white glue characterized by a strong stiffness is used.
The system was supported by a rigid frame through two soft springs, as shown in figure 2.
Before starting with the experimental measurements of the energy distribution among the subsystems, some preliminary analysis are necessary. In fact, the application of the theoretical-numerical procedure described in the previous chapter requires the knowledge of the modal parameters of the structure, in particular the natural frequencies, the mode shapes and the modal damping. The first two parameters were evaluated from a commercial Finite element software (FEMLab), whereas the modal damping was experimentally obtained. Moreover to verify the goodness of the numerical modal parameter evaluated, some preliminary measurements were performed to compare the numerical and the experimental natural frequencies.
In tab.4 a comparison between the first numerical and the experimental natural frequencies in the case of two plates coupled by means of 3 straps are presented showing a good agreement.

Experimental and numerical natural frequencies: two plate assembly			
Frequency	**Numerical [Hz]**	**Experimental [Hz]**	**Error %**
1	2.4	2.6	7.7
2	3.4	3.6	5.5
3	7.5	7.8	3.8
4	10.8	11	1.8
5	12	12.4	3.2

6	15	15.8	4.2
7	17.6	18	2.2
8	20	20.5	2.4
9	23	23	0
10	26	25.4	2.3
11	28.6	28	2.1
12	30.6	31	1.3
13	36	36.5	1.4
14	38	38.5	1.3
15	43	43	0
16	45	45	0
17	46.8	47	0.4
18	48.2	48.4	0.4
19	53.8	53	1.5
20	59	59.2	0.3

Tab.4

Except at very low frequency, the discrepancy between the natural frequency measured and those obtained using a FE package is very small. The disagreement at low frequency could be caused by two different motivations: the former is related to the modeling of the coupling between plates and straps and the second with an incorrect working of the accelerometers.

The modal damping was evaluated using the half power points defined by the following expression (Cremer et al., 1987):

$$\eta_i = \frac{\omega_a^2 - \omega_b^2}{\omega_{res}^2}$$

The obtained results are presented in figure 5.

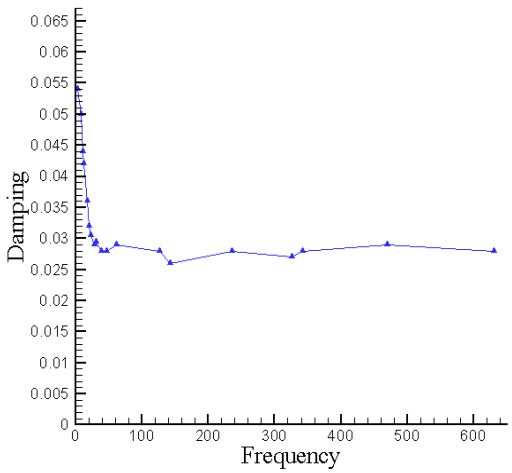

Fig.5

Modal damping

For most structures the loss factor tends to decrease with frequency, but in practice the choice of a constant value is often a good approximation. In the analysed case, it is evident that, except at very low frequency, the internal damping can be considered constant and equal to 0.029.

The first experiment was performed on two plates (plate 1 and plate 2 in tab.3). The plates were coupled by means of three straps as shown in figure 6.

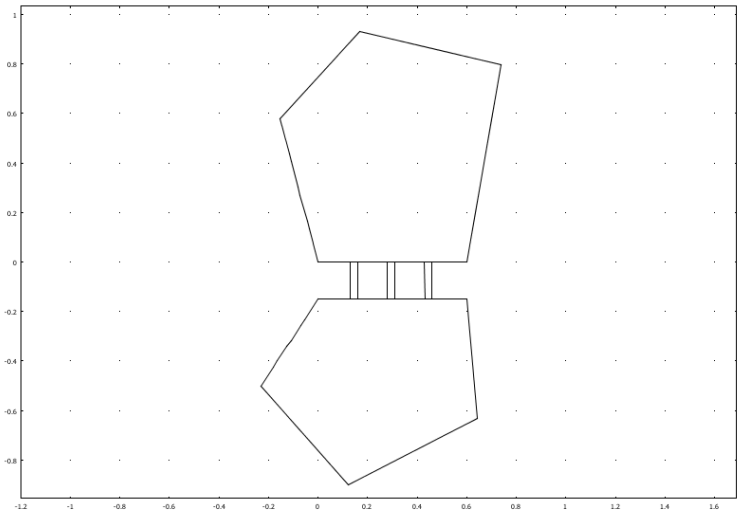

Fig. 6

Two plates: first configuration

The shaker was connected to the upper plate (plate 2) and the dynamical responses were obtained in 30 points for each plate. In figures 7 and 8 the energies time histories of the receiver system and of the excited system are shown, respectively.

The energy time histories shown in those figures were obtained only by averaging the data among the measured points of the plates, without doing any kind of filtering or smoothing actions while in figure 9 the dynamics of the two subsystems are plotted together after having done a time average.

It is evident that an equilibrium condition, where the two subsystems have the same energies, is rapidly reached.

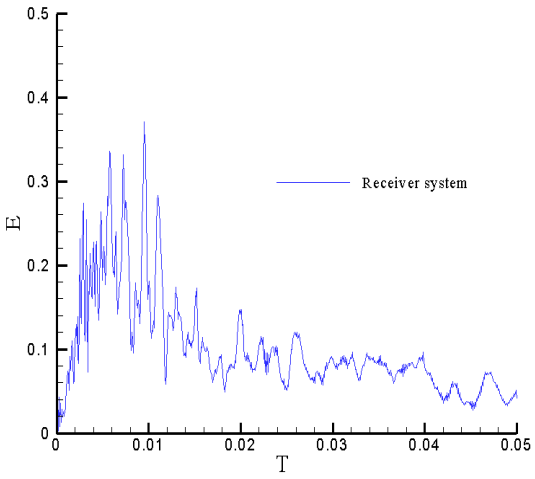

Fig.7

Energy time history of the receiver

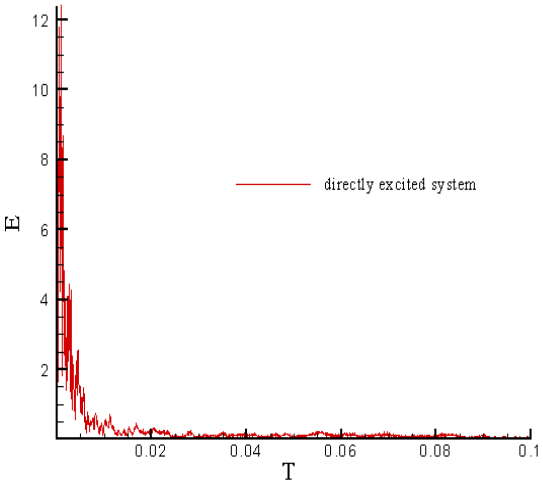

Fig.8

Energy time history of the excited system

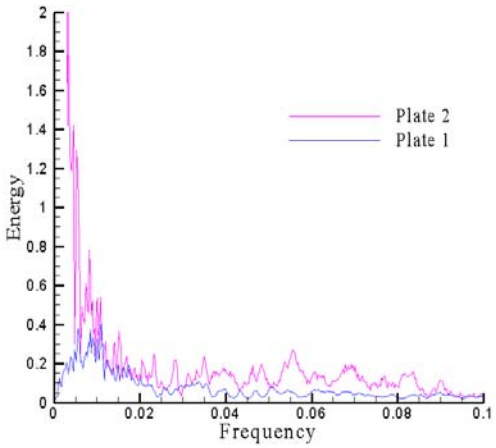

Fig.9

Averaged energy time histories

The maximum energy achieved by the receiver subsystem is quite low compared with the initial value provided to the plate directly excited. The motivation of this behaviour lies on the high value of the internal damping and in the weak coupling between the subsystems. In fact as already shown in a similar experimental measurement by Fahy and James, (1996) the stronger is the coupling the higher is the energy transmitted to the plate not directly excited. This increase of the energy level is unfortunately coupled to a fast decrease of the rise time, that, as already underlined in chapter 3, it could imply a difficulty to distinguish the dynamical behaviours of the two subsystems.

It is interesting to analyze in the system under analysis the changes in the energy distribution that appears increasing the strength of the coupling between the subsystems. For this reason another connecting element was inserted between the two plates, as shown in figure 10.

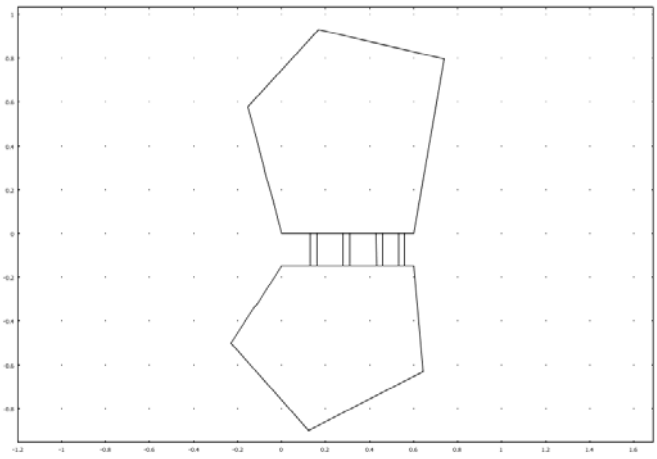

Fig.10

Two plates: second configuration

The effects produced adding another strap is also a reduction of the natural frequencies of the system, since it becomes stiffer. In table 5 a comparison of the first 5 natural frequencies of the systems with 3 and 4 connecting elements are presented.

Numerical natural frequencies: Two plates assembly, first and second configurations			
Frequency	**3 straps**	**4 straps**	**Difference %**
1	2.4 Hz	2.8 Hz	7.7
2	3.4 Hz	3.7 Hz	5.5
3	7.5 Hz	7.8 Hz	3.8
4	10.8 Hz	10.9 Hz	1.8
5	12 Hz	12.5 Hz	3.2

Tab.5

The difference between the natural frequencies for the two analysed systems is less than 6%.

While it is impossible to appreciate differences in the time histories of the direct excited subsystem, an increase of the maximum energy achieved by the receiver subsystem is evident, as shown in figure 11.

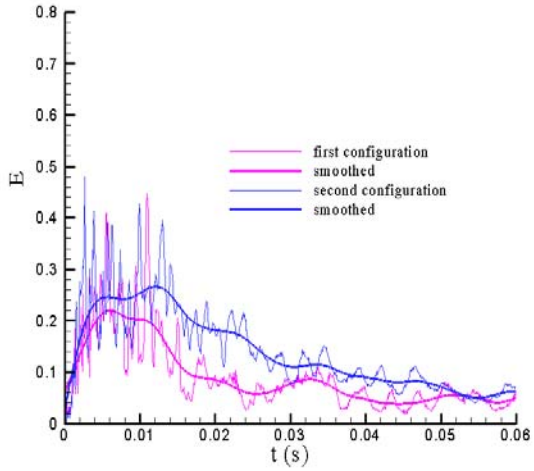

Fig.11

Energy time histories of the receiver subsystems for two different strength of the coupling

6.1.4 THREE-PLATE ASSEMBLY

The third configuration analysed is composed by three plate structures connected by straps. Notwithstanding the great interest demonstrated by the research community in the analysis of multi-body interaction [Finnveden, 1995; Heron, 1994; Mace, 2005], many problems are still open. In the previous chapter it was already underlined the difficulties met in SEA in the attempt the classical analysis to the case of three or more subsystems, due to the presence of the indirect coupling loss factor. Moreover, as the author's knowledge, no experimental measurements have been performed to check the validity of the developed theories.

The analysed configuration was obtained adding to the last configuration another plate of the same material, as shown in figure 4. The third plate is lighter than the other two, being its area quite small. The metallic structure that supports the system is connected with the heaviest plate through two springs. The shaker is located in the plate number 2.

A preliminary analysis of the frequency response function has allowed obtaining the natural frequencies of the system in order to compare the results obtained by the FEM package. In table 6, the results for the first 20 natural frequencies are compared with the

experimental results obtained using the same excitation force and measuring instruments of the previous experiment.

Experimental and numerical natural frequencies: three plate assembly			
Frequency	**Numerical [Hz]**	**Experimental [Hz]**	**Error %**
1	1.8	(*)	
2	3.1	3.9	20
3	3.7	4	7.5
4	6.3	6.6	4.5
5	9	9.8	8.1
6	11	11	---
7	14.9	15	0.6
8	16.6	16.8	1.2
9	17.8	18	1.1
10	24.8	25	0.8
11	27.2	27	0.73
12	31.3	32	2.1
13	35	36	2.7
14	37.2	37.4	0.53
15	42.3	43	1.6
16	44	44.54	1.12
17	47.3	48	1.45
18	49	49	---
19	52.5	53	0.94
20	58	60	3.3

Tab.6

Being the first natural frequency very low, it was impossible with the instrument used to measure it.

The system responses were average among 20 measuring points for each plate. The obtained average energies are shown in figure 12. The behaviours of the subsystem energies do not strongly vary from the test case made up of two coupled plates. In fact, like in the previous configuration, the energy of the directly excited subsystem decreases due to its internal damping and to the energy flow to the other two plates. The receiver subsystems after an initially increase of their energy, given from the direct excited subsystem, decreases their energy due to their internal dissipation. An “equilibrium” condition is achieved after approximately 0.01 second, when the three energies are equal. Starting from this condition, the subsystem energies continue to oscillate but tend to zero in the same way.

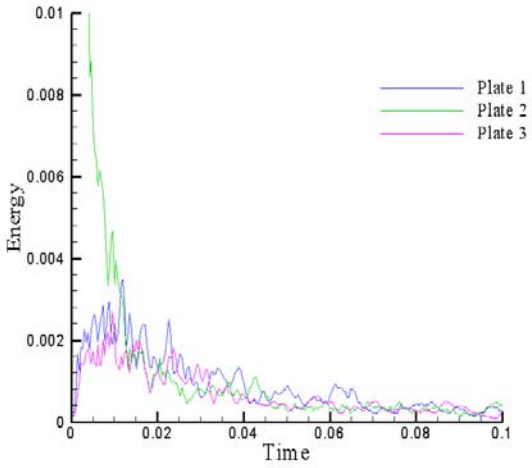

Fig.12

Averaged energy time histories

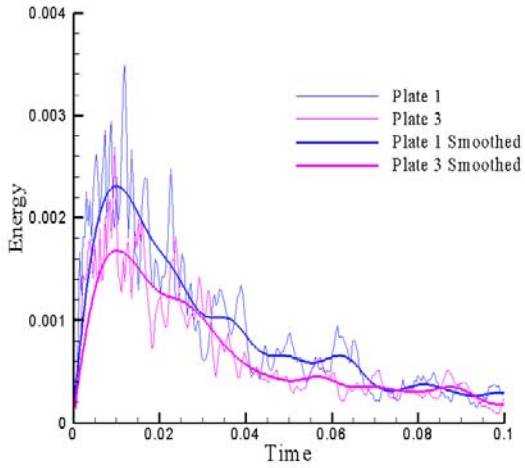

Fig. 13

Energy time histories of the receivers

It is interesting to compare the dynamical behaviour of the two receiver subsystems (figure 13). Even if the trends are almost the same, some differences can be observed in the maximum value reached. In fact, the first plate, characterized by a higher area, achieves a higher maximum energy with respect to the third plate. Unfortunately it is not easy to discern the rise times, i.e. the times at which they assumes their maximum energy, for the two subsystems. Probably to distinguish a change in the rise time, it would have been necessary to strength more the coupling between the subsystems, increasing the number of coupling elements.

6.2 COMPARISON WITH THE THEORETICAL RESULTS

In this paragraph the energies measured in the experimental campaign described in the previous sections are compared with the results obtained by applying the TAEA method. The theoretical evaluation of the energy of each subsystem is obtained through 5 steps:

1. Evaluation of the mass M and the stiffness K matrices of the analysed systems, using the commercial finite element package FemLab.
2. Determination of the eigenvalues λ_i and the eigenvectors U of the whole system
3. Partition of M, K, λ and U into subcomponents corresponding to different subsystems

4. Determination of the coefficients $a_{ij}, b_{ij}, c_{ij}, d_{ij}$ defined in chapter 5.

5. Evaluation of the energies of each subsystem using the formula (5.13).

To simplify the expressions that provide the energy distribution among the subsystems (eq 5.13), an uniform probability density function is assumed. In this case the *i*-th marginal probability of the system $\Pi_i(\omega_i)$ values 0 except for a frequency band $\left[\omega_i^-, \omega_i^+\right]$, where:

$$\omega_i^- = \omega_i - \frac{D\omega}{2}$$

$$\omega_i^+ = \omega_i + \frac{D\omega}{2}$$

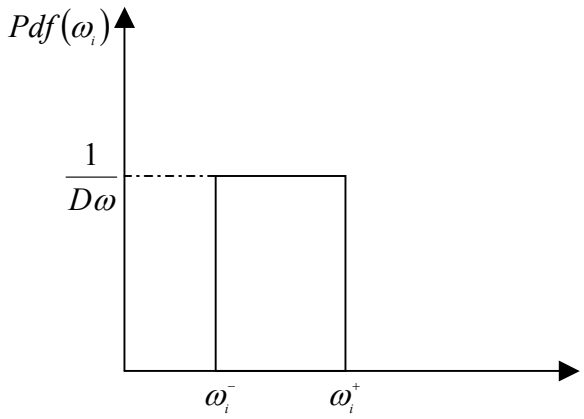

Fig. 14

Uniform *Pdf*

in which $\Pi_i(\omega_i)$ is equal to $\frac{1}{D\omega}$, as shown in figure 14. Since $D\omega$ is independent of frequency, the *Pdf* for all the natural frequencies are similar. It is interesting to notice that Lyon (Lyon, 1975) used the same hypothesis to achieve the Sea equations.

The first analysed configuration is the coupling between two plates, connected through three straps. Using a commercial FE package with approximately 2000 degrees of freedom (see figure 15), the mass and the stiffness matrices of the whole system are obtained. Hence, the eigenvalues and the eigenmodes of the system are determined. This data are later post-processed to discern the components related to the first and to the second subsystems.

After having compared the measured natural frequencies and those evaluated with the FE package (as already underlined in the previous section), these data are introduced in a Fortran code that provides the energy time histories of the subsystems.

Only the first 200 natural frequencies are taken into account in the summation (5.13), implying a quite low computational cost. Increasing the number of terms added in the summation (i.e. increasing the mode order taken into account), none significant variation appears in the energy time histories of the subsystems.

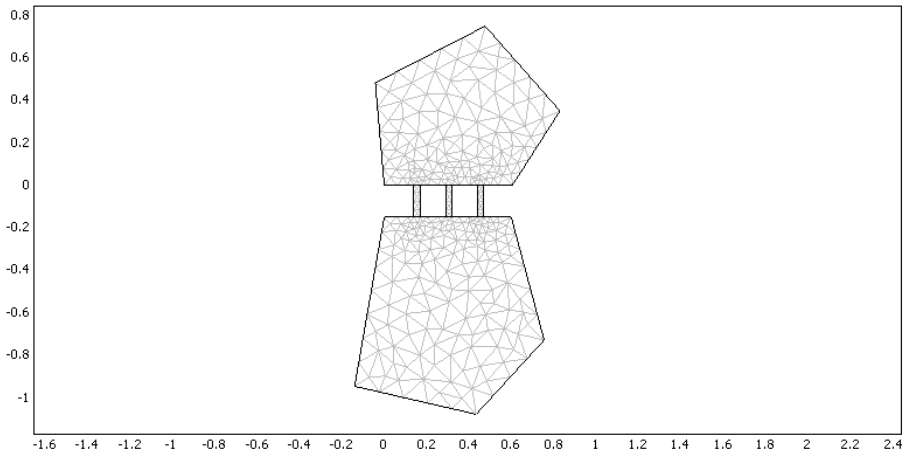

Fig.15

Numerical mesh: 2000 Degrees of Freedom

This means that only the lower order eigenmodes affects the energy distribution, since increasing the frequency, the amplitude of the vibrations becomes small and provides small contribution to the dynamic response of the system. The last assertion confirms the theoretical property underlined in chapter 3, that states the ensemble energy average can be obtained on the basis of the lowest natural frequencies and mode-shapes, since the coefficients $a(\omega_i)$ tends to zero as the frequency increases.

In figure 16 the measured energy time histories of the two subsystems are compared with the theoretical results, showing a very good agreement.

To better understand the behaviour of the two subsystems an enlargement of the behaviour of the direct excited subsystem and of the receiver one are shown in figures 17 and 18.

Only at an early stage the discrepancy between the two curves (the numerical curve and the theoretical one) is quite relevant.

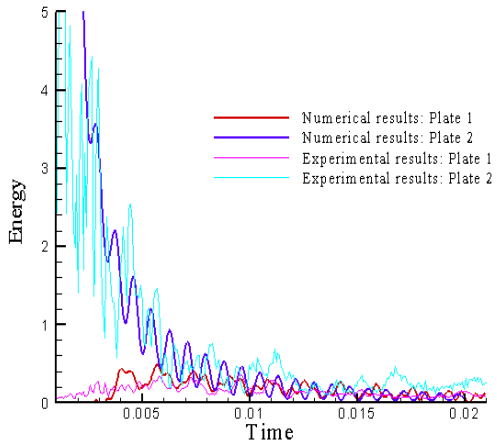

Fig.16

Experimental and numerical energy time histories

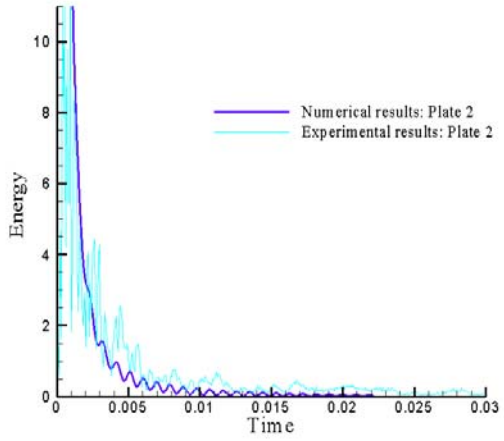

Fig 17

Experimental and numerical energy time histories

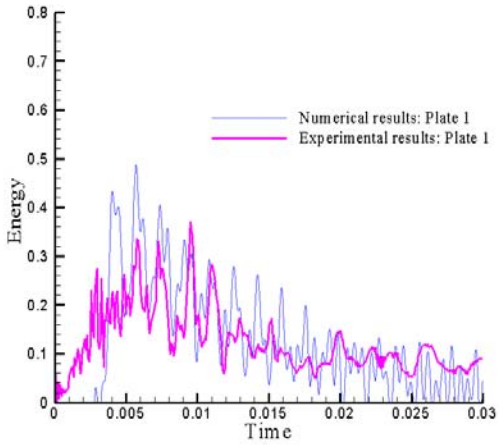

Fig 18

Experimental and numerical energy time histories

But, as shown in chapter 3, the time asymptotic envelope presents a lower bound time limit of validity, which represents the condition that allow to neglect the terms of order t^{-3} with respect to those of order t^{-2} that are included in the formulation. Hence, at early times the asymptotic energies are not representative of the real response of the system.

Increasing the number of natural frequencies used in the numerical computation of the energies, none significant changes appear in the energy time histories of the two subsystems. This confirms the behaviour of the $a_{ij}(\omega_i)$ coefficients described in chapter 3, *i.e.* that the coefficients $a(\omega_i)$ in the summation (3.7) tend rapidly to zero as *i*

increases. This means that the prediction of the energy sharing between two subsystems can be obtained from the sole knowledge of the first eigenvalues of the system, which can be easily evaluated using a mesh with few degrees of freedom and consequently low computational cost.

Let us consider the three-plate system. A mesh of 4000 degrees of freedom is used to resolve the system (figure 19). The system is partitioned into three different subsystems, each of them composed by the degree of freedom corresponding to a single plate, as shown in figure 20.

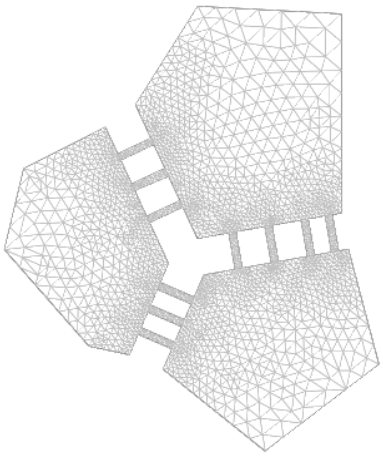

Fig.19

FE mesh for the three plate assembly

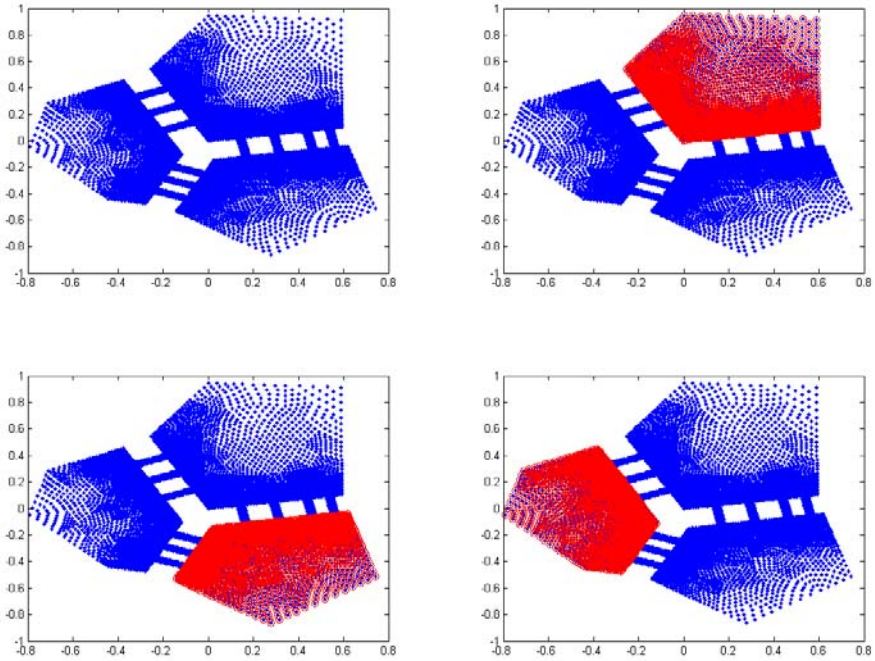

Fig.20

Partitioned into three different subsystems

In figures 21, 22 and 23 the measured energy time histories of each subcomponents are compared with the numerical results obtained by applying the procedure previously described.

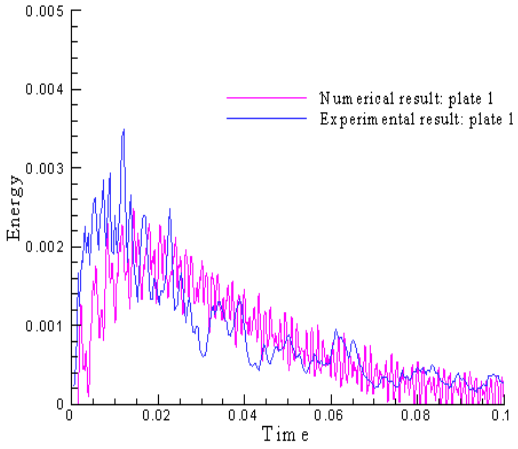

Fig.21

Energy time history of the first plate

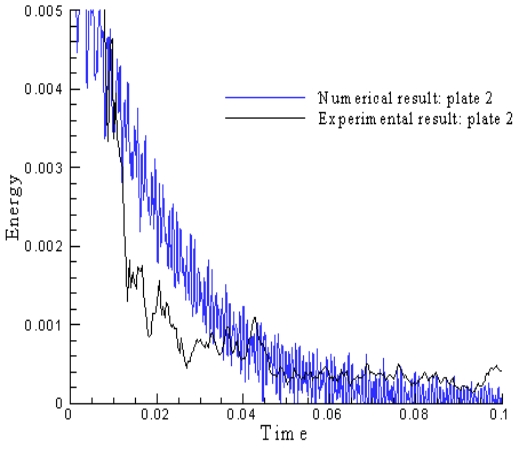

Fig.22

Energy time history of the second plate

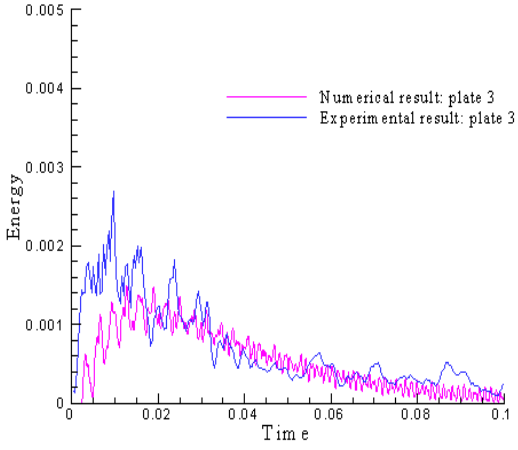

Fig.23

Energy time history of the third plate

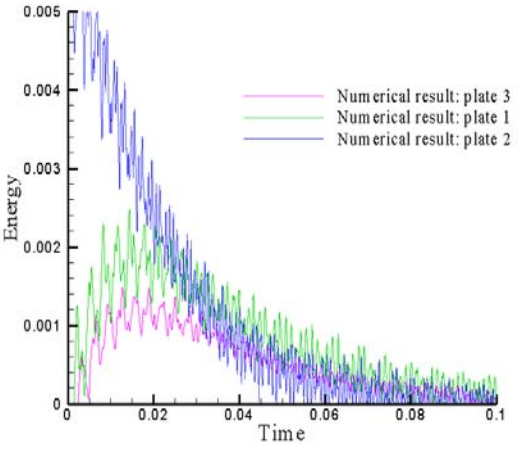

Fig.24

Energy distribution among the subsystems: theoretical results

As already underlined for the configuration composed by two coupled plates, a discrepancy between the theoretical results and experimental ones is present at the first instants, where the time asymptotic envelope does not match the experimental results. The dynamical behaviour of the system under analysis seems to be a bit faster than the theoretical trends obtained. Different motivations could have caused this disagreement; the most important are the damping characterization and the modelling of the

connecting elements. As the former, to simplify the expression in the theoretical procedure the damping is chosen constant and equal to 0.027, this is obviously an approximation, as shown in figure 4. In fact, at low frequencies the damping level is quite higher than the asymptotic value. Since the low order modes are those which higher affect the system behaviours, the introduction of the correct damping, as a function of the frequency, could provide better results.

Another parameter which introduces a certain degree of variability is the coupling among the subsystems. In fact, to improve the agreement between the theoretical and numerical results, it could be important to improve the finite element modelling of the real structure, making greater care on the characterization of the straps.

CHAPTER 7: CONCLUSION

There are many areas of engineering in which the systems under analysis are very complicated, since they consist of a very large number of different jointed subcomponents, such as ship hulls or aircraft fusalages.

It has already underlined the direct correlation that the complexity has with the uncertainty. In a complex system the presence of a high number of heterogeneous subsystems (beams, plates, acoustic cavities, etc.) and, above all, the high number of joints connecting the components are sources of a certain degree of variability. Moreover, at high frequency the response of the system becomes increasingly sensitive to small perturbations of its parameters: even small variations in geometrical component dimensions, material properties and assembly tolerances imply large variations in the mid- and high- frequency responses.

These considerations lead to introduce a different way of tackling the vibro-acoustic problem of complex systems, rather than classical deterministic approaches based on a discretization of the continuum domain, that would allow a reduction of the computational cost, decreasing the number of degrees of freedom and also takes into account the random nature of the phenomena.

In this work the time asymptotic ensemble energy average has been used to deal with complex and uncertain systems, namely TAEA. This new approach belongs to the class of the energetic methods, since the system dynamic is described in terms of global parameters (the energies of a subset of the system) and a statistical approach is developed by introducing random natural frequencies, whose variability is due to stochastic perturbations of physical and geometrical parameters of the system.

The originality of this method lies in the development of an asymptotic expansion technique, that permits to evaluate the energy distribution among the subcomponents of a system in both transient and steady state conditions in terms of only few modes of the system and the related marginal probabilities, determined with a low computational cost.

TAEA allows evaluating the unsteady energy sharing between two coupled conservative as well as nonconservative systems. In the first case two different phases can be distinguished: an initial transient controlled by a term vanishing with t^{-1}, which is responsible for the energy sharing between the two subsystems and a second phase where the energy flow tends to zero approaching to a steady-state condition, where a

particular energy distribution that is something reminiscent of the EEP in statistical mechanics, is obtained.

The possibility to obtain an energy distribution law in structural dynamics of complex systems similar to the EEP stated in Statistical Mechanics has led to investigate the EEP in depth, trying to understand the conditions under which it holds, the definitions introduced in SM and how these last could be translated to structural dynamics. Its importance relies on the immediate prediction it provides of the energy distribution among the particles, or degrees of freedom, of the considered system.

An important element of this thesis has represented the attempt to define the conditions that can lead to the appearance of EEP in engineering systems and to identify the factors that inhibit or promote the reaching of energy equipartition conditions.

The analysis has explored the field of linear and nonlinear vibrations, the effects of non-homogeneity and localization, the weak and strong coupling as well as the effect of the initial energy distribution among the subsystems.

TAEA also deals with non conservative systems. With respect to conservative case, the dynamics of a damped system is more complicated. While the trend of the system directly excited remains monotonic because of the dissipation effects and the energy flow going to to the receiver, this last undergoes two opposite effects: an energy increase due to the energy flow from the directly excited subsystem and a tendency to decrease due to its inherent dissipation. The combination of the two effects leads to an increasing of the energy of the receiver at the early stage, while its energy decays at later times because of the dissipation effects acting in both systems; hence, the resulting trend of the receiver energy exhibits a maximum.

It is important to underline that in both cases (conservative and nonconservative systems) the developed method makes a breakthrough in the analysis of complex and uncertain system, since it allows to describe the energy sharing between two subsystems from the sole knowledge of a few macro parameters of the systems easy to evaluate. In particular, when identifying the first natural frequencies and mode-shapes of the whole system (this analysis has low computational cost, since a numerical grid with few degrees of freedom is sufficient for their evaluation), a numerical simulation allows to evaluate the energy time histories of the system components.

When attempting to establish a new tecniques for the prediction of structural dynamic and structural acoustic response of a complex system a necessary comparison with SEA, which represents the most widely used method up to now, is necessary to consider.

In the proposed method two main problems met in the attempt applying SEA to the study of complex systems are overcome: the former is the necessity of *a priori* informations upon the systems, for instance the coupling loss factors, the second is the impossibility to have information of the transient dynamics, since only steady state excitations are up to now be considered (except for simple structures, where a modified SEA, namely TSEA, would provide the transient dynamics of the system).

The developed method (TAEA) does not need any *a priori* information, since this method allows describing the energy sharing between two subsystems from the sole knowledge of a few macro parameters of the systems easy to evaluate.

As to the second critical element of SEA, it is important to underline that TAEA provides the energy time histories of system components loaded by an impulsive excitation. Considering the possibility to extend easily the theory to the case of a general time dependent excitation, it is evident the wide class of engineering problems that can be analysed, such as the analysis of the vibro-acoustical response of a section of the ship hull excited by slamming loads, breaking waves and so on.

An important element of this thesis has represented the numerical and experimental validation of TAEA, that were lacking before.

A core element of this thesis was the improvements performed on the TAEA to render the procedure applicable to a more wide class of engineering problems.

The first has regarded the possibility to take into account the effects of the coupling forces, overcoming the limitation of weak coupling that restricted the use of the previous method. This has implied the evaluation of subsystem energies as a sum of two terms: the first is the energy component obtained when the other subsystems are considered blocked, the second is related with the motion of the other subsystems, instead.

The second innovating element is given by the inclusion of interaction between more than two subsystems. In fact, the theory developed allows the determination of the energy sharing among three subsystems, being very easy the extension to the general case of N subsystems.

The TAEA method and these new extension of the theory were validated through numerical simulations and experimental measurements performed on two different setup (the two-plate and the three-plate assemblies) showing a good agreement.

CHAPTER 8: PERSPECTIVES

This work is concerned with the development of a predictive method for describing the energy sharing among complex engineering vibrating system. For the purpose of validation, the applications have been limited to deal with some simple structures. Thus, the work in this thesis offers a starting point to further study, the investigation in the near future and some possible perspectives may be summarized as follows.

A great potentiality of the method lies in the possibility to describe the energy sharing between two generic complex subsystems from the sole knowledge of the first natural frequencies and mode-shapes of the whole system. This analysis has low computational cost, since a numerical grid with few degrees of freedom is sufficient for their evaluation. To fully understand this ability, the TAEA method should be applied to a more complex system; in particular the possibility to verify this method in a real structure, such as a section of a ship, is under construction.

In chapter 6, some preliminary results regarding a sensitivity analysis of the energy distribution from the strength of the coupling among the subsystems are shown. A systematic experimental campaign should be performed to better understand this phenomenon, varying the strength of the coupling in a wider range.

Moreover, in that frame the study of the maximum energy achieved by the receiver subsystem has a central role in prediction capabilities of a structural tool at the design stage. For this reason, it would be important to obtain a theoretical determination of this condition, validated through an experimental campaign.

From a theoretical point of view, an important improvement to obtain is the possibility to generalize the TAEA to include the case of an arbitrary excitation force varying in time; in this way the procedure would become applicable to a more wide class of engineering problems.

CHAPTER 9: REFERENCES

Anderson, P.W., 1958. *Absence of diffusion in certain random lattices*. Physical Review 109(5), 1492-1505.

Arnold, V. I. and Avez, A., 1968 Ergodic problems of classical mechanics, W. A. Benjamin, Inc., New York.

Baowen, L., Hong, Z. and Bambi, H., 2001. *Can disorder induce a finite thermal conductivity in 1D lattice?*. Physical Review Letters 86 (1), 63-66.

Benettin, G., 2005. *Time-scale for energy equipartition in a two dimensional FPU model*. Chaos 15, 015108.

Bies, D.A.and Hamid, S., 1980. *In Situ determination of loss and coupling loss factors by the power injection metho*d. Journal of Sound and Vibration 70(2), 187-204.

Bogadanov, J.L. and Kozin, F., 1962. *Moments of the output of linear random systems*, Journal of Acoustical Society of America, 34, 1063-1068.

Bolt, R.H. and Roop, R.W., 1950. *Frequency response fluctuations in rooms.* Journal of the Acoustical Society of America, 22(2), 280-289.

Bouthier, O.M. and Bernhard, R.J., 1995. *Simple models of energy flow in vibrating membranes*. Journal of Sound and Vibration, 182(1), 129-147.

Brebbia, C.A., 1984. *The Boundary Element Method for Engineers*. Pentech, London.

Cacciolati, C. and Guyader, J.L, 1994. *Measurement of S.E.A. Coupling Loss Factors using Point Mobilities*. Philosophical Transactions of the Royal Society: Physical and Engineering Sciences, A 346, 465-475.

Carcaterra, A., 1992. *An entropy formulation for the analysis of energy between mechanical resonators*. Mechanical Systems and Signal Processing, 16(5), 905-920.

Carcaterra, A., 2005. *Ensemble energy average and energy flow relationships for nonstationary vibrating systems.* Journal of Sound and Vibration 288, 751-790.

Carcaterra, A., 2005a. *Time asymptotic ensemble energy average: modelling the energy dynamics of uncertain and large vibrating systems*. Keynote Lecture, NOVEM 2005, St. Raphael, France.

Carcaterra, A. and Adamo, L., 1999. *Thermal analogy wave energy transfer: theoretical and experimental analysis*. Journal of Sound and Vibration, 226(2), 253-284.

Carcaterra, A., Dessi, D., Mastroddi, F., 2005. *Hydrofoil vibration induced by a random flow: a stochastic perturbation approach.* Journal of Sound and Vibration, 283, 401-432.

Carcaterra, A. and Sestieri, A., 1995. *Energy density equations and power flow in structures.* Journal of Sound and Vibration 188(2), 269-282.

Carcaterra, A., and Sestieri, A., 2003. *High frequency vibrations and dynamics of complex resonators.* In Recent Research Developments in Structural Dynamics. Angelo Luongo Trivandrum, 195-223.

Çelik, C. and Akay, A., 2000. *Dissipation in solids: thermal oscillations of atoms*. Journal of acoustical society of America 108(1), 184-191.

Chirikov, B.V., Izrailev, F.M. and Tayursky, V.A., 1973. *Numerical experiments on the statistical behaviour of dynamical systems with a few degrees of freedom.* Computer Physics Communications, 5, 11-16.

Cremer, L., Heckl M. and Ungar, E.E., 1987. *Structure-borne sound*. second edition. Springer-Verlag, Berlin.

Cretegny, T., Dauxois, T., Ruffo, S. and Torcini, A., 1998. *Localization and equipartition of energy in the beta-FPU chain: Chaotic breathers*, Physica D, 121, 109-115.

DeJong, R.G., 1997. *An approach to the statistical energy analysis of strongly coupled systems*. Proc. IUTAM Symposium on Statistical Energy Analysis, Southampton (UK).

De Luca J., Lichtenberg, A.J.and Ruffo, S., 1999. *Finite times to equipartition in the thermodynamic limit.* Physical Review E, 60(4), 3781-3786.

De Rosa, S., Franco, F. And Ricci, F., 1999. *Introduzione alla tecnica statistico-energetica (S.E.A)*. Liguori Editore, Napoli.

Dowell, E.H., and Tang, D., 2003. *Dynamics of very high dimensional systems.* World Scientific Publishing Co., Singapore.

Fahy, F.J., 1994. *Statistical energy analysis: a critical overview*. Philosophical Transactions of the Royal Society of London, A346, 431-447.

Fahy, F.J. and James, P.P., 1996. *A study of the kinetic energy impulse response as an indicator of the strength of coupling between SEA subsystems.* Journal of Sound and Vibration 190(3), 363-386.

Fahy, F.J. and Mohammed, A.D., 1992. *A study of uncertainty in application of SEA to coupled beam and plates systems, part I: computational experiments.* Journal of Sound and Vibration 158(1), 45-67.

Fermi, E., Pasta, J. and Ulam, S.M., 1965. *Studies of non linear problems*, Los Alamos 1940,1955; in: Fermi E. Collected papers, II, 978, Academia de Lincei and Univ. of Chicago Press.

Finnveden, S.F., 1995. *Ensemble averaged vibration energy flows in a three element structure*. Journal of sound and vibration 187 495-529.

Finnveden, S., 1998. *Coupling strength as an indicator of the applicability of Statistical Energy Analysis*, ISVR Technical Report 268.

Ford, J., 1961. *Equipartition of energy for nonlinear systems.* Journal of mathematical Physics 2, 387-393.

Ford, J., 1992. *The Fermi-Pasta-Ulam problem: paradox turns discovery*. Phys Rep 213 271-310.

Garrido, P.L., Hurtado, P.I. and Nadrowsky, B., 2001. *Simple one-dimensional model of heat conduction which obeys Fourier's Law*. Physical Review Letters 86, 5486-5489.

Gibbs, J.W., 1902. *Elementary principles in Statistical Mechanics developed with especial reference to the rational foundation of thermodynamics*. Charles Scribner's Sons, New York.

Ghanem, R.G. and Spanos, P.D., 2003. *Stochastic Finite Elements. A spectral approach* Revised Edition. Dover Publications, New York.

Graff, K.F., 1975. *Wave motion in elastic solid*, Dover Publications, Inc. New York.

Heron, K.H., 1994. *Advanced statistical energy analysis*. Phylosophical Transactions: Royal Society of London 346, 501-510.

Ibrahim, R.A., 1987. *Structural dynamics with parameters uncertainties.* Applied Mechanics Review 40(3), 309-328.

Ichchou, M.N., Le Bot, A., and Jezequel, L., 1997. *Energy models of one-dimensional multi-propagative systems*. Journal of Sound and Vibration, 201, 535-554.

Ichchou, M.N., Le Bot, A., and Jezequel, L., 2001. *A transient local energy as an alternative to transient SEA: wave and telegraph equations*, Journal of Sound and Vibration, 246, 829-840.

James, P.P. and Fahy, F.J., 1997. *A technique for the assessment of strength of coupling between SEA subsystem: experiments with two coupled and two coupled rooms*. Journal of Sound and Vibration 203(2), 265-282.

Kato, A. and Jou, D., 2001. *Breaking of equipartition in one-dimensional heat-conducting systems*. Physical Review E, 64 0522011, 1-4.

Khinchin, A. I. and Khinchin, A.Y., 1949. *Mathematical Foundations of Statistical Mechanics*. translated from the Russian by G. Gamow, Dover Publications, Inc., Mineola, New York.

Lai, M.L. and Soom, A., 1990. *Prediction of transient vibration envelopes using statistical energy analysis techniques.* Journal of Vibration and Acoustics, 112, 127-137.

Lai, M.L. and Soom, A., 1990a. *Statistical energy analysis for the time integrated transient response of vibrating systems.* Journal of Vibration and Acoustics, 112, 206-213.

Landau, L.D. and Lifšits, E.M., 1978. *Fisica Statistica.* Editori Riuniti, Roma (in Italian).

Langley, R.S., 1989. *A general derivation of the statistical analysis equation for coupled dynamic systems.* Journal of Sound and Vibration, 135, 499–508.

Langley, R.S., 1992. *A wave intensity technique for the analysis of high frequency vibration*. Journal of Sound and Vibration, 159(3), 483–502.

Langley, R.S., 1995. *On the vibrational conductivity approach to high frequency dynamics for twodimensional structural components.* Journal of Sound and Vibration, 182, 637–657.

Langley, R.S. and Bremner, P.G., 1999. *A hybrid method for the vibration analysis of complex structural-acoustic systems.* Journal of the Acoustical Society of America 105, 1657-1671.

Langley, R.S. and Cotoni V., 2004. *Response variance prediction in the statistical energy analysis of built-up systems.* Journal of the Acoustical Society of America 115(2), 706-718.

Lase, Y., Ichchou, M.N. and Jézéquel, L. , 1996. *Energy flow analysis of bars and beams: theoretical formulations,* Journal of sound and vibration 192 (1), 281-305.

Le Bot, A., Ichchou, M.N. and Jezequel, L., 1995. *Smooth energy formulation for multi-dimensional problem*. Proc. Euro-Noise 95, Vol 2, 423-428.

Livi, R., Pettini, M., Ruffo, S., Sparpaglione, M. And Vulpiani, A., 1985. *Equipartitions thresholds in nonlinear large Hamiltonian systems: The Fermi Pasta Ulam*. Physics Rev A 31(2), 1039-1045.

Lyon, R.H., 1975. *Statistical energy analysis of dynamical systems: theory and applications*. Cambridge MIT Press.

Lyon, R.H. and DeJong, R.G., 1995. *Theory and application of statistical energy analysis 2nd edition.* Butterworth- Heinemann, Boston.

Lyon, R. H. and Maidanik, G., 1962. *Power flow between linearly coupled oscillators.* Journal of the Acoustical Society of America, 34, 623-639.

Mace, B.R., 1992. *Power flow between two continuous one-dimensional subsystems: a wave solution*. Journal of Sound and Vibration 154, 289-319.

Mace, B.R., 1994. *On the statistical energy analysis hypothesis of coupling power proportionality and some implications of its failure*. Journal of Sound and Vibration, 178(1), 95–112.

Mace, B.R., 2005. *Statistical energy analysis: coupling loss factors, indirect coupling and system modes*. Journal of Sound and Vibration 279, 141-170.

Mace, B:R. and Rosenberg, J., 1998. *The Sea of two coupled plates: an investigation into the effects of subsystem irregularity*. Journal of Sound and Vibration 212(3), 395-415.

Maidanik G., 1962. *Response of ribbed panels to reverberant acoustic field*. Journal of Acoustical Society of America 34, 809-826.

Magionesi, F. and Carcaterra, A., 2005. *An investigation on the energy equipartition principle in structural dynamics of uncertain system*. Proc. International Conference of Sound and Vibration (ICSV12), Lisbon (Portugal).

Maidanik, G., and Dickey, J., 1997. *On the external input power into coupled structures*. Iutam Symposium on Statistical Energy Analysis, 197-208. Kluwer Academic Publishers, Dordrecht.

Manning, J.E. and Lee, K., 1968. *Predicting mechanical shock transmission.* Shock and Vibration bulletin, 37(4), 65-70.

Maxit, L. and Guyader, J.L., 2001. *Estimation of SEA coupling los factors using a dual formulation and FEM modal information, part I: theory*. Journal of Sound and Vibration, 239(5), 907-930.

Morse, P.M., and Uno Ingard, K., 1968. *Theoretical Acoustics*. Princeton University Press, Princeton, New Jersey.

Nefske, D.J. and Sung, S.H., 1987. *Power flow finite element analysis of dynamic systems: basic theory and application to beam.* ASME Publication NCA-3: Statistical Energy Analysis, 47-54.

Nelson, E., 2001. *Theories of Brownian Motion. Second edition*. Princeton University Press, Princeton, New Jersey.

Newland, D.E., 1987. *An introduction to random vibrations and spectral analysis. Second Edition*. Longman Scientific & Technical, London.

Pinnington, R.J. and Lednik, D., 1996. *Transient statistical energy analysis of an impulsively excited two oscillator system.* Journal of Sound and Vibration 189, 249-264.

Pinnington, R.J. and Lednik, D., 1996. *Transient energy flow between two coupled beams*. Journal of Sound and Vibration 189, 265-287.

Pradlwarter, H.J. and Schueller, G.I., 1997. *On advanced Monte Carlo simulation procedures in stochastic structural dynamics*. International Journal of Non-linear Mechanics, 32(4), 735-744.

Rayleigh, J.W.S., 1945. *The theory of sound*, Dover, New York.

Rice, S.O., 1954. *Mathematical analysis of random noise*. Bell System Technical Journal, 23 1944 46-156. Reprinted in Selected papers on noise and stochastic processes, Dover, New York.

Schuss, Z., 1980. *Theory and Applications of Stochastic Differential Equations*. Wiley, New York.

Sestieri, A., Salvini, P. and D'Ambrogio, W., 1991. *Reducing scatter from derived rotational data to determine the FRF of connected structures*. Mechanical System and Signal Processing 5(1), 25-44.

Smith, P.W., 1979. *Statistical models of coupled dynamical systems and the transition from weak to strong coupling*. Journal of Acoustical Society of America 65, 695-698.

Snyder K.A. and Kirkptrick T.R., 1999. *The influence of Anderson localization on the mode decay of excited nonlinear systems*. Annalen der Physik (Leipzig) **8**, 241-244.

Soize, C., 1993. *A model and numerical method in the medium frequency range for the vibroacoustic predictions using the theory of structural fuzzy*. Journal of Acoustical Society of America, 94, 849-865.

Soize, C., 1999. *Reduced models for structures in the medium-frequency range coupled with internal acoustic cavities.* Journal of Acoustical Society of America, 106, 3362-3374.

Soong, T.T., 1973. *Random Differential Equations in Science and Engineering*. Academic Press, New York.

Soong, T. and Bogdanoff, J., 1963. *On the natural frequencies of a disordered linear chain of n degrees of freedom*. International Journal of Mechanical Sciences, 5, 237-265.

Szopa, J., 1986. *Application of stochastic sensitivity functions to chaotic systems*. Journal of Sound and Vibration, 104 (1), 176-178.

Tolman, R.C., 1980. *The principles of Statistical Mechanics*. Dover Publications, New York.

Totaro, N. and Guyader, J.L., 2006. *SEA substructuring using cluster analysis: The MIR index*. Journal of Sound and Vibration, 290(1-2), 264-289.

Weaver, R.L. and Lobkis, O.I., 2000. *Anderson localization in coupled reverberation rooms*. Journal of Sound and Vibration 231(4), 1111-1134.

Wolhever, J.C. and Bernhard R.J., 1992. *Mechanical energy flow models of rods and beams.* Journal of Sound and Vibration 153(1), 1-19.

Woodhouse, J., 1981. *An approach to the theoretical background of statistical energy analysis*

applied to structural vibration. Journal of Acoustical Society of America, 69(6), 1695-1709.

Xing, J.T. and Price, W.G., 1997. *The energy flow equation of continuum dynamics.* Iutam Symposium on Statistical Energy Analysis, 83-94. Kluwer Academic Publishers, Dordrecht.

Yap, F.F. and Woodhouse, J., 1996. *Investigation of the damping effects on statistical energy analysis of coupled structures.* Journal of Sound and Vibration 197 (3), 351-371.

Zienkiewicz, O.C., and Taylor, R.L., 1989. *The Finite Element Method: Basic Formulation and Linear Problems.* Mac Graw-Hill Book Company , London.

APPENDIX A: the probabilistic asymptotic expansion of the energy term for conservative system.

In this appendix, the asymptotic expansion of the time dependent integrals in equation (5.16) is developed.

In the expression of the ensemble energy average two different types of terms are present: the term for, which $i = j$, which are dependent on ω_i, and those for which $i \neq j$, which are dependent on ω_i and ω_j.

Let us considered the first type. Integration by parts of this term with respect to ω_i produces:

$$\int_{\omega_i^-}^{\omega_i^+} \Pi(\omega_i) d_{ii}^{(12)}(\omega_i) \cos 2\omega_i t \, d\omega_i = \cdot$$

$$\frac{1}{2t}\left[\Pi(\omega_i) d_{ii}^{(12)}(\omega_i) \sin 2\omega_i t\right] \Big|_{\omega_i^-}^{\omega_i^+} - \frac{1}{2t} \int_{\omega_i^-}^{\omega_i^+} \frac{d}{d\omega_i}\left[\Pi(\omega_i) d_{ii}^{(12)}(\omega_i)\right] \sin 2\omega_i t \, d\omega_i$$

Integrating again by parts the last integral, the following expression is obtained:

$$\int_{\omega_i^-}^{\omega_i^+} \Pi(\omega_i) d_{ii}^{(12)}(\omega_i) \cos 2\omega_i t \, d\omega_i = \frac{1}{2t}\left[\Pi(\omega_i) d_{ii}^{(12)}(\omega_i) \sin 2\omega_i t\right] \Big|_{\omega_i^-}^{\omega_i^+} + \frac{1}{4t^2}\left[\frac{d}{d\omega}\left(\Pi(\omega_i) d_{ii}^{(12)}(\omega_i)\right) + \right.$$

$$\left. - \frac{1}{4t^2} \int_{\omega_i^-}^{\omega_i^+} \frac{d^2}{d\omega^2}\left[\Pi(\omega_i) d_{ii}^{(12)}(\omega_i)\right] \cos 2\omega_i t \, d\omega_i \right.$$

Integration by parts can be iterated, leading to an infinite series of terms of order t^{-1}, t^{-2}, t^{-3}....., that can be expressed as follows:

$$\int_{\omega_i^-}^{\omega_i^+} \Pi(\omega_i) d_{ii}^{(12)}(\omega_i) \cos 2\omega_i t \, d\omega_i = \sum_{i=1}^{\infty} \left\{ \frac{(-1)^{n+1}}{(2t)^{2n-1}}\left[\frac{d^{2n-2}}{d\omega^{2n-2}}\left(\Pi(\omega_i) d_{ii}^{(12)}(\omega_i)\right) \sin 2\omega_i t\right]\right\|_{\omega_i^-}^{\omega_i^+} +$$

$$\left. + \frac{1}{(2t)^{2n}}\left[\frac{d^{2n-1}}{d\omega^{2n-1}}\left(\Pi(\omega_i) d_{ii}^{(12)}(\omega_i)\right) \cos 2\omega_i t\right]\Big|_{\omega_i^-}^{\omega_i^+} \right\}$$

(A.1)

On the other hand, integration by parts with respect ω_j of the second type of terms provides the following expression:

$$\int_{\omega_i^-}^{\omega_i^+}\int_{\omega_j^-}^{\omega_j^+}\Pi(\omega_i,\omega_j)d_{ij}^{(12)}(\omega_i,\omega_j)\cos(\omega_i+\omega_j)t\,d\omega_i d\omega_j=\int_{\omega_i^-}^{\omega_i^+}\left\{\frac{1}{t}\left[\Pi(\omega_i,\omega_j)d_{ij}^{(12)}\sin(\omega_i+\omega_j)t\right]\Big|_{\omega_j^-}^{\omega_j^+}-\right.$$

$$\left.\frac{1}{t}\int_{\omega_i^-}^{\omega_i^+}\frac{d}{d\omega_j}\left[\Pi(\omega_i,\omega_i)d_{ij}(\omega_i,\omega_i)\right]\sin(\omega_i+\omega_i)t\;d\omega_j\right\}d\omega_i$$

Neglecting the second order term in the integrand, and integrating by part with respect ω_i, it is produced:

$$\int_{\omega_i^-}^{\omega_i^+}\int_{\omega_j^-}^{\omega_j^+}\Pi(\omega_i,\omega_j)d_{ij}^{(12)}(\omega_i,\omega_j)\cos(\omega_i+\omega_j)t\,d\omega_i d\omega_j=-\frac{1}{t^2}\left[\Pi(\omega_i,\omega_j)\cos(\omega_i+\omega_j)t\right]\Big|_{\omega_j^-}^{\omega_j^+}+$$

$$+\frac{1}{t^2}\int_{\omega_i^-}^{\omega_i^+}\frac{d}{d\omega_i}\left[\left(\Pi(\omega_i,\omega_j)d_{ij}^{(12)}(\omega_i,\omega_j)\right)\cos(\omega_i+\omega_j)t\right]\Big|_{\omega_j^-}^{\omega_j^+}d\omega_i$$

Keep on integrate per parts, the following serie is obtained:

$$\int_{\omega_i^-}^{\omega_i^+}\int_{\omega_j^-}^{\omega_j^+}\Pi(\omega_i,\omega_j)d_{ij}^{(12)}(\omega_i,\omega_j)\cos(\omega_i+\omega_j)t\,d\omega_i d\omega_j=\sum_{n=1}^{\infty}\left\{-\frac{(-1)^{n+1}}{t^{2n}}\left[\frac{d^{2n-2}}{d\omega^{2n-2}}\left(\Pi(\omega_i,\omega_j)\right)\right.\right.$$

$$\left.d_{ii}^{(12)}(\omega_i,\omega_j)\left[\cos(\omega_i+\omega_j)t\right]_{\omega_j^-}^{\omega_j^+}\Big|_{\omega_i^-}^{\omega_i^+}-\frac{1}{(2t)^{n+1}}\left[\frac{d^{2n-1}}{d\omega^{2n-1}}\left(\Pi(\omega_i,\omega_j)d_{ii}^{(12)}(\omega_i,\omega_j)\right)\sin(\omega_i+\omega_j)t\right]\Big|_{\omega_j^-}^{\omega_j^+}\Big|_{\omega_i^-}^{\omega_i^+}\right\}$$

(A.2)

The lower time order of eq. (A.2) is the second, *i.e.* this kind of integrals generates only term of order t^{-2} and higher order terms.

Therefore, on the basis of eqs. (A.1) and (A.2), when considering only the terms up to the first order, the asymptotic expansion is proven.

APPENDIX B: the probabilistic asymptotic expansion of the coupling energy term for a non conservative systems.

The system response in presence of damping can be expressed in the form:

$q_i = A_i e^{-\partial_i \omega_i t} \sin \omega_i t$

Where the ω_i's are the damped natural frequencies of the whole systems, ∂_i's are modal damping coefficients and A_i's are coefficients related with the initial conditions.

Substituting the expression of the lagrange coordinates and its derivatives into eq.(5.8), the explicit time dependencies of the coupling energy between S_1 and S_2 are given by:

$$E^{(12)} = \frac{1}{4}\sum_{i,j=1}^{N} \alpha_{ij}^{(12)} A_i A_j \omega_i \omega_j \, e^{-(\delta_i\omega_i+\delta_j\omega_j)t}\left[(1-\delta_i\delta_j)\cos(\omega_i+\omega_j)t + (1+\delta_i\delta_j)\cos(\omega_i-\omega_j)t\right.$$
$$\left. -(\delta_i+\delta_j)\sin(\omega_i+\omega_j)t + (\delta_j+\delta_i)\sin(\omega_i-\omega_j)t\right] + \frac{1}{4}\sum_{i,j=1}^{N}\beta_{ij}^{(12)} A_i A_j e^{-(\delta_i\omega_i+\delta_j\omega_j)t} \cdot$$
$$\left[-\cos(\omega_i+\omega_j)t + \cos(\omega_i-\omega_j)t\right] \qquad \text{(B.1)}$$

Introducing the following coefficients:

$$m_{ij}^{(12)} = \frac{1}{4} A_i\, A_j \left[\alpha_{ij}^{(12)}(1-\delta_i\,\delta_j)\omega_i\,\omega_j - \beta_{ij}^{(12)}\right]$$

$$n_{ij}^{(12)} = \frac{1}{4} A_i\, A_j \left[\alpha_{ij}^{(12)}(1+\delta_i\,\delta_j)\omega_i\,\omega_j + \beta_{ij}^{(12)}\right]$$

$$p_{ij}^{(12)} = \frac{1}{4} A_i\, A_j\, \alpha_{ij}^{(12)}(\delta_i+\delta_j)\omega_i\,\omega_j$$

$$q_{ij}^{(12)} = \frac{1}{4} A_i\, A_j\, \alpha_{ij}^{(12)}(\delta_i-\delta_j)\omega_i\,\omega_j$$

and dividing the terms in the summation into a part for which $i=j$ and the others, equation (B.1) becomes:

$$E^{(12)} = \sum_{i=1}^{N} m_{ii}^{(12)} \cos(2\omega_i t) e^{-2\delta_i\omega_i t} + \sum_{i=1}^{N} n_{ii}^{(12)} e^{-2\delta_i\omega_i t} - \sum_{i=1}^{N} p_{ii}^{(12)} \sin(2\omega_i t) e^{-2\delta_i\omega_i t} +$$
$$\sum_{\substack{i,j=1\\ j\neq i}}^{N} m_{ij}^{(12)} \cos(\omega_i+\omega_j)t\; e^{-(\delta_i\omega_i+\delta_i\omega_i)t} + \sum_{\substack{i,j=1\\ j\neq i}}^{N} n_{ij}^{(12)} \cos(\omega_i-\omega_j)t\; e^{-(\delta_i\omega_i+\delta_i\omega_i)t} + \qquad \text{(B.2)}$$
$$\sum_{\substack{i,j=1\\ j\neq i}}^{N} p_{ij}^{(12)} \sin(\omega_i+\omega_j)t\; e^{-(\delta_i\omega_i+\delta_i\omega_i)t} + \sum_{\substack{i,j=1\\ j\neq i}}^{N} q_{ij}^{(12)} \sin(\omega_i-\omega_j)t\; e^{-(\delta_i\omega_i+\delta_i\omega_i)t}$$

Following the same procedure used for the conservative case, in analogy with eq.(5.14b), it is possible to obtain the ensemble energy average of a population of similar systems affected by inherent uncertainty of their paramter as:

$$\overline{\mathrm{E}}^{(12)}(t)=\int_{\Re^N}\mathrm{E}^{(12)}(t)\,p(\Omega)d\Omega \tag{B.3}$$

Eq.(B.2) is introduced into eq.(B.3), each terms of eq.(B.2) was integrated, leading to an asymptotic expansion of the integrals with respect to time.

Let us considered the first type. Considering only the first and second order terms, integration by parts of this term with respect to ω_i produces:

$$\int_{\omega_i^-}^{\omega_i^+}\Pi(\omega_i)m_{ii}^{(12)}(\omega_i)\cos 2\omega_i t\; e^{-2\delta_i\omega_i t}\,d\omega_i=\cdot$$

$$\frac{1}{2t\left(1+\delta_i^2\right)}\left[\Pi(\omega_i)m_{ii}^{(12)}(\omega_i)(\sin 2\omega_i\, t-\delta_i\cos 2\omega_i\, t\,)e^{-2\delta_i\omega_i t}\,\right]\Big|_{\omega_i^-}^{\omega_i^+}+$$

$$-\;\frac{1}{4t^2\left(1+\delta_i^2\right)^2}\left\{\frac{d}{d\omega_i}\left[\Pi(\omega_i)m_{ii}^{(12)}(\omega_i)\right]\cdot\left[\left(\delta_i^2-1\right)\cos 2\omega_i\, t-2\,\delta_i\sin 2\omega_i\, t\right]e^{-2\delta_i\omega_i t}\right\}\Big|_{\omega_i^-}^{\omega_i^+}$$

The second term in eq.(B.3) produces:

$$\int_{\omega_i^-}^{\omega_i^+}\Pi(\omega_i)n_{ii}^{(12)}(\omega_i)\,e^{-2\delta_i\omega_i t}\,d\omega_i=\cdot-\frac{1}{2\delta t}\left[\Pi(\omega_i)n_{ii}^{(12)}(\omega_i)e^{-2\delta_i\omega_i t}\right]\Big|_{\omega_i^-}^{\omega_i^+}+$$

$$-\frac{1}{(2\delta t)^2}\left\{\frac{d}{d\omega_i}\left[\Pi(\omega_i)n_{ii}^{(12)}(\omega_i)\right]e^{-2\delta_i\omega_i t}\right\}\Big|_{\omega_i^-}^{\omega_i^+}$$

For the third term, the asymptotic expansion poduces:

$$\int_{\omega_i^-}^{\omega_i^+}\Pi(\omega_i)\,p_{ii}^{(12)}(\omega_i)\sin(2\omega_i t)e^{-2\delta_i\omega_i t}\,d\omega_i=\cdot$$

$$-\frac{1}{2\,t\left(1+\delta_i^2\right)}\left[\Pi(\omega_i)g_{ii}^{(12)}(\omega_i)(\cos 2\omega_i t+\delta\sin 2\omega_i t)e^{-2\delta_i\omega_i t}\right]\Big|_{\omega_i^-}^{\omega_i^+}+$$

$$+\frac{1}{4\,t^2\left(1+\delta_i^2\right)^2}\left\{\frac{d}{d\omega_i}\left[\Pi(\omega_i)g_{ii}^{(12)}(\omega_i)\right]\left[-2\,\delta\cos 2\omega_i t+\left(1-\delta_i^2\right)\sin 2\omega_i t\right]e^{-2\delta_i\omega_i t}\right\}\Big|_{\omega_i^-}^{\omega_i^+}$$

The second type of terms for which $i\neq j$, integration by parts with respect ω_j and ω_i provides the following expression:

$$\int_{\omega_i^-}^{\omega_i^+}\int_{\omega_j^-}^{\omega_j^+}\Pi\left(\omega_i,\omega_j\right)m_{ii}^{(12)}\left(\omega_i,\omega_j\right)\cos\left(\omega_i+\omega_j\right)t\;e^{-\left(\delta_i\omega_i+\delta_j\omega_j\right)t}\,d\omega_i d\omega_j=$$

$$\frac{1}{t^{\,2}\left(1+\delta_i^2\right)\left(1+\delta_j^2\right)}\left\{\;\Pi\left(\omega_i,\omega_j\right)m_{ii}^{(12)}\left(\omega_i,\omega_j\right)\left[\left(\delta_i\delta_j-1\right)\cos\left(\omega_i+\omega_j\right)t-\left(\delta_i+\delta_j\right)\sin\left(\omega_i+\omega_j\right)t\right]\right.$$

$$\left.e^{-\left(\delta_i\omega_i+\delta_j\omega_j\right)t}\;\right\}\Bigg|_{\omega_i^-}^{\omega_i^+}\Bigg|_{\omega_j^-}^{\omega_j^+}$$

The second integrand of this type is given by:

$$\int_{\omega_i^-}^{\omega_i^+}\int_{\omega_j^-}^{\omega_j^+}\Pi\left(\omega_i,\omega_j\right)n_{ii}^{(12)}\left(\omega_i,\omega_j\right)\cos\left(\omega_i-\omega_j\right)t\;e^{-\left(\delta_i\omega_i+\delta_j\omega_j\right)t}\,d\omega_i d\omega_j=$$

$$\frac{1}{t^{\,2}\left(1+\delta_i^2\right)\left(1+\delta_j^2\right)}\left\{\;\Pi\left(\omega_i,\omega_j\right)n_{ii}^{(12)}\left(\omega_i,\omega_j\right)\left[-\left(1+\delta_i\delta_j\right)\cos\left(\omega_i-\omega_j\right)t-\left(\delta_j-\delta_i\right)\sin\left(\omega_i-\omega_j\right)t\right]\right.$$

$$\left.e^{-\left(\delta_i\omega_i+\delta_j\omega_j\right)t}\;\right\}\Bigg|_{\omega_i^-}^{\omega_i^+}\Bigg|_{\omega_j^-}^{\omega_j^+}$$

Taking into account only the first and second order term in the asymptotic expansion provides:

$$\int_{\omega_i^-}^{\omega_i^+}\int_{\omega_j^-}^{\omega_j^+}\Pi\left(\omega_i,\omega_j\right)p_{ij}^{(12)}\left(\omega_i,\omega_j\right)\sin\left(\omega_i+\omega_j\right)t\;e^{-\left(\delta_i\omega_i+\delta_j\omega_j\right)t}\,d\omega_i d\omega_j=$$

$$\frac{1}{t^{\,2}\left(1+\delta_i^2\right)\left(1+\delta_j^2\right)}\left\{\;\Pi\left(\omega_i,\omega_j\right)p_{ij}^{(12)}\left(\omega_i,\omega_j\right)\left[\left(\delta_j^2+\delta_i^2\right)\cos\left(\omega_i+\omega_j\right)t+\left(\delta_i\delta_j+1\right)\sin\left(\omega_i+\omega_j\right)\right]\right.$$

$$\left.e^{-\left(\delta_i\omega_i+\delta_j\omega_j\right)t}\;\right\}\Bigg|_{\omega_i^-}^{\omega_i^+}\Bigg|_{\omega_j^-}^{\omega_j^+}$$

The last term provides the following expression:

$$\int_{\omega_i^-}^{\omega_i^+}\int_{\omega_j^-}^{\omega_j^+} \Pi(\omega_i,\omega_j)\, q_{ii}^{(12)}(\omega_i,\omega_j)\sin(\omega_i-\omega_j)t\; e^{-(\delta_i\omega_i+\delta_j\omega_j)t}\, d\omega_i d\omega_j =$$

$$\frac{1}{t^2(1+\delta_i^2)(1+\delta_j^2)}\left\{ \Pi(\omega_i,\omega_j)\, q_{ij}^{(12)}(\omega_i,\omega_j)\left[(\delta_j^2-\delta_i^2)\cos(\omega_i-\omega_j)t+(1+\delta_i\delta_j)\sin(\omega_i-\omega_j)t\right]\right.$$

$$\left. e^{-(\delta_i\omega_i+\delta_j\omega_j)t} \right\}\Bigg|_{\omega_i^-}^{\omega_i^+}$$

APPENDIX C: the mass loading effect

The experimental data are affected by systematic errors induced by the experimental set-up or by the data acquisition instrumentation. Among the others, the mass loading effect, due to the presence of the accelerometers upon the plates, is responsible of a modification of the system characteristics. In general, mass loading induces an increase of the total mass of the system, that implies a shift of the system eigenfrequencies to lower frequency value. This effect is obviously as much pronounced as lighter is the system under analysis with respect the mass of the instrumentation.

To analyse the mass loading effect on the plate due to those accelerometers, a preliminary test was carried out on the lightest plate among the three presented in table 3.

Two accelerometers were mounted very close on the lightest plate, but only the dynamical response of one of those accelerometers was analysed, since the other was used only as a mass loading the plate. In figures 1 the dynamical responses of the accelerometer in presence and in absence of the second accelerometer are shown

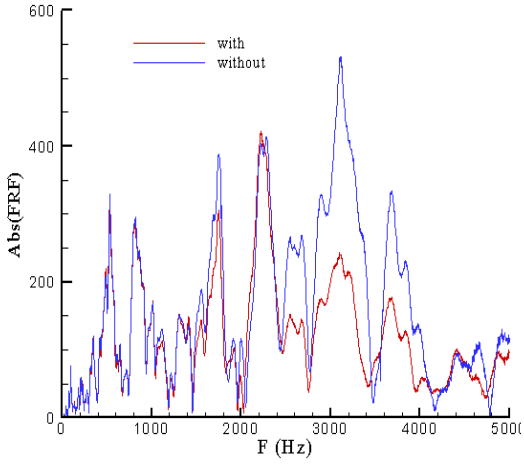

Fig.1

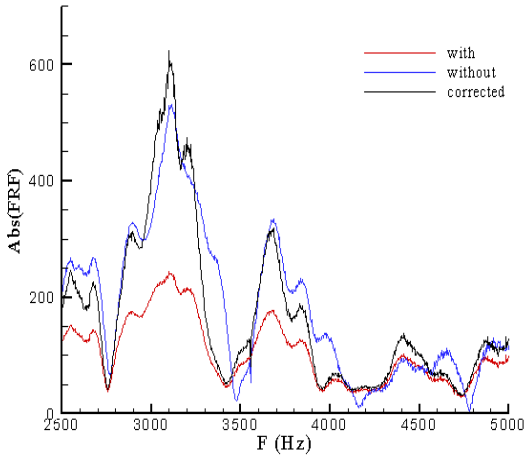

Fig.2

For a frequency lower than 2.5 KHz the absolute values of the frequency response function of the system does not appear to be significantly affected by the mass of the second accelerometer. At higher frequency the dynamical behaviour of the system measured in the absecnce of the other mass diverges from the one obtained in presence of that, instead. In this frequency range the measured signals can be corrected using eq

(C.1) and eq (C.2) which provide the real value of the FRF from the knowledge of the accelerometer mass (m_a) and the measured FRF $H_{jj}(\omega)_m$ (Sestieri et al. 1991).

$$H_{jj}(\omega)_r = \frac{H_{jj}(\omega)_m}{1 - m_a H_{jj}(\omega)_m} m_a \qquad \text{(C.1)}$$

$$H_{ij}(\omega)_r = H_{ij}(\omega)_m \left(1 + \frac{H_{ij}(\omega)_m}{1 - m_a H_{ij}(\omega)_m} m \right)_a \qquad \text{(C.2)}$$

In figure 2 the same curves shown in figure 1 are presented in the high frequency range to show better the disagreement between them. Moreover another curve (the black line), which is obtained by applying the theoretical correction (eq.C.1 and C.2), is superimposed. A good agreement between the corrected spectra and the dynamical response obtained in absence of the other accelerometer is evident. It is important to underline that the frequency limitation imposed by the accelerometer weight lightly affects the kinetic energy of the system. In fact, comparing the punctual energy response of the accelerometer obtained in the two conditions described below, it is evident that the differences between them is very small. This remarks that the energy response of a structure is strictly dependent on the lower modes, being not very sensitive to variation at high frequency.

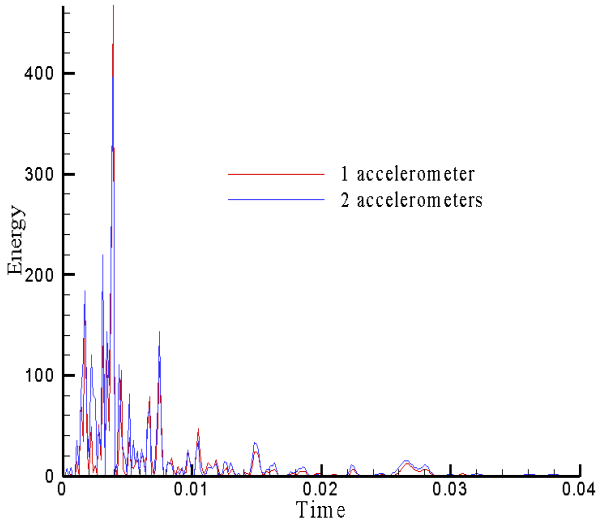

Fig.3